Isolation, Expansion and Characterization of Circulating Tumor Cells using Microfluidic Technologies

by

Zhuo Zhang

A dissertation submitted in partial fulfillment
of the requirements for the degree of
Doctor of Philosophy
(Chemical Engineering)
in the University of Michigan
2016

Doctoral Committee:

Professor Sunitha Nagrath, Chair
Professor Erdogan Gulari
Professor Jennifer J. Linderman
Professor Gary D. Luker

Dedication

I dedicate this thesis to my mother, who taught me to believe in hard work and stay strong to overcome hardship in life. I also dedicate this thesis to my father, who has left my Mom and me ten years ago because of cancer but who has never failed to influence my life. Their love and support set the foundation for me to complete this work.

Acknowledgements

I would like to express my sincere gratitude to my supervisor, Dr. Sunitha Nagrath, who has been guiding me through my PhD dissertation research. As a role model for me, Dr. Nagrath demonstrates the unlimited possibilities biotechnologies can aid in clinical medicine. Her enthusiasm for science, engineering and her compassion for cancer patients will always be aspirations for my future pursuit in research and medicine.

I am sincerely grateful to my supervisor, Dr. Nithya Ramnath, who inspired me to embark on my voyage in medicine. Dr. Ramnath supervised me to test technologies with patient samples. Together, we have been exploring the possibility to bridge the gap between technologies and their clinical applications. Her devotion to cancer research and her care for patients are great motivations for me to continue my endeavor in medical research.

I would like to thank Dr. Hiroe Shiratsuchi, for her guidance and help for my research. I learned molecular biology techniques from her and I enjoyed greatly my time working with her.

I also greatly appreciate all the help and support from Dr. Rishindra Reddy, Dr. Guoan Chen, Dr.Gary Luker, Dr. David Beer, Dr. Nallasivam Palanisamy, Dr. Diane Simeone, Dr. Max Wicha, Dr. Erdogan Gulari, Dr. Jennifer Linderman, Dr. Ebrahim Azizi, Dr. Shamileh Fouladdel, Dr. Hui Jiang, Dr. Meghan Waghray, Dr. Lin Lin, Dr. Jules Lin and Dr. Andrew Chang.

All my colleagues in Nagrath lab and Beer lab are greatly appreciated for their kind support over the years.

Table of Contents

List of Tables

List of Figures

List of Abbreviations

CTCs: circulating tumor cells
NSCLC: non-small cell lung cancer
SCLC: small cell lung cancer
SCC: squamous cell carcinoma
PDMS: polydimethylsiloxane
GO: graphene oxide
EpCAM: epithelial cell adhesion molecule
CK: cytokeratin
TTF-1: thyroid transcription factor-1
EGFR: epidermal growth factor receptor
EMT: epithelial-mesenchymal transition
AC: adenocarcinomas
NGS: next generation sequencing
LNF: Lurie Nanofabrication Facility
GMBS: N-gamma-maleimidobutyryl-oxysuccinimide ester
PBS: phosphate buffered saline
BSA: bovine serum albumin
PFA: paraformaldehyde
DAPI: 4',6-Diamidino-2-Phenylindole, Dihydrochloride
DMSO: Dimethyl sulfoxide
IF: immunofluorescence
HMFs: human mammary fibroblasts
CAFs: cancer associated fibroblasts
GFP: green fluorescent protein
ECM: extracellular matrix
FFPE: formalin-fixed, paraffin-embedded
IARC: International Agency for Research on Cancer
ALK: anaplastic lymphoma kinase
FISH: fluorescence in-situ hybridization
H&E: hematoxylin and eosin
IHC: immunohistochemistry
EDTA: ethylenediaminetetraacetic acid
TKI: tyrosine kinase inhibitors
EML4: echinoderm microtubule-like protein 4

Abstract

Circulating tumor cells (CTCs) are the tumor cells shed from primary tumor, which enter the bloodstream and travel to distant anatomic sites to form metastasis. With emerging sensitive micro- and nanotechnologies, CTCs have been identified as blood-based biomarkers to guide cancer diagnosis and prognosis. Detecting CTCs, as a means of "liquid biopsy", allows monitoring cancer progression in real time and predicting therapeutic response. The major challenge that limits the clinical utility of CTCs, especially in early stage cancer patients, is their rarity; specifically, there are only 1-10 CTCs in one milliliter of whole blood. One way to overcome this critical limitation is to *ex vivo* expand CTCs through culturing. Previously, a few studies have shown limited success with CTC culturing from metastatic cancer patients.

In this thesis, a microfluidic CTC capture device is optimized and tested for the capture and analysis of CTCs from lung cancer patients. A novel microfluidic co-culture model is developed to facilitate CTC expansion followed by downstream genomic, functional analysis and xenograft implantation. CTCs were isolated from more than 50 lung and esophageal cancer patients of various stages including patients with Stage I disease and cultured *ex vivo*. Using a 3D, on chip co-culture model, CTCs were successfully expanded in 70% of the patient samples. Cultured CTCs were characterized with immunostaining, RNA profiling, mutation analysis and invasion assays. We found concordant *TP53* mutation in CTCs and matched primary tumors. Next-generation sequencing further revealed mutations in additional genes.

It was found that, patients whose CTCs exhibited the greatest capacity to expand *ex vivo* had earlier recurrence. In one of the patient samples, expanded CTCs implanted in mice resulted in a xenograft tumor, demonstrating the expanded CTCs' ability to metastasize. CTC-derived xenograft was compared with cultured CTCs and the primary tumor through IHC staining and RNA sequencing. We were able to demonstrate that the

xenograft had the same histology as the primary tumor. Genes related to EMT and tumor microenvironment were enriched in the xenograft. In addition, building upon this co-culture model, CTCs from one of the *ALK* positive metastatic lung cancer patients were isolated and cultured. The cultured CTCs harbored the concordant *EML4-ALK* rearrangement as the tumor biopsy specimen and further served as an *in vitro* model for drug testing.

Taken together, this study demonstrated that CTCs from early stage lung cancer are tumorigenic and mirror the phenotypic and genotypic status of primary tumors. *Ex vivo* culturing of CTCs changed the current paradigm of CTC research, and will make a significant impact in the era of personalized medicine. It will bring about opportunities for individualized drug screening, such as predicting treatment response to targeted therapies and the emergence of acquired drug resistance. Cultured CTCs will also serve as tools for understanding metastatic spread of cancer cells.

Chapter 1
Introduction

1.1 Motivation

Circulating tumor cells (CTCs) are the lethal drivers of metastasis. They are tumor surrogates that carry relevant genomic and proteomic information of primary tumors. Sampling CTCs via blood drawn from peripheral veins can be non-invasive. It permits routine clinical monitoring and causes less pain than solid biopsy. Isolating CTCs has been a great challenge because of the low number of cells present in the bloodstream. To enhance the capture efficiency and specificity, microfluidic technologies have emerged to detect and analyze CTCs. Detecting and diagnosing cancer early in its progression increases survival. Isolating CTCs from early stage cancer patients will examine the potential of the cells to aid in early cancer detection. Furthermore, there is a need to increase the CTC number to expand the clinical utility of CTCs such as performing drug susceptibility testing and *in vivo* implantation. In this thesis, we aim to address this need by culturing CTCs *ex vivo* through a microfluidic co-culture model.

1.2 Microfluidics and CTCs

1.2.1 Microfluidics for cancer research

Microfluidics handles microliter volumes in microchannels of 1μm to 1000μm size. In such a regime, fluid flow is laminar, hence concentrations of molecules can be controlled [1]. Microfluidics was introduced as a biological tool in the early 1990s [2]. Since then, this interdisciplinary technology, known for manipulating reagents within miniaturized platforms, has been developing rapidly [3, 4]. The material used for preparing microfluidic devices has evolved from traditional silicon and glass, to elastomers rendering the device more biocompatible and of lower cost [1]. There are several inherent advantages of microfluidics, including reduced sample size and reagent consumption, short processing time, enhanced sensitivity, real-time analysis and automation [5]. One of the motivations for applying microfluidic techniques in life science is to automate the labor-intensive experimental processes similar to that accomplished in electronic circuits [2]. Polymerase chain reaction, electrophoresis on chip and DNA microarrays are among the earliest microfluidic ventures [2]. With a decade of development, microfluidic integrated systems are expanded to manipulate RNA, proteins and mammalian cells; and as biosensors, single cell assays for disease diagnosis and prognosis. Microfluidic devices are utilized to explore and investigate cancers in new and unconventional ways.

Cancer research has long been at the forefront of medical and scientific research. Its seemingly incurable nature and large prevalence in society has made cancer a popular and well-funded area of research for decades. Cancer is a chronic disease involving multitude genetic alterations. It was estimated that in 2008, 12.7 million cancer cases and 7.6 million cancer-related deaths occurred globally [6]. In 2011 in the United States alone, 1.6 million people were newly diagnosed with cancers and 571,950 cancer-related deaths were projected. Prostate, breast, lung and colorectal cancers are the leading cause of cancer deaths in the US [7]. Since 2004, considerable funding has been allocated for technology advancement in search of more effective anti-cancer strategies [8].

Traditionally, cancer diagnosis is highly dependent upon sampling tumor tissues or indirect quantification of proteins [9]. Often, these conventional sampling approaches are invasive, which lead to tissue damage, limited access and inability to get reliable

samples and cause high levels of patient discomfort. Although proteomic and genomic research have identified a list of candidate cancer biomarkers in body fluids such as blood and saliva [10], there is still a lack of point-of-care devices for rapid and non-invasive diagnosis. Possible biomarkers in the blood include DNA, miRNA, proteins, serum microvesicles and circulating tumor cells (CTCs) [11-14]. However, these biomarkers are often present at low levels against massive background signals. For example, there are only 1-10 CTCs in 1mL of whole blood containing 10^6-10^7 blood cells [15, 16]; the ratio between targeted proteins versus the background is approximately $1{:}10^5$ [17]. Given the challenge of detecting the actual signal from vast noises, researchers turn to MEMS (Microelectromechanical systems) based approaches. Inherently, microfluidics is suitable for analyzing complex fluids *in vitro* and thus offers a promising approach for cancer diagnosis and disease management [1]. In addition, because of the ease of manufacturing and low cost of microfluidic devices, biomarkers can be assessed routinely, which is essential for developing personalized medicine [18].

1.2.2 Circulating tumor cells (CTCs)

Circulating tumor cells (CTCs) are cells shed by underlying tumors and circulate in blood and lymphatic vessels. CTCs are the likely drivers of metastasis, which accounts for nearly 90% of cancer-related deaths [19]. They can ultimately lodge, invade and proliferate at distant organs initiating metastatic lesions (Figure 1). In some cancers, metastasis may occur in the early stage of tumor progression [20]. In addition, metastatic cells acquire mutations beyond those initiated within primary tumors [21].Therefore, detecting CTCs can be extremely valuable for cancer diagnosis in early stages and help with treatment decisions.

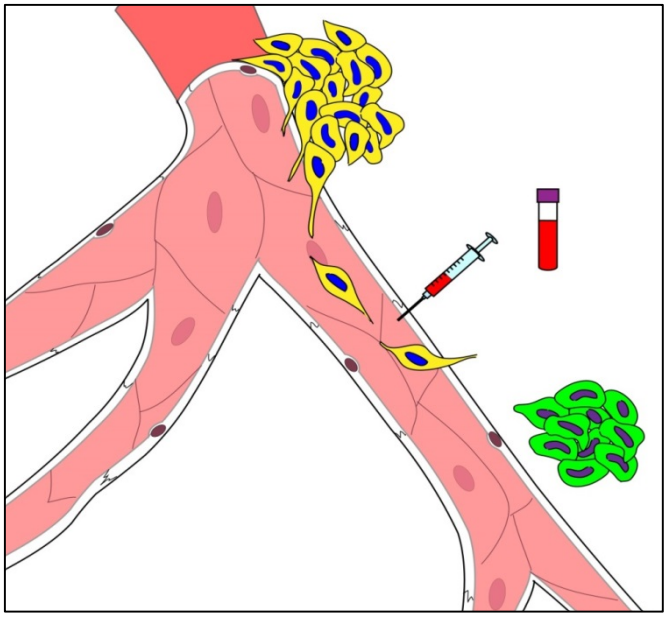

Figure 1. CTCs and the metastatic cascade. CTCs are the cells shed by the primary tumor, which enter the bloodstream, ultimately extravasate and form metastases in distant organs.

1.2.3 Microfluidic technologies for isolating CTCs

The emerging microfluidic technologies can isolate CTCs based on their biological or physical properties (Figure 2).

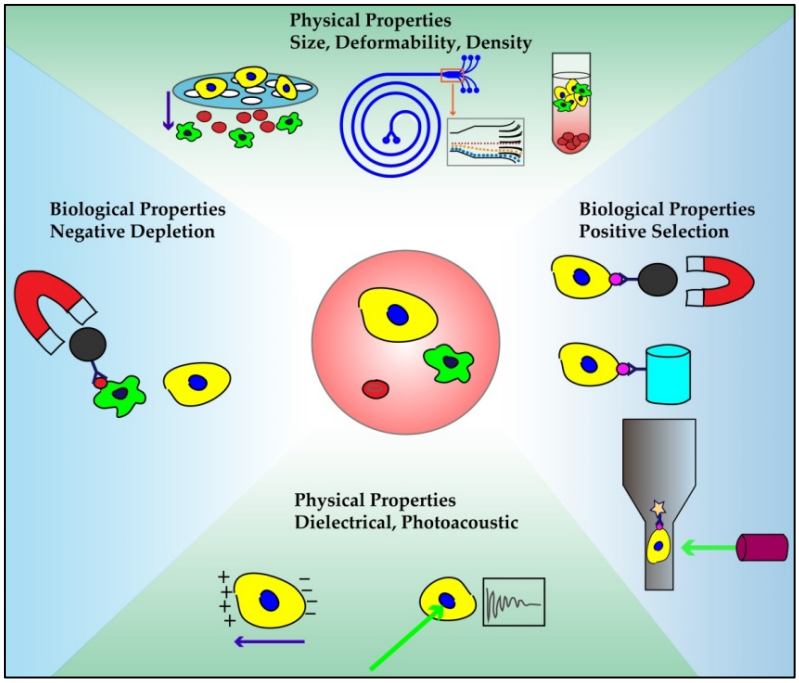

Figure 2. CTC isolation technologies. CTCs can be isolated based on their physical or biological properties.

Immunoaffinity-based Isolation

One of the major CTC isolation methods is based on antibody-antigen interactions. The most commonly used surface antigen is the epithelial cell adhesion molecule or EpCAM, first identified in the late 70's [22]. EpCAM is overexpressed in breast, colon, lung, prostate, gastric, ovarian and renal carcinomas [22-24] and hence widely employed as the target in almost all immunoaffinity-based CTC isolation strategies.

Early in 2004, CellSearch, demonstrated CTC-based diagnostic potential by separating CTCs using EpCAM-coated magnetic beads and correlating the number of isolated CTCs to prognosis in breast cancer patients. It is the only device approved by the U.S. Food and Drug Administration for isolating CTCs in metastatic breast, colon and prostate cancers [25]. In the CellSearch system, blood specimens are fixed prior to CTC isolation. Although it can prolong the storage time of the blood samples, the available downstream analysis is limited because of the fixed cells.

In 2007, Nagrath *et al*. reported a microfluidic-based CTC capture device, which was composed of 78,000 EpCAM-coated microposts embedded on a silicon chip [26].

The chip can capture cancer cells from milliliters of unprocessed whole blood with high sensitivity and purity. The captured cancer cells were maintained in an appropriate condition for molecular analysis through immunostaining and RNA profiling. The chip successfully detected CTCs in all but one of 116 blood samples from 68 patients with metastatic lung, prostate, pancreatic, breast and colon cancer.

Later in 2008, Maheswaran *et al*. showed that the CTC-chip technology monitored the epidermal growth factor receptor (EGFR) mutations in patients with non-small-cell lung cancer (NSCLC). Sufficient DNA was isolated from the captured CTCs to allow allele specific assay testing and in few instances direct sequencing. Somatic genetic mutations were detected in 19 out of 20 EGFR positive patient samples. In addition, the secondary resistant mutations from 11 out of 12 patients, who developed resistance to tyrosine kinase inhibitors, were also shown [27]. This type of information, which is vital for diagnosis, prognosis, and therapeutics, was earlier provided only by repeated tissue biopsies. Non-invasive genotyping or "blood biopsies" provide possible alternatives.

In 2010, Stott *et al*. developed an automated strategy to characterize CTCs of metastatic prostate cancer [28]. CTCs were stained for the prostate-specific antigen (PSA). The chip was imaged in a semiautomated fashion and CTCs were characterized by an image processing algorithm in terms of fluorescence intensity, cell shape and other morphological traits. This method enabled easier monitoring of CTCs in different patients during the course of therapy.

The CTC isolation devices discussed so far immobilized antibodies on microposts through surface chemistry. In another approach, magnetic arrays coated with antibodies self-assembled in plain microchannels for CTC capturing [29]. This system was used to sort B-lymphocytes from patients with leukemia and lymphoma. In addition, cancer cells were separated from endothelial cells with an efficiency of 80% using the same device. Dharmasiri *et al*. demonstrated another immobilization technique using aptamers. This method captured prostate cancer cells with high efficiency and purity [30]. Dickson *et al*. reported a streptavidin coated microfluidic device to isolate cancer cells from blood [31].

Despite the ability to specifically target CTCs, challenges for CTC isolation remain. CTCs are very rare (1 to 10 per mL of whole blood) compared with billons of white blood cells and red blood cells. The rarity poses a significant engineering problem when designing a device to capture CTCs for high specificity, purity and simultaneously keeping the cells viable for subsequent molecular analysis [15]. Researchers have been developing sophisticated microfluidic devices to address these issues.

Stott *et al*. made a high-throughput polydimethylsiloxane (PDMS) based device with enhanced capture efficiency and optical properties [32]. The microchannel was fabricated into a herringbone shape, which generated passive mixing via microvortices. It can process larger volume of blood than the micropost-based CTC-chip while maintaining the same capture efficiency. For example, the herringbone chip maintained >40% capture efficiency at flow rate up to 4.8mL/hr but the efficiency of the CTC-chip dropped significantly above 2-3mL/hr. After being captured, cancer cells were viable and intact for molecular characterization and imaging.

Gleghorn *et al*. reported a geometrically enhanced differential immunocapture (GEDI) chip to capture prostate CTCs with high-efficiency and high-purity [33]. The researchers optimized the displacement, size and shape of posts to maximize the interaction between CTCs (15-25um) and the antibody coated surface while small blood cells (4-18um) can escape.

Myung *et al*. demonstrated the immobilization of E-selectin and anti-EpCAM on the microfluidic channels for CTC isolation. E-selectin induced rolling of leukocytes and cancer cells at different velocities resulting in enhanced antibody accessibility to cancer cells [34]. The cancer cells tended to roll faster as the shear stress increased while the rolling velocity of leukocyte remained stable. Therefore, this approach achieved separation of leukocytes and CTCs with increased cell capture efficiency.

Dharmasiri *et al.* recently reported an integrated microfluidic system, which incorporated immunoaffinity-based capture, enzymatic release, conductivity enumeration and electrokinetic enrichment of colorectal CTCs [35]. This method allowed consequent manipulation and molecular profiling of CTCs using PCR coupled with a ligase detection

reaction (LDR) assay. Since this system contained an electrokinetic enrichment component, it can concentrate the mass-limited DNA samples extracted from CTCs. They were able to detect the *KRAS* mutation in the SW620 cell line but not in the HT29 cell line, which was consistent with the known genotypes.

Hoshino *et al*. utilized immunomagnetic separation mechanism to isolate cancer cells in a microchip. Blood samples containing spiked cancer cells were incubated with magnetic nanoparticles conjugated with anti-EpCAM prior passing through the device. This device can isolate as few as 5 cells per mL of blood and can be operated at 10ml/hr flow rate without a significant reduction of capture rate [36].

Most recently, Kang *et al*. presented a novel CTC isolation approach which incorporated magnetic separation with microfluidic devices that permitted removal of captured CTCs from the device followed by culturing [37]. The device consisted of a main channel flanked by two rows of dead-end side chambers for CTC collection. One mouse blood sample was first treated with EpCAM coated magnetic beads followed by flowing through the isolation channel. After that, CTCs can be released by moving the magnet to the opposite side of the device. CTCs were then cultured and checked for viability.

The major drawback of immunoaffinity-based isolation is that the EpCAM expression level on CTCs varies. Some of the CTCs might not express EpCAM, particularly cells that undergo the epithelial-mesenchymal transition(EMT) [38]. Therefore, immunoaffinity approaches miss subpopulations of CTCs, which may carry important molecular information about primary tumors. Utilizing size-based separation and filtration in addition to immunoaffinity methods could increase the yield with minimal loss of low/none EpCAM expressing cells.

Size-based biomarker independent Separation

CTCs are often larger in size and may have a different specific gravity than blood cells therefore they can be separated from blood cells either by physical filtration or by hydrodynamic forces [39]. One advantage of the size-based separation is that cells can be enriched without using a specific antibody. With hydrodynamic separation, there is an

added advantage that the system can be operated at a relatively high flow rate, which is valuable to enriching rare CTCs. Furthermore, isolated CTCs can be collected without compromising cell viability or genetic contents thereby enabling off-chip cellular and molecular characterizations. Microfluidic devices enable sorting of CTCs based on size followed by single cell analysis and culturing.

Zheng *et al*. presented an efficient membrane microfilter device made of parylene-C for isolating prostate cancer cells from whole blood [40]. The membrane filter contained 16,000 evenly distributed pores of 10μm diameter with 20μm space in between. The membrane was integrated with electrodes for direct electrolysis of the retained cancer cells followed by the polymerase chain reaction (PCR). Later, researchers used two-layer membranes to filter viable prostate and breast cancer cells [41]. The captured cells were cultured on device for 2 weeks. Two issues arose with increasing volumes of blood processed: the membrane was easily clogged and whole blood needed to be diluted before filtering.

Kuo *et al.* demonstrated a microfluidic filtration system which separated breast cancer cell spiked into whole blood with 50-90% recovery rate [42]. The device consisted of a serpentine channel interconnected with two outer filtrate channels with rectangular apertures. The force experienced by cells during the filtration process was carefully assessed and the dimensions of the apertures were adjusted accordingly to minimize cell damage.

Hur *et al*. presented a device to enrich cancer cells in diluted blood by a factor of 5.4 [43]. Inertial lift forces and viscoelastic forces created distinct focusing positions of deformable particles in microchannels having high aspect ratios. Despite high-throughput and ease of operation, blood samples needed to be diluted to avoid defocusing caused by cancer and blood cell interactions.

Lim *et al*. utilized a particle tracking analysis (PTA) method to study the particle-focusing in microchannels [44]. Polystyrene beads, white blood cells and prostate cancer cells (PC-3) were tested in both diluted and whole blood. Two-dimensional focusing profiles were generated as guidelines for isolating CTCs.

Despite some key advantages of the size-based separation, the performance of this technique is still limited with heterogeneous sizes and morphologies of CTCs [45]. To overcome this challenge, additional downstream processes are needed to increase detection accuracy and sensitivity.

Other MEMS based Methods

Talasaz *et al.* demonstrated a magnetic sweeper utilizing an immunomagnetic mechanism [46]. The device used magnetic rods to sweep wells of a six-well plate to isolate magnetically labeled breast cancer cells from blood. The cells were released and were analyzed by genomic sequencing and other molecular assays. Moon *et al*. combined both hydrodynamic focusing and dielectrophoresis to isolate cancer cells with high flow rates [47]. Diluted blood was passed through a multi-orifice microchannel. Blood cells and cancer cells held different equilibrium positions in the stream to facilitate cell separation. Cancer cells, now pooled with fewer blood cells were then flowed into a non-uniform electric field for further separation. The combined modules achieved efficient enrichment of cancer cells in a short period. Chen *et al*. presented a microfluidic disk to negatively deplete non-tumor cells via immunomagnetic principles [48]. Non-targeted cells were labeled with magnetic beads. As samples passed through a multistage magnetic field, the labeled cells were trapped. Compared with the positive selection methods, negative depletion accommodates the need to capture CTCs, which don't express known surface markers [49].

List of Technology	Principle	Application	Clinical Study
CTC-chip [26]	Immunoaffinity	Isolation of CTCs (1ml/hr flow rate,60-65% efficiency,50% purity from patient samples)	68 patients with metastatic lung, prostate, pancreatic, breast and colon cancer
CTC-chip [27]	Immunoaffinity	Identify EGFR mutations	27 patients with metastatic non-small-cell lung cancer
CTC-chip [28]	Immunoaffinity	Automated imaging of captured CTCs	62 patients with prostate cancer
CEE microchannel [31]	Immunoaffinity	Isolate of cancer cells from blood cells	N/A
Herringbone-chip [32]	Immunoaffinity	High-throughput mixing and isolation of CTCs (1.5-2.5ml/hr flow rate, 90%	15 patients with metastatic prostate cancer

		efficiency, 14% purity from spiking cells in blood)	
Self-assembled magnetic arrays [29]	Immunomagnetic	Isolation of B-lymphocytes (9ul/hr flow rate, 94% yield)	7 patients with B-cell hematological malignant tumors (leukemia and lymphoma)
Aptamer selection chip [30]	Immunoaffinity through aptamers	Isolation of prostate cancer cells from blood (2ml/hr flow rate, 90% recovery, 100% purity—cell line test)	N/A
Geometrically enhanced differential immunocapture (GEDI) chip [33]	Immunoaffinity	Isolation of prostate cancer circulating tumor cells (1ml/hr flow rate, 85% efficiency, 68% purity from spiking cells in blood)	Blood samples of castrate-resistant prostate cancer patients
E-selectin biomimetic chip [34]	Immunoaffinity & Biomimic	Isolation of cancer cells from mixture of leukocytes (1.2ml/hr flow rate, 35% efficiency)	N/A
Integrated CTC selection chip [35]	Immunoaffinity & electrokinetics	Isolation, enumeration, enrichment of CTCs (1.5ml/hr flow rate, 96% efficiency) PCR/LDR detection of KRAS colorectal cancer cell mutations	N/A
Immunomagnetic chip [36]	Immunomagnetic Nanoparticles	Capture cancer cells spiked in blood	N/A
Micromagnetic chip [37]	Immunomagnetic	Isolation CTCs and release for culturing (90% efficiency)	N/A
Membrane microfilter [40, 41]	Size	Separation of cancer cells from blood (89% recovery)	N/A
Filtration chip [42]	Size & Deformability	Separation cancer cells from blood cells (0.72-0.96ml/hr flow rate 50-90% recovery,)	N/A
Deformability-based chip [43]	Size & Deformability	High-throughput separation and enrichment of CTCs from diluted blood (1.5-27ml/hr flow rate, 96% yield, 3.2-5.4 fold enrichment)	N/A
Particle focusing chip [44]	Size	Use particle trajectory analysis to study cancer cell focusing in whole blood	N/A
MagSweeper [46]	Immunomagnetic	Isolation and enrichment of breast cancer cells from whole blood (process 9ml blood per hour, 62% efficiency, 51% purity)	Blood samples from 17 female patients with metastatic breast cancers
MOFF and DEP chip [47]	Size and Dielecrophretic properties	Isolation of breast cancer cells from blood (126ul/min flow rate, 99% efficiency)	N/A
Negative selection disk [48]	Immunomagnetic	Isolation of breast cancer cells from mononuclear cells mixture (60% yield)	N/A

Table 1. Microfluidic technologies for isolating CTCs

1.3 Current Status of CTCs as liquid biopsy in lung cancer

CTCs have garnered a lot of attention in the past few decades. Isolation of these rare cells from the billions of blood cells has been a challenge until recent times. With the advent of new sensitive technologies that permit live cell isolation and downstream genomic analysis, the existing paradigm of CTC research has evolved to explore clinical utility of these cells. CTCs have been identified as prognostic and pharmacodynamic biomarkers in many solid tumors, including lung cancer. As a means of liquid biopsy, CTCs play a major role in the development of personalized medicine and targeted therapies. The following part of the chapter discusses the state of various isolation strategies, cell separation techniques and key studies that illustrate the application of liquid biopsy to lung cancer.

1.3.1 Background

Lung cancer is the leading cause of cancer worldwide, accounting for 160,000 deaths in the United States in 2014 [50] with a 5-year survival rate of 20% [51]. Approximately 224,000 new cases of lung cancer were reported in 2014 [51]. Smoking is the leading risk factor [52]. Non-small-cell lung cancer (NSCLC) constitutes 80% of all new lung cancer cases [53]. Over 50% of patients are diagnosed initially with locally advanced or metastatic disease with worse outcomes. Surgically resectable Stage I-III non-small cell lung cancer (NSCLC) constitutes 25% of all lung cancers [54]. Despite the performance of seemingly “curative” surgery for locally confirmed disease in these patients, more than 50% will recur in 5-years and succumb to the disease [55]. Survival is improved through screening, early diagnosis and treatment [56]. However, currently approved screening strategies involving low dose CT scans have a low sensitivity and high false positive rates of >90% [56]. There is an unmet need for additional biomarkers that can improve the sensitivity of low dose CT screening, particularly in patients with indeterminate pulmonary nodules. Following a diagnosis of lung cancer and stage specific therapy, currently, the only available techniques to monitor disease progression other than clinical symptoms, are periodic CT scans done every 3-6 months. Earlier detection of recurrence in cases of earlier stages of lung cancer (Stage I and II) is needed

to direct certain subsets of patients for treatment of oligometastatic disease; this may include surgery and/or radiation therapy. In cases of patients with more advanced lung cancers, surveillance CT scans may demonstrate progression of disease; repeat biopsies of these recurrent/progressive lesions allow us to determine the underlying resistance mechanisms, in cases of lung cancers associated with specific molecular targets [57]. This type of surveillance may miss early recurrence/resistance and identification of treatable oligometastatic disease. In addition, repeat biopsies are invasive and not without risk. There is an unmet need for earlier detection of resistance in this subgroup of patients using a minimally invasive approach, which could potentially serve as decision aid for subsequent alternative therapies targeting secondary mutations or alternative pathway activation [58, 59]. Furthermore, a better non-invasive approach for serial monitoring is necessary to address other clinical and research unmet needs, not only for early response assessment for targeted therapies, but also for novel immunotherapies where radiologic response may lag behind or be erroneous (e.g.: pseudo-progression).

Emerging research in blood-based biomarkers provides new opportunities to diagnose lung cancer earlier and to assist with detection of earlier recurrence. These biomarkers include circulating tumor cells [60] and circulating cell free nucleic acids (CfNA) [61-63]. CfNA are released from apoptotic or necrotic tumor cells [64]. Besides plasma, tumor nucleic acids have also been detected in other fractions of blood, such as platelets [65], extracellular vesicle exosomes [66], and buffy coat (leukocyte-enriched) [67]. New technologies are being developed to increase the sensitivity and specificity of cfNA detection in the blood [68]. Circulating tumor cells (CTCs), on the other hand have been extensively studied as prognostic and pharmacodynamic biomarkers in many cancers [69-73]. Both cfNA and CTCs were demonstrated to correlate with tumor burden and revealed genetic signatures of primary and metastatic tumors [27, 74]. CTC processing technologies however, have unique advantages over cfNA, by permitting a vast array of molecular and functional studies including cell culture, xenograft implantation, and *ex-vivo* drug testing (Figure 3) [75]. CTCs represent a subset of tumor cells that have acquired the ability to disseminate from the primary tumor and intravasate to the circulatory system [76]. CTCs may be a viable non-invasive alternative to tissue

biopsies for diagnosis of lung cancers. In many patients, however, CTCs are quite low in number, and they need to be isolated from an overwhelming majority of blood cells (1 CTC: 1 billion blood cells). We have reported capability of detecting and characterizing CTCs from early stages lung cancer [77]. CTCs have demonstrated utility in surveillance of patients and their changing numbers predict PFS and OS in several cancers [45, 70]. Additionally, CTCs have been proposed as surrogate biomarkers in a multitude of research areas, including the selection of neoadjuvant and adjuvant therapy, detection of recurrent disease and as pharmacodynamic biomarkers of novel therapeutics [73, 76, 78-83]. We summarize current technological and scientific advancements in CTC research specifically pertaining to lung cancer (Figure 4).

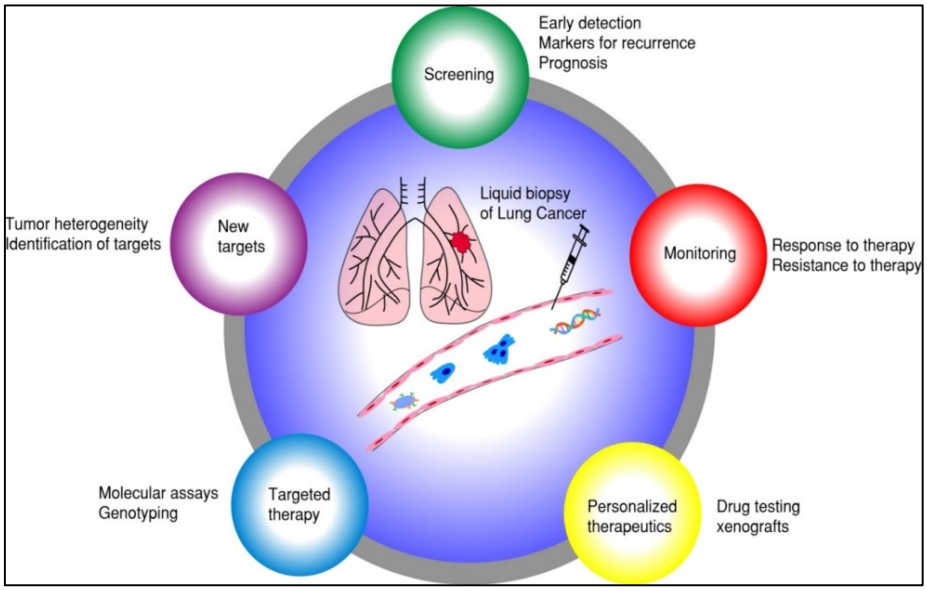

Figure 3. Liquid biopsy of lung cancer. Different aspects of using CTCs as surrogate biomarkers in lung cancer.

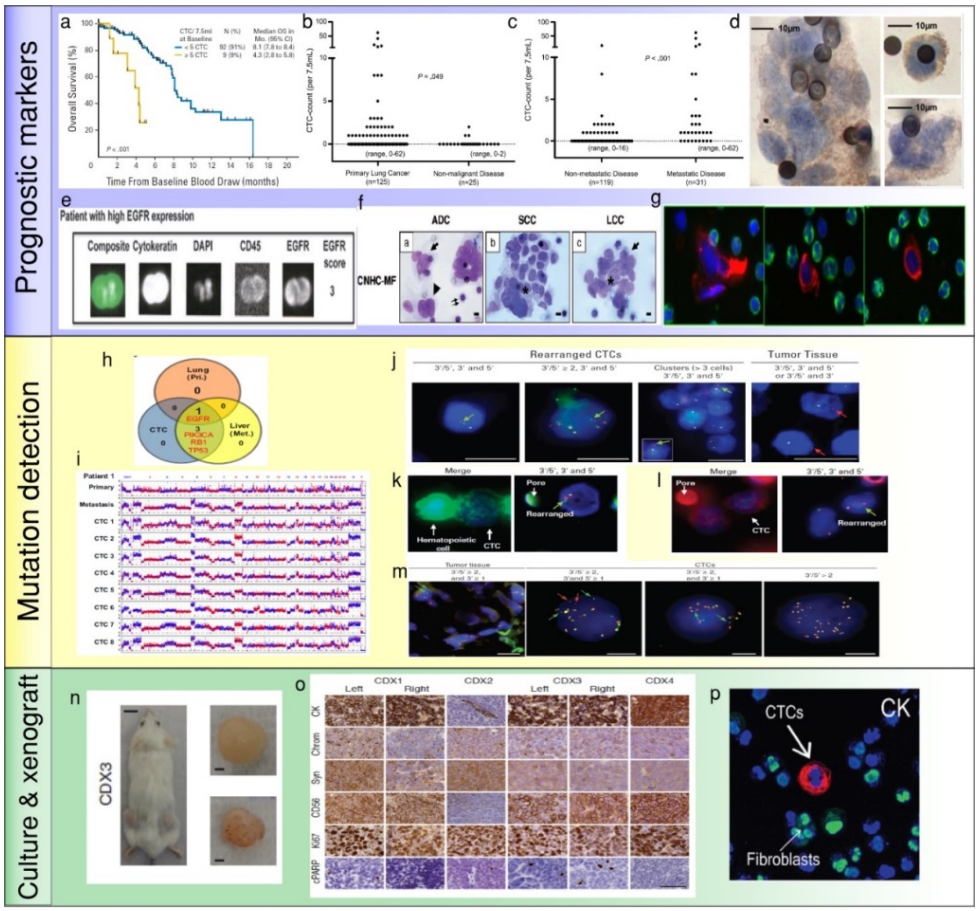

Figure 4. Application of CTCs in lung cancer. a. Less than 5 CTCs/7.5ml of blood predict improved survival by CellSearch system [70]. b and c. Higher numbers of CTCs are detected in metastatic lung cancer than cancer without distant metastasis [84]. d. NSCLC CTCs are detected by ISET technology and stained positive for EGFR [85]. e. NSCLC CTCs isolated by CellSearch system are stained positive for EGFR and CK [82]. f. Morphologic features of NSCLC CTCs [86]. g. CTCs detected by HD-CTC assay are stained positive for CK (red) and negative for CD45 (green) [87]. h and i. Mutations detected in CTCs, primary tumors and metastatic sites. Copy number variation patterns among single CTCs, primary tumor and metastatic sites [88]. j. *ALK* rearrangements in CTCs and primary tumor [89]. k and l. *ALK* rearranged CTCs are stained positive for vimentin (k) and N-Cadherin (l) [89]. m. *ROS1*-rearranged CTCs are compared to primary tumor[90]. n. CTCs isolated from SCLC patients generate xenografts [91]. o. CTC-derived xenografts are stained for different protein markers [91]. p. NSCLC CTCs are isolated and expanded by a microfluidic co-culture model and stained positive for CK [77].

1.3.2 CTC isolation technologies demonstrated in lung cancer

CTCs have now been proposed as surrogate biomarkers in over 270 clinical trials [61]. However, to date, CTCs have not been incorporated into routine clinical practice for management of patients with cancer. The efforts to identify biological relevance and clinical utility of CTCs parallel the development of CTC isolation technologies. There are several key parameters worthy of consideration when designing a method to isolate CTCs: a) specificity, b) sensitivity, c) purity, d) viability, e) throughput. All the downstream assays such as molecular and genomic analysis and culturing for *ex vivo* drug testing depend on these factors. We will discuss about pros and cons associated with current isolation technologies generally and specifically as they pertain to lung cancer (Table 2).

Technology	**Approach**	**Flow rate mL/hr**	**Recovery cell lines**	**Purity WBCs/mL**	**Patient samples**	**Whole blood**	**Genomic analysis**	**Live cells**	**Culture**	**Drug testing**
Cell Search	EpCAm coated magnetic beads	NA	>80%	Low	< 50% in breast [92] 32% in **lung cancer**, 5CTCs/7.5 ml [70]	N	N	N	N	N
Epic Sciences	No enrichment, RBCs lysed blood deposited on slides	NA	NA	None	73% in **lung cancer** [87], 55% in melanoma [93]	N	Y, single cell for copy number	N	N	N
Mag Sweeper	Flow through immunomagnetic capture		62% ± 7%		100% in metastatic breast cancer, 12CEpCs/9 mL [94]	Y, need dilution	Y	Y	N	NA
ISET	Size based filtration	NA	One CTC per 1ml of blood	NA	80% in **lung cancer** [85, 89, 95]	N	Y, FISH	N	N	N
CTC iChip	Size based separation +ve or –ve selection with mag beads	9.6	> 95% for –ve 78%-98% for +ve	>10,000 for –ve <10,000 for +ve	90% from multiple types of metastatic cancers including **lung cancer** [96]	Y, not a single step	Y, single cell RNA expression	Y	Y	Y

FACS Sorting	Surface marker based selection	Very Low	NA	Very Low	<10% [97]	Y	Y	Y	Y	N
RosetteSep kit	Depletion of WBCs	NA	NA	NA	NA [91, 98, 99]	multiple steps	Y	Y	Y	NA
CTC chip	Positive selection	1	>95%	NA	72% in **lung cancer** [77]	Y	Y	Y	Y	N
GO Chip	Nano pillars with Graphene Oxide	1-3	> 95% 2-5 CTCs	<1000	> 95% sensitivity, 10CTCs/mL [100]	Y	Y	Y	Y	N

Table 2. Comparison of CTC isolation technologies pertaining to lung cancer

Collectively, there are two major approaches; one is anti-epithelial cell adhesion molecule (EpCAM) dependent while the other is EpCAM independent. The FDA approved CellSearch technology utilizes EpCAM coated magnetic beads to isolate CTCs in a multitude of cancers in spite of limited detection efficiency (32% in lung cancer) [70, 92, 101, 102]. Microfluidic-based technologies have changed the existing paradigm for recovery of CTCs. Microfluidic chips coated with EpCAM and microfluidic systems utilizing immunomagnetic principles have been shown to capture CTCs from lung cancer samples with 100% efficiency [26, 100, 103, 104]. These antibody-based microfluidic devices have the advantages of high sensitivity, low numbers of white blood cells contamination (can be as low as 1500 WBCs), as well as preserving the viability of CTCs due to minimal handling of whole blood. The drawbacks are that they suffer from limited throughput due to low flow rates (1-3 ml/hour) and a requirement for antibody-antigen interaction. Another problem with EpCAM dependent methods is that they can only capture a subset of CTCs and miss cells undergoing the epithelial-mesenchymal transition (EMT) [61]. Wit *et al*. recovered lung CTCs by filtration from the waste of CellSearch system [105]. The percentage of patients having more than 5 cells per 7.5ml of blood increased from 15% (EpCAM positive) to 41% (EpCAM positive and negative). This suggests that including the EpCAM negative population increases CTC recovery.

In contrast, the label-free approaches for isolating CTCs do not rely on the expression of specific cell surface markers but instead on inherent CTC properties such as size, deformability, or dielectric susceptibility, and/or negative selection of WBCs [41, 106-114]. While improvements in size-based and other physical separation techniques have allowed higher throughput over the years, they suffer from limitations related to heterogeneity of tumor cells, contamination with blood cells and result in lower yield and specificity compared with the antigen-based systems [115]. For example, CTCs within a patient may have a wide range of sizes (>4 to 30 μm) and many of them may overlap in size with blood cells [116]. More recently, several new integrated platforms have emerged for CTC isolation. Liu *et al*. introduced an integrated device that separated blood cells and CTCs by deterministic lateral displacement followed by an affinity-based enrichment (9.6 ml/hour) [117]. The CTC-iChip by Ozkumur *et al*. combined magnetic labeling and high-throughput sorting of cells (8 ml/hour) [96], which was based on the principle of conjugating capturing antibodies on magnetic particles and enriching rare cells by applying external magnetic forces [118]. While EpCAM independent systems allow high throughput and an unbiased, surface-marker independent approach, which can capture cells undergoing EMT [119], the need for multiplexing and pre-processing of blood samples makes it cumbersome and time consuming. Chang *et al*. employed similar principles by labeling CTCs with antibody cocktail conjugated with magnetic beads followed by size-based filtration to trap CTCs on chip for immunofluorescence staining [120]. This system also operated at high flow rates (2ml/min) but required RBC lysis and the average WBC contamination was around 4000.

Other label-free technologies, which are not microfluidic based, are also employed in clinical evaluation of lung CTCs. The ISET (isolation by size of epithelial tumor cells) technology, isolating CTCs based on their larger size, is among the earliest EpCAM independent approaches which filter CTCs from blood cells as they pass through a membrane filter [95]. CTCs were detected in 80% of samples from stages IIIA to IV NSCLC patients using ISET compared with 23% using CellSearch [85]. Using the same approach, CTCs were present in 65% of NSCLC patients in a more recent report [121]. In another study, an automatic microscope scanning and analysis technology called high-

definition CTC (HD-CTC) assay was utilized to examine CTCs from stage I to IV NSCLC patients [87, 122]. This technology permitted high-resolution imaging of CTCs and was not biased towards size or surface markers. Recently, DNA aptamers were utilized to isolated CTCs from NSCLC patients [123]. CTCs were identified in 86% of the samples that were positive to aptamers and pan-CK. The ISET, HD-CTC assay and aptamer approach require RBC lysis and have limited purity of isolated CTCs, therefore posing constraints on molecular and functional studies of the cells.

In summary, CTC technologies have evolved rapidly over the last decade, yet there is none that has FDA approval other than CellSearch. However, to incorporate CTCs into basic as well as small cohort clinical research, there are more tools than ever before, with microfluidic devices leading the way with higher sensitivity. Any ideal CTC technology should offer high throughput, minimal handling (whole blood) that can separate live CTCs with high sensitivity and specificity. Presently, there is no single technology that is optimal for every downstream analysis; the choice of technology is driven more by the end user application and ease of accessibility to the technology. Immunoaffinity-based technologies offer both sensitivity and specificity albeit with dependence on the known biomarkers. A high-throughput system that requires minimal pre-manipulation of whole blood and that can operate with either positive selection or negative depletion approach seems to be most promising for lung cancer CTC isolation. Furthermore, the efficiency of positive selection depends on the discovery of lung cancer specific surface markers such that a cocktail of capturing antibodies can be applied to target a broader range of lung CTCs.

1.3.3 CTCs as prognostic and predictive markers in lung cancer

Previously, the oncology community believed that there was little merit in diagnosing recurrence or progression earlier in patients who had surgery for earlier stages of lung cancer or following initial therapy for locally advanced /metastatic NSCLC. This was related to poor therapy choices at recurrence/progression that often did not alter clinically significant outcomes such as progression free survival (PFS) and overall survival (OS). There has been a re-think of this approach in a small but significant

minority of patients. This relates to the emerging field of therapy directed at oligometastatic disease such as local radiation or use of immunotherapy or newer biologics that may render patient disease free for a significant amount of time, even if overall survival is not affected. Many of these therapies are also better tolerated with broader therapeutic windows. We will outline various studies relating CTCs to prognosis in lung cancer as well as studies that predict therapy response.

Hofman *et al*. used ISET technology to isolate CTCs from 208 NSCLC patients with stages I to IV cancer. Fifty percent of these patients had CTCs by morphological examination [86]. A cut-off value of >50 corresponded to shorter progression-free-and overall survival (PFS and OS). There was however, no direct correlation between numbers of CTCs and disease stage, or other clinicopathologic parameters. Therefore, CTCs and tumor staging appeared to be independent prognostic factors. In another study using the CellSearch system, there were greater numbers of CTCs in metastatic lung cancer patients ($P<0.001$) compared to patients without distant metastases [84]. Similarly, another study using the CellSearch system found that in 101 patients with Stage III/IV NSCLC, numbers of CTCs were higher in stage IV compared to stage III patients [70]. With a threshold of 5 CTCs in 7.5 ml blood, patients were categorized into favorable and unfavorable groups. Both the PFS (6.8 v 2.4 months) and OS (8.1 v 4.3 months) were higher in the favorable group than the unfavorable ($P<0.001$). Additionally, CTC numbers decreased with one cycle of chemotherapy. Reduction in numbers of CTCs with therapy correlated with improved PFS (6.9 v 2.4 months; $P=0.005$) and OS (8.8 v 3.9 months; $P<0.001$). This study highlights that CTC numbers are not only prognostic, but also that a change in CTC number with therapy predicts disease progression dynamically.

Dorsey *et al*. investigated the change of CTC number in patients with localized NSCLC undergoing radiation treatment. Using a telomerase-based detection assay, 65% of the patients were positive for CTCs prior to treatment. CTC numbers significantly reduced after radiation (9.1 CTCs per ml v 0.6 CTCs per ml; $P<0.001$). This study suggested analyzing CTC could serve as “real-time liquid biopsies” accompanying treatment to monitor tumor progression [124]. Several studies examining CTCs in advanced NSCLC patients receiving chemotherapy showed that >2 CTCs/7.5mL or any

increase in CTC numbers after therapy predicted lower OS and PFS (P=0.05) [82, 83, 125]. To improve detection sensitivity, CTCs from pulmonary vein blood were examined in patients undergoing surgery [126-128]. Compared to peripheral CTCs (2 out of 30 positive), pulmonary CTCs were present in 22 out of 30 samples before surgery (0-1122 cells/2.5ml, median, 4 cells/2.5ml) [127]. Surprisingly, the number of pulmonary CTCs increased significantly after surgical manipulation (0-1855 cells/2.5ml, median, 60 cells/2.5ml); this increase also correlated with pathological evidence of microscopic lymphatic invasion (P=0.043). Chudasama *et al*. investigated the effect of endobronchial cryotherapy on shedding of CTCs before and after the procedure in peripheral blood [129]. CTC count increased following cryotherapy in 15 out of 20 advanced stage patients (P=0.0086), which predicted poor prognosis during follow-up. In summary, these studies suggest that monitoring change of CTC numbers during therapy is prognostic for NSCLC. An increase of CTC counts may entail additional follow-up examinations.

More recently, several groups reported on the prognostic value of CTC clusters called circulating tumor microemboli (CTM) [85, 122]. Krebs *et al*. observed the prevalence of CTM by ISET technology in 43% of patients with stage IIIB/IV NSCLC [85]. In another study using HD-CTC assay, 50% of NSCLC patients with stage I to IV disease had CTM [122]. It was shown CTM can be used to diagnose lung cancer when combined with clinical and imaging data. CTMs were also observed in pulmonary venous blood of NSCLC patients [128]. Among 130 patients tested, 74% of them were positive for CTCs. CTM were detected in 33% of samples which predicted tumor recurrence and worse disease-free survival rate (P<0.01).

Other studies correlated prognosis to the presence/absence of protein expression of CTCs in NSCLC. As demonstrated by Wu *et al*., CTCs in multiple types of cancer including lung cancer harbored a mixed population of epithelial and mesenchymal phenotypes [130]. Nel *et al*. stained CTCs for both epithelial markers such as EpCAM and pan-cytokeratin (CK) as well as mesenchymal markers such as N-cadherin and CD133 [131]. Different subsets of CTC populations were identified with heterogeneous combinations of epithelial and mesenchymal characteristics. CD133 expression correlated positively with N-cadherin. The presence of these mesenchymal markers

predicted shorter PFS (2 vs 8 months, P=0.003) likely due to emergence of chemoresistant populations.

Small cell lung cancer (SCLC) accounts for 13% of newly diagnosed lung cancer. It is considered aggressive with early dissemination and poor prognosis [132]. Hou *et al*. demonstrated that CTCs were present in 85% of SCLC compared to 21% in NSCLC patients [70, 133]. Higher CTC numbers were noted in SCLC than NSCLC; > 50 CTCs/7.5ml of blood predicted shorter PFS (4.6 months vs 8.8 months; 95% CI) and OS (5.4 months vs 11.5 months; 95% CI). A reduction in CTC number after chemotherapy was associated with longer PFS (9.6 months vs 4.1 months; 95% CI) and OS (10.4 months vs 4.1 months; 95% CI). Huang *et al*. evaluated prognostic significance of CTCs in SCLC. CTCs were enumerated before and after chemotherapy [134]. A reduction of CTCs was observed in 16/26 patients after treatment. However, CTC count at baseline and the percentage change of CTCs was not statistically significantly associated with survival. A summary of the studies investigating the prognostic value of CTCs in lung cancer is shown in Table 3.

Study	**Technology**	**Sensitivity (% of patients positive for CTCs)**	**Prognostic significance**
Hofman et al. **[86]** 208 NSCLC patients Stage I to IV	ISET	50%	> 50 CTCs corresponded with shorter OS and PFS
Tanaka et al. **[84]** 125 lung cancer patients Stage I to IV 25 patients with nonmalignant diseases	CellSearch	30% in all patients 71% in metastatic patients	CTC count was higher in lung cancer than nonmalignant patients. CTC count was higher in patient with distant metastasis.
Kreb et al. **[70]** 101 NSCLC patients Stage III to IV	CellSearch	21% at baseline (32% at Stage IV, 7% at Stage IIIB)	> 5 CTCs/7.5ml blood predicted shorter PFS and OS. A reduction in CTC count after chemotherapy predicted improved survival.
Dorsey et al. **[124]** 30 NSCLC patients received radiation therapy	Telomerase-based assay	65% before RT	CTC count decreased in patients responding to to RT.
Juan et al. **[125]** 37 NSCLC patients Advanced stage (IIIB-IV)	CellSearch	24% at baseline	No significant prognostic conclusion was made
Muinelo-Romay et al. **[83]** 43 NSCLC patients Stage IIIB and IV	CellSearch	42% at baseline	> 5 CTCs/7.5ml blood at baseline predicted shorter PFS and OS. CTC count increase during chemotherapy correlated with worse PFS and OS.

Punnoose et al**. [82]** 41 NSCLC patients Advanced stage	CellSearch	76% at baseline	Reduction in CTC count after chemotherapy predicted longer PFS.
Sienel et al. **[126]** 62 NSCLC patients Stage I to III	Ficoll-Hypaque Centrifugation	18% in pulmonary venous (PV) blood	Presence of CTCs in PV blood was associated with shorter survival especially in patients with lymph node involvement.
Hashimoto et al. **[127]** 30 NSCLC patients Stage I to IV	CellSearch	73% in PV blood before surgery	CTC count in PV blood significantly increased after surgery, which predicted lymphatic tumor invasion.
Funaki et al. **[128]** 130 NSCLC patients Stage I to IV	RosetteSep kit	74% in PV blood after tumor resection circulating tumor microemboli (CTM) in 33%	The presence of CTM in PV blood predicted worse PFS.
Chudasama et al. **[129]** 20 NSCLC patients Stage III-IV	ScreenCell	25% at baseline, 75% after endobronchial cryotherapy (EC)	CTC count increased after EC.
Carlsson et al. **[122]** 104 NSCLC patients Stage I to IV 25 patients with benign diseases	HD-CTC assay	50% positive to CTM	CTM along with clinical and imaging data can serve as predictor of malignant versus benign diseases.
Pirozzi et al. **[135]** 45 NSCLC patients Stage I to III	Ficoll-Hypaque Centrifugation	24% in PV blood	No association found between presence of CTCs and prognosis.
Nel et al. **[131]** 43 NSCLC patients Stage IIB-IV	Ficoll-Paque CD45 magnetic depletion	100%	Presence of mesenchymal markers CD133 and N-cadherin in CTCs predicated shorter PFS.
Hou et al. **[133]** 97 SCLC patients	CellSearch and ISET	CTCs in 85% CTM in 32%	More than 50 CTCs/7.5ml blood predicated shorter OS. .
Huang et al. **[134]** 26 SCLC patients	CellSearch	Not reported Median CTC count at baseline is 75 (0-3430)	CTC count decreased after chemotherapy. CTC count at baseline and change of CTC numbers after treatment not associated with survival.

Table 3. CTCs as prognostic markers in lung cancer

Taken together, several studies have demonstrated the prognostic utility of CTCs in lung cancer. CTC count and change of CTC number after surgery, radiation and chemotherapy may serve as predictors of recurrence. At the current time, however, CTCs are not routinely used as prognostic or predictive markers in clinic. There are several reasons for this. Most of the previous studies used CellSearch or traditional approaches without pre-enrichment that limited sensitivity of the tests for detecting CTCs. Many of the studies had small sample sizes (<100) limiting statistical significance, which resulted in contradictory or inconclusive findings. Given newer and more sensitive technologies that allow isolation and accurate characterization of CTCs, large numbers of patients within specific stages of lung cancer need to be enrolled. Stringent biomarker studies using training and test sets will allow independent validation and reproducibility.

1.3.4 Applications of CTCs in the era of targeted therapies in lung cancer

The past 2 decades have seen a large discovery effort such that lung cancer is not considered one homogenous cancer. Over 64% of all lung cancers have an underlying driver mutation that is responsible for proliferation of the cancer and many of these mutations are mutually exclusive [136]. Nearly 30% cases of these driver-mutant lung cancers have an approved therapy (targeted therapy). The most common ones are adenocarcinomas (AC) that are associated with mutations in the *EGFR* gene or rearrangements in the *ALK* and *ROS-1* gene [137]. Additional genomic aberrations include those in *BRAF*, *AKT1*, *ERRB2*, *PIK3CA*, and fusions in *RET* [138]. Detection of mutations by biopsy may not fully reflect intra-tumoral heterogeneity [139]. In this regard, sampling CTCs as "liquid biopsy" may complement solid biopsy to inform effective targeted therapies. Liquid biopsy is also noninvasive allowing dynamic monitoring of disease progression [64].

One of the earliest investigations was identifying *EGFR* mutations in CTCs from metastatic NSCLC known to harbor these mutations. In 11 out of 12 patients, expected mutations were validated including the appearance of the resistance mutation T790M. In this study, CTC numbers paralleled radiographic response and offered first insights into genomic profiling of CTCs as a way to monitor genotypic changes during therapy [27]. Two recent studies examined *EGFR* mutation in advanced NSCLC patients. Marchetti *et al*. demonstrated that *EGFR* mutation was detected in CTCs of 84% of the patients carrying *EGFR* mutant primary tumors [140]. In 94% of the cases, mutations found in CTCs matched the mutations in tumor tissues. The unmatched mutations in CTCs and primary tumors were likely due to tumor heterogeneity between primary lesions and metastatic sites. Breitenbuecher *et al*. utilized a RT-PCR assay to detect in-frame deletions in the *EGFR* exon 19 [141]. All 8 *EGFR*-mutant patients demonstrated identical mutations in the CTCs. *EGFR* mutations were also detected from circulating DNA of advanced lung adenocarcinoma patients with 73% sensitivity [142]. Both CTCs and cfDNA can be used in future research to determine the "best in class" *EGFR* tyrosine kinase inhibitors (TKI) for individual patients.

Other studies focused on investigating *ALK* rearrangement in CTCs [89, 143]. By performing filter-adapted fluorescent in situ hybridization (FA-FISH), researchers identified unique *ALK* rearranged pattern in CTCs with mesenchymal phenotypes. This unique population of CTCs may be highly invasive, behaving as metastasis initiating cells [144]. Adapting the similar approach, *ROS1* rearrangement was investigated in NSCLC CTCs and compared to tumor biopsy specimens [90]. Among 4 patients tested, CTCs harbored similar split patterns as tumors but exhibited an increase in *ROS1* copy number. The number of *ROS1* rearranged CTCs increased in one patient who didn't respond to crizotinib treatment. In another study, whole-genome amplification of single CTCs from lung cancer patients was performed followed by analyzing copy number variation (CNV) in addition to somatic mutations [88]. It was demonstrated that CTCs obtained from the same patient exhibited similar CNV pattern but was distinguishable from CTCs obtained from a different histology of lung cancer. These studies suggest that profiling CTC genome predicts cancer progression as well as emergence of secondary resistant mechanisms, which can be further targeted by second-line therapies.

1.3.5 CTCs as biomarkers for early diagnosis of lung cancer

Sensitive detection of CTCs provides opportunities for early diagnosis of lung cancer. CTCs can be shed by primary tumor even at early stages of tumor development [145, 146]. It was demonstrated that the presence of CTCs in 5 out of 168 chronic obstructive pulmonary disease patients predicted occurrence of lung nodules 1 to 4 years after initial detection of CTCs [147]. In one study, CTCs were isolated from 84% of lung cancer patients of various stages including early stage of lung cancer (57.1%) [148]. CTCs were identified with CD45-FISH method, which was reported to increase detection sensitivity by including cells deficient in epithelial markers like CK. Two studies utilized tumor-specific ligand folate and an oligonucleotide followed by qPCR and immunofluorescence staining to identify NSCLC CTCs [149, 150]. CTCs were observed in more than 70% of all stages with 67.2% in stage I cancer. It was further demonstrated that CTCs can be more sensitive for early diagnosis of lung cancer than blood serum markers such as cyfra21-1 or CEA. More recently, one study evaluated CTCs from potential lung cancer patients to predict malignancy of the lung lesions as a way to

circumvent sampling bias by solid biopsy [151]. CTCs shared similar morphological features and histology (72%) with biopsy specimens. In stage I patients (42%), the numbers of CTCs correlated with tumor size (P=0.001). Our group also demonstrated that CTCs were detectable in early stages of lung cancer (68%) [77]. Early diagnosis of cancer aided by liquid biopsy is challenging due to low abundance of CTCs. Therefore, it is necessary to develop more sensitive and specific technologies such that more inclusive characterization methodologies will aid in early detection of lung cancer.

1.4 CTCs in esophageal cancer

Esophageal cancer is one of the least studied and most aggressive cancers worldwide. The five-year survival rate is 20% [152]. In the year 2015, 16,980 new cases and 15,590 deaths are estimated in the US [153]. Esophageal cancer has a tendency to spread early in the tumor development [154]. More than 50% of the patients have either unresectable tumor or visible metastases at the time of diagnosis. Alcohol and smoking are the risk factors for esophageal cancer [155]. Consuming extremely hot beverages frequently also increases the risk [156]. In addition, the gastroesophageal reflux disease is associated with an increased risk [157]. Clinical diagnostic methods of esophageal cancer include esophagogram and endoscopy. A computed tomographic (CT) scan, positron-emission tomography (PET) scan or endoscopic ultrasonography is used to detect invasion to the lymph nodes and other metastatic diseases [158]. Serum marker tests such as carcinoembryonic antigen and cancer antigen (CA) are normally conducted to accompany with the CT examination. However, the blood marker tests are limited with low sensitivity and specificity [159]. There is an unmet need to incorporate additional biomarkers for accurate preoperative/pretreatment staging and stratification of patients as well as post-therapy monitoring.

Several studies have investigated the role CTCs plays in prognosis and predicting treatment response in esophageal cancer. Sclafani *et al*. conducted a small pilot study of 18 patients with advanced esophageal or gastric adenocarcinoma and evaluated CTC counts in the patients during the course of chemotherapy using the CellSearch technology [160]. More than 2 CTCs were detected in 44% of patients at baseline. Recently,

Matsushita *et al*. reported a larger cohort study [161]. Ninety patients with esophageal squamous cell carcinoma (ECSS) were enrolled. Using CellSearch technology, CTCs were identified in 27.8% of patients at baseline. CTCs were evaluated in the follow-up samples from 71 patients during treatment. CTC positivity was shown to correlate with worse OS (P=0.002). A reduction in CTC number after treatment predicted partial response and positive therapeutic efficacy (P=0.034). Consoli *et al*. observed the presence of CTCs after one esophageal cancer patient developed cardiac metastasis [162]. Reeh *et al*. examined the prognostic significance of CTCs in 100 esophageal cancer patients [163]. CTC were identified in 18% patients and CTC positivity predicted worse OS (P<0.001) and tumor recurrence (P<0.001). They found that the presence of CTCs was correlated with metastatic stage (P=0.013).

To account for heterogeneous CTC populations by including cells that are negative for EpCAM, Li *et al*. recently detected CTCs using both CellSearch and ISET technologies [164]. Sixty-one patients with esophageal squamous cell carcinoma were recruited and their CTC numbers were analyzed by the two methods. CTCs were detected in 32.8% patients by ISET and 1.6% by CellSearch. CTM were observed in 4.9% patients by ISET and undetectable by CellSearch. This suggests CTC counts may be underestimated using CellSearch. Bobek *et al*. used another size-based technology (MetaCell) to detect CTCs in 43 esophageal cancer patients [165]. 62.8% of patients were positive for CTCs. The CTCs were cultured directly on the filters allowing further immunohistochemical analysis.

These studies highlight the potential utility of CTCs in monitoring tumor progression and treatment response. This is likely to help with pretreatment evaluation of patients, follow-up monitoring and predicting tumor recurrence. However, there is a discrepancy of CTC detection rate in ESCC patients between different studies, which is likely due to small cohort of patients, different tumor stages, and ethnicities. Most studies evaluating prognostic value of esophageal CTCs used the FDA approved CellSearch technology which is limited with detection sensitivity and available downstream assays [166]. Further studies need to incorporate more sensitive detection methods and esophageal cancer specific markers for CTC identification or characterization.

Chapter 2
CTC isolation by a transparent polymer based microfluidic CTC-capture device

2.1 Abstract

Microfluidic based isolation technologies offer high sensitivity and specificity due to the microscale manipulation of cells. CTCs can be positively selected by antibodies targeting cell surface antigens. One of the most widely used antibodies is the antibody against the epithelial cell adhesion molecule (EpCAM). We developed a microfluidic CTC-capture device utilizing the immunoaffinity principle. The device is made of polydimethylsiloxane (PDMS) and exhibits high optical property. The CTC-capture device consists of arrays of microposts, which enhance the interaction between fluid and surface, thereby increasing the CTC capture efficiency. We evaluated the device with H1650 and A549 cells (lung cancer cell lines). The capture yields are 100% and 50% respectively due to different level of EpCAM expression. Furthermore, the CTC-capture device successfully detected CTCs in the peripheral blood of early stage lung (68%) and esophageal (86%) cancer patients. We show that the CTC-capture device provides an effective method to identify and characterize CTCs in early stage cancer patients and contributes to early cancer detection.

2.2 Introduction

The presence of CTCs in the blood stream is prognostic for cancer patients[167]. Detecting CTCs in early stage cancer patients aids in cancer diagnosis and staging[60]. In the past decade, microfluidic technologies have been developed to enhance the isolation efficiency and specificity of rare CTCs[168]. Microfluidic devices apply low shear stress on cells with minimal damage to them. One of the major CTC detection methods is targeting antigens uniquely expressed by cancer cells but not by blood cells. Early in 2007, Nagrath *et al*. reported that the CTC-chip coated with EpCAM identified CTCs in metastatic breast, lung and prostate cancer patients [26]. This silicon based microfluidic device had limited optical property, which might hinder the subsequent characterization of CTCs. Later, an alternative strategy called the Herringbone (HB)-chip was developed to capture CTCs from patients with metastatic prostate cancer [32]. Both the CTC-chip and HB-chip utilized complex geometries in the microchannel to increase the contact between cells and antibody-coated surfaces. In the present study, we introduce a CTC-capture device using polydimethylsiloxane (PDMS), an organic polymer, and a glass slide. The CTC-capture device is transparent and of low cost. In addition, the functionalized area of the device for CTC capturing is increased compared to the CTC-chip because the glass slide is also coated with antibodies. Hence, the CTC capture efficiency is enhanced.

2.3 Methods

2.3.1 Design and computational fluid dynamic simulation of the CTC-capture device

The CTC-capture device was based on the micropost architecture originally published by Nagrath *et al.* in 2007 [26]. The dimension of the device was determined such that it can fit onto a 1 inch by 3 inch glass slide. Specifically, the channel contained one inlet and one outlet. In the middle of the channel, there were arrays of cylindrical microposts. Each post was 100μm in diameter and the array was shifted every 10 columns. The depth of the channel is 100μm. This shift helped to increase fluid-surface interactions such that cancer cells could encounter the surfaces more efficiently.

A Comsol simulation using finite element fluidic solver was conducted to demonstrate the efficiency of the post arrangement. The flow rate at inlet was 1mL/hr. Due to the memory limitation of the computer, a section of the post structure was drawn in the software only to demonstrate the fluid interactions with the posts. We evaluated the fluid flow using both the "Laminar fluid" module and the "Particle tracing" module.

2.3.2 Fabrication and functionalization of the CTC-capture device

The mold of the CTC-capture device was fabricated in the Lurie Nanofabrication Facility (LNF) at the University of Michigan. Specifically, a small amount of negative photoresist SU-8 100 (MicroChem) was deposited on one 4 inch silicon wafer (UniversityWafer). The wafer was spun initially at 500rpm for 10 seconds immediately followed by spinning at 2280-2300rpm for 60 seconds. Then the wafer was baked on a hot plate at 65 degree C for 10 minutes followed by baking at 95 degree C for 60 minutes. Then the SU-8 coated wafer was taken to expose for 18 seconds under the UV light in a MA/BA-6 Mask/Bond Aligner in the clean room of LNF. The exposed wafer was then developed in the Wet Chemistry lab at the LNF. Before developing, the wafer was baked at 65 degree C for 5 minutes followed by baking at 95 degree C for 10 minutes. The wafer was then placed in the SU-8 developer for 8 min for the SU-8 to develop. Since SU-8 is a negative photoresist, the UV exposed areas remain after developing. Therefore the micropost areas in the film mask were black and got washed away through development. The developed SU-8 mold was further baked at 150 degree C to seal the micro-cracks near the edges of the structures. Finally, PDMS polymer mixed with its curing agent was poured on the SU-8 mold. After degasing in a dessicator for 2-3 hours, the mold with PDMS was transferred to a 75 degree oven to cure PDMS overnight. The next day, the cured PDMS was cut and peeled from the mold. The PDMS containing post structures was then treated with plasma and bonded to one plasma activated glass slide. The bonded device was then placed on a hot plate at 85 degree C to reinforce the bonding.

To functionalize a device, surface chemistry treatment was conducted after bonding the PDMS to a glass slide. Specifically, immediately after hot plate treatment of the bonded device, 4% mercaptopropyltrimethoxysilane (Gelest) in 200 proof ethanol was injected into the device three times from inlet and three times from outlet followed

by incubation for 1 hour. Then, silane was washed away with pure ethanol. 280ng/µL N-gamma-maleimidobutyryl-oxysuccinimide ester (GMBS) (Thermo Scientific) was then injected into the device three times from inlet and three times from outlet followed by incubation for 30 minutes. Then GMBS was washed away with ethanol. 100µg/ml of NeutrAvidin (Invitrogen) was then injected to the device. The device can be used after 1 hour of incubation in NeutrAvidin or it can be stored at 4 degree C for up to months before the solution was dried up. Figure 5 demonstrates the fabrication and surface treatment process. Biotinylated antibody in 1% bovine serum albumin (BSA) (Sigma-Aldrich) solution was injected into the device. It was achieved by injecting from the inlet and incubating for 30 minutes followed by injecting from the outlet and incubating for another 30 minutes. Finally, 1mL of 3% BSA solution was flowed through the device at 3mL/hr. The device was ready to flow with blood for CTC capturing.

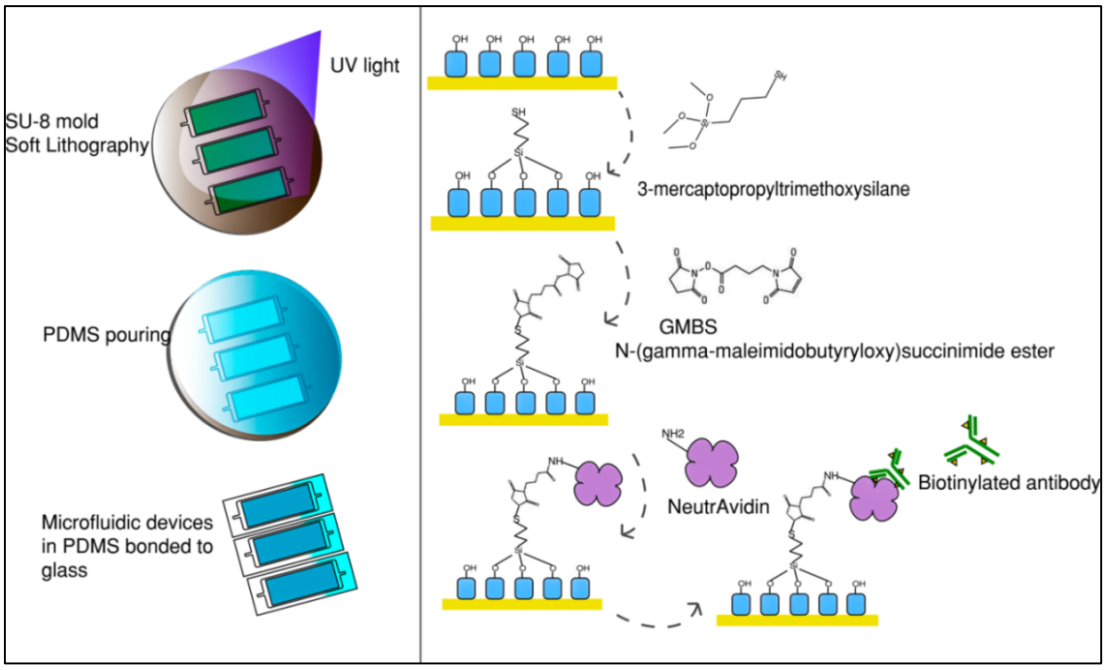

Figure 5. Process of device fabrication and functionalization. A SU-8 mold is fabricated using soft-lithography method. After the PDMS is bonded to a glass slide, silane is first reacted with plasma activated glass and PDMS, then GMBS is reacted with silane and serves as a linker molecule. NeutrAvidin is then applied to link to GMBS and finally the biotinylated antibody is attached.

2.3.3 Preparation of spiked cells

To characterize the capture efficiency of the device, known numbers of cancer cells were spiked into phosphate buffered saline (PBS) or whole blood drawn from healthy donors. The spiked cancer cells were prepared as follows. Cultured cancer cells were trypsinized and pre-labelled with CellTracker Green CMFDA Dye (Invitrogen). Specifically, cell pellets were washed one time in PBS followed by re-suspending in 5mL of serum free medium. Each vial of the CellTracker dye was dissolved in 10μL of dimethyl sulfoxide (DMSO). 5μL of the CellTracker dye solution in DMSO was then added to the 5mL of serum free medium containing cancer cells. The cells were then incubated at 37 degree C for 30 minutes. After that, the cells were washed twice in 5mL of PBS and re-suspended in complete medium followed by incubating at 37 degree C for another 30 minutes. Then the cells were washed two more times in PBS. Finally 1000 or 100 cells were counted either using a hemocytometer or by spot counting under a fluorescence microscope. The cells were spiked into 1mL whole blood or PBS to complete the preparation procedure.

2.3.4 Cell capture experiments

Typically, 1mL of the sample containing spiked cancer cells was flowed through the EpCAM coated device at 1mL/hr for CTC capturing. The device was then washed with PBS at 10mL/hr for 10mL to get rid of non-specifically bound cells. 1mL of 4% paraformaldehyde solution was then flowed through the device at 3mL/hr to fix the captured cells. After the labelled cancer cells were captured and fixed. 1mL of 0.2% triton solution in PBS was flowed through the device followed by flowing 1mL of DAPI solution into the device to stain nucleus of the cells. After that, the device was ready to be imaged and scanned under a fluorescence microscope with an automated moving stage. Normally there would be around 800 images acquired under a 10X objective. Each image was reviewed and captured cancer cells were enumerated. The capture efficiency was calculated by dividing this number by the initial spiked cell number. Each experiment was performed in triplicate.

2.3.5 Immunofluorescence staining of captured cancer cells on chip

To test the on-chip immunofluorescence (IF) staining protocol, unlabeled cancer cells were counted and spiked into whole blood. Specifically, after the captured cells were fixed and permeabilized. 1mL of 2% normal goat serum and 3% BSA solution was flowed through the device to block the cells for 1 hour. Then 1mL of 5 μg/mL of cytokeratin 7/8 (CK 7/8) (CAM5.2, BD) and CD45 (HI30, BD) was flowed through the device at 3mL/hr and incubated for 1 hour. After that, primary antibodies were washed by PBS at 10mL/hr for 3 mL followed by applying secondary antibodies, goat anti-mouse IgG2a-AF546 and goat anti-mouse IgG1- AF488, at 1:200 dilution for 1 mL in 1% BSA. The secondary antibodies were incubated in device for 1 hour followed by washing with 3mL PBS. Finally, 1mL of DAPI solution was flowed through the device and incubated for 30 minutes. The device was washed again with 3mL of PBS and could be scanned with microscope or stored at 4 degree C.

2.3.6 Acquisition of blood samples from early stage cancer patients

The CTC-capture device was tested with patient samples from early stage lung and esophageal cancer patients. Peripheral blood samples were drawn from cancer patients prior surgery at University of Michigan Hospital under an IRB-approved protocol. All patients involved in this study had surgically resectable early stage cancers. Upon CTC isolation, the devices were IF stained with antibodies for enumerating CTCs. The staining method is the same as the one described in the cell line experiments.

2.4 Results

2.4.1 The CTC-capture device

The design and appearance of the CTC-capture device is shown in Figure 6. Figure 6a is an AutoCAD drawing demonstrating the arrangement of the microposts. The surface area of the device is greatly enhanced with the post structures. Figure 6b is a SEM image of the microposts. In addition, Figure 6c is an actual CTC-capture device with blood running through the device. The Comsol simulation shown in Figure 7 demonstrates the fluid interaction with the microposts. Because of the column-shift,

streamlines are shifted periodically to enhance the interaction between fluid and microposts. The interaction enables CTCs to come closer to the surface and get specifically captured by the antibodies coated on the surface. This is simulated by "Particle Tracing" module in Comsol, which demonstrates how the particles are stuck by the post structures in the channel.

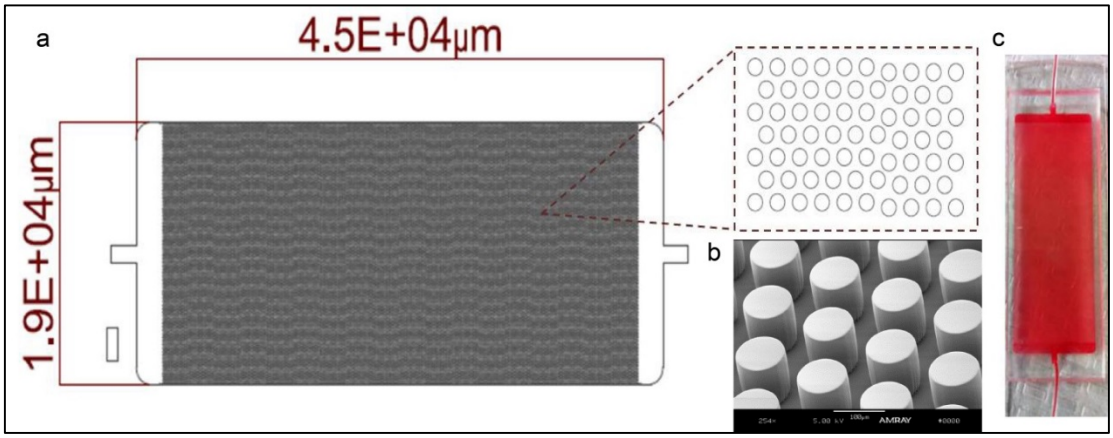

Figure 6. The CTC-capture device. a. The post arrangement is drawn with AutoCAD. b. Post structures are imaged with the Scanning Electron Microscope. c. An actual device made of PDMS is running with whole blood.

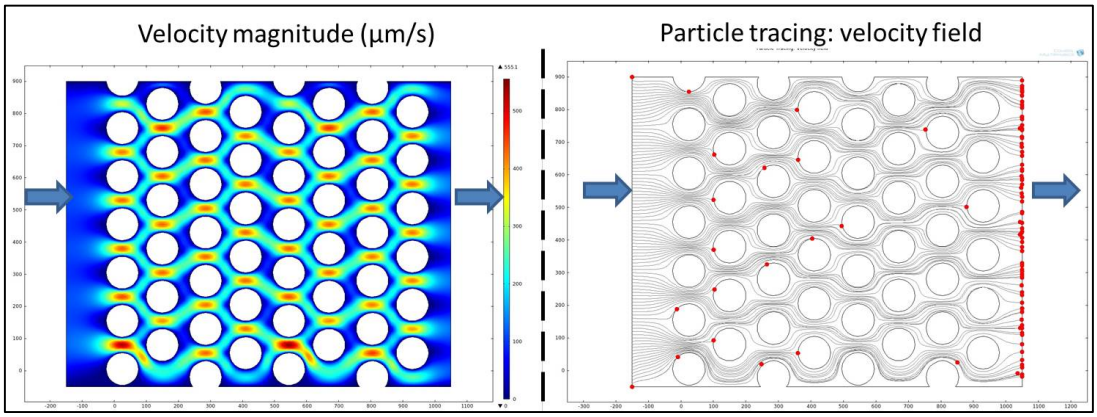

Figure 7. Comsol simulation of the micropost structures. Fluid simulation is performed to show the velocity field and particle tracing of the post arrangement inside the microfluidic device.

2.4.2. Characterization of the CTC capture efficiency using cancer cell lines

Figure 8 demonstrates the capture yield of two different lung cancer cell lines. H1650 cells express EpCAM abundantly (10^6 markers/cell) while A549 only have moderate (10^4 markers/cell) EpCAM expression [169]. The capture efficiency of H1650 was 87% at a 10 cells/mL concentration and almost 100% at concentrations of 100 and 1,000 cells/mL of whole blood. The capture efficiency was lower in PBS because the cell-surface interaction was enhanced by blood cells. The capture efficiency of A549 was lower than H1650, around 60% with 1000 cells and 50% with 100 or 10 cells. This was due to lower EpCAM expression. The immunofluorescence images demonstrate that cancer cells are specifically captured by the micropost structures. The device exhibits good optical properties for acquiring images of high quality, which is demonstrated by the confocal microscopy images shown in Figure 8c. To distinguish cancer cells from blood cells for CTC enumeration, the captured H1650 lung cancer cells were immunofluorescence (IF) stained for CK 7/8(green), white blood cells were stained for CD45 (red) and nuclei were counterstained for DAPI. These results demonstrate that the CTC-capture device can reliably isolate CTCs from whole blood with high sensitivity and efficiency even for low numbers of cells.

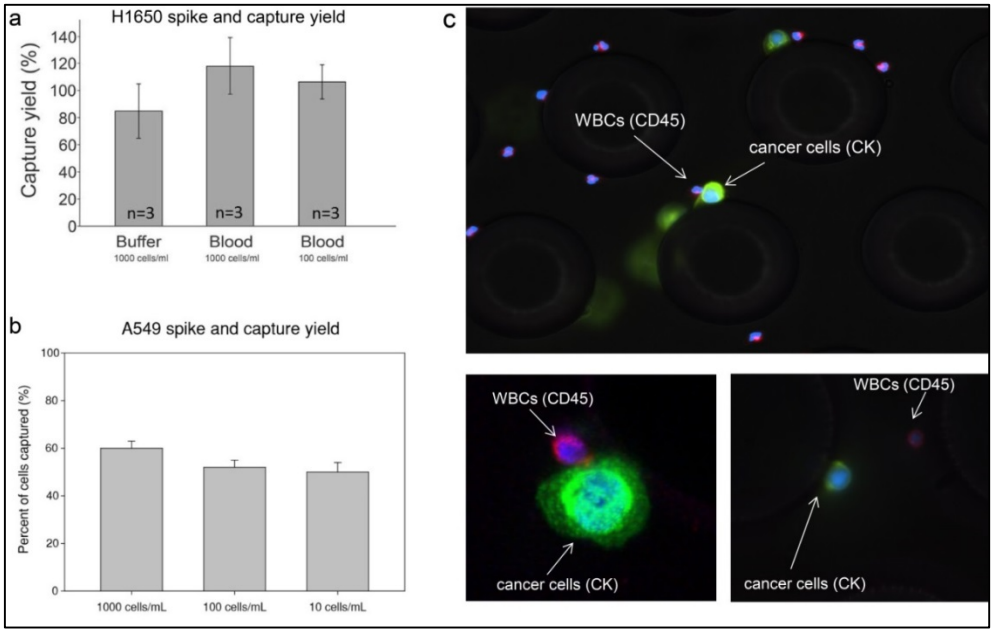

Figure 8. Characterization of the CTC capture device with cancer cell lines. a. Capture yield of H1650 lung cancer cell lines spiked in buffer or whole blood; b. Capture yield of A549 lung cancer cell lines spiked in whole blood; c. Immunofluorescence staining of the captured H1650 lung cancer cells in the device, CK(green), CD45(red).

2.4.3 Isolation of CTCs from patients with early stage lung and esophageal cancers

After the CTC-captured device was tested with cancer cell lines and demonstrated high capture efficiency, we evaluated the device with actual patient samples, which were peripheral blood samples from early stage lung and esophageal cancer patients. We observed the CTC numbers ranged from 1-11/mL (mean=4, median=3, SD=3) in lung cancer patients and 1-21/mL (mean=8, median=6, SD=6) in esophageal cancer patients. CTCs were identified in 68% of lung cancer patients (total=19, positive=13) and 86% of esophageal cancer patients (total=14, positive=12), whereas none of the healthy volunteers (n=7) showed CK positive cells greater than 2/mL (Figure 9). Figure 10 demonstrates the stained CTCs recovered from lung and esophageal cancer patients. The patient CTCs were identified as CK (red) positive and CD45 (green) negative cells.

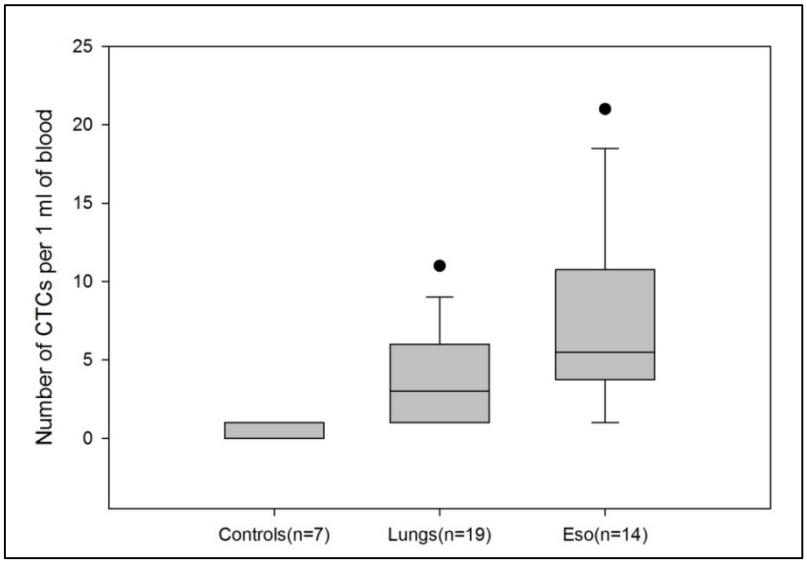

Figure 9. Number of CTCs captured from 1mL peripheral blood of healthy controls, NSCLC cancer patients and esophageal cancer patients. Healthy controls (n=7), mean=0.6; lung cancer patients (n=19), mean=4; esophageal cancer patients (n=14), mean=8. CTC positive samples are determined as >2 CTCs/mL.

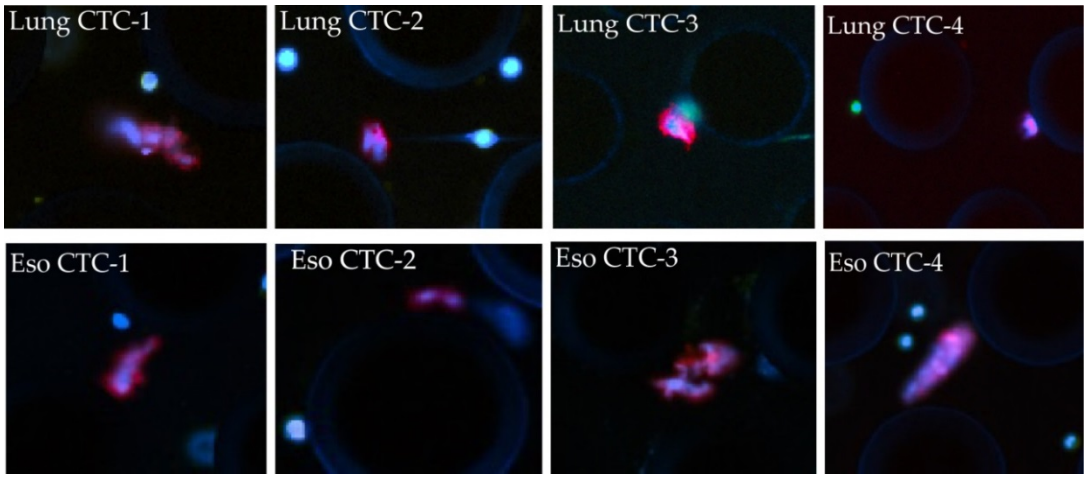

Figure 10. A gallery of captured CTCs from lung and esophageal cancer patients. CTCs are stained with CK(red) and CD45 (green). CTCs are identified as CK positive and CD45 negative cells. White blood cells are CK negative and CD45 positive.

2.5 Discussion

We developed a CTC-capture device to specifically isolate CTCs using immunoaffinitiy-based approach. The micropost structures enhance the fluid and surface interactions. Based on the spiked cell results, we demonstrate the CTC-capture device isolates CTCs with high yields. The capture efficiency of H1650 was nearly 100%, and A549 was 50% due to the low level of EpCAM expression on the cells. To circumvent this problem, other capturing antibodies such as those against epidermal growth factor receptors (EGFR) and CD133, a stem cell marker, can be incorporated in the future to enhance the capture efficiency. The ability of isolate CTCs with high specificity and efficiency depends on the choice of detection technologies. Microfluidic devices have emerged to provide versatile platforms to isolate CTCs with high sensitivity and purity. Building upon the previous published CTC-chip technology, the present CTC-capture device offers advantages such as enhanced optical property, biocompatibility and low cost. These improvements will facilitate its translation from bench to bedside in the future.

Shedding CTCs by primary tumors can be an early event in tumor development [20]. Previous studies have demonstrated that CTCs can be detected in patients with early stage cancers [149, 150]. In this study, we also observed CTCs were identified in patients

having early stage lung and esophageal cancers. The isolated CTCs were either single cells or cell clusters. Although our study is limited to a small number of patient samples and the CTC numbers vary substantially between samples, the present study indicates the possibility of detecting CTCs in large cohorts and monitoring the change of CTC number during treatment. Isolating CTCs can have vast implications in cancer diagnosis, prognosis and assist with early lung and esophageal cancer detection.

Chapter 3
Three-dimensional microfluidic co-culture model for the expansion of CTCs

3.1 Abstract

Microfluidic devices have been demonstrated as *in vitro* systems for cell culture. The microsystems handle small volumes of materials and allow dynamic control of the cellular environment. Here, we developed a multi-inlet microfluidic device that could pattern cancer cells and stromal cells using laminar flow. The patterned cells were cultured in a mix of collagen and Matrigel representing a tumor microenvironment, which allows the study of cell-cell communications. The microfluidic co-culture methodology was further applied to culture CTCs on chip. The motivation of culturing CTCs comes from the need to increase CTC yield for downstream assays, especially in the early stage cancer patients. Using the three dimensional co-culture model, a tumor microenvironment was simulated to support tumor development. CTCs were isolated and expanded from 14 of 19 lung cancer patients and 10 of 14 esophageal cancer patients. All of the cancer patients had surgical resectable tumors. Expanded lung CTCs carried mutations of the *TP53* gene identical to those observed in the matched primary tumors. Next-generation sequencing further revealed additional matched mutations between primary lung tumors and CTCs of cancer-related genes. This strategy sets the stage to further characterize the biology of CTCs derived from patients with lung and esophageal cancers, thereby leading to a better understanding of these putative drivers of metastasis.

3.2 Introduction

3.2.1 Cell patterning and culturing by microfluidic platforms

Polydimethylsiloxane (PDMS) has become a standard material for microfluidic research community due to its ease of fabrication, versatility for making various geometries, and compatibility with imaging. PDMS-based microfluidic platforms have also been utilized to culture mammalian cells *in vitro*. PDMS permits gas exchange, which is essential for cells to grow. Although there are some concerns about PDMS absorbs hydrophobic molecules in culture such as estrogen, it has been widely used as the material to construct microfluidic devices for cell culture [170] and the adverse effect on cells is minor. The motivation of culturing cells in a microfluidic device is the ability to control the cellular microenvironment through spatial and temporal gradients [171]. In addition, cells can be patterned to study the dynamic interplay between different cell types. Compared to conventional cell culture techniques, microfluidics provides a better approximation to cellular environment by precisely controlling concentration gradients, extracellular matrix components and cell-cell interactions [172].

In the tumor microenvironment, there are the surrounding non-malignant cells and extracellular matrix (ECM). The tumor microenvironment plays a dynamic role during tumor progression, which evolves from tumor inhibiting to promoting. Cancer cells and surrounding stromal cells communicate through paracrine signaling pathways such as the transforming growth factor beta (TGFβ), epidermal growth factor (EGF), colony stimulating factor 1 (CSF1), C-X-C chemokine receptor 4 (CXCR4) and stromal cell-derived factor 1 (SDF1 or CXCL12) [173]. These pathways are important for cancer proliferation and invasion. Understanding the tumor microenvironment will have vast implications in drug development and screening.

In this present study, we created a multi-inlet microfluidic device to pattern cancer cells and fibroblasts, which are the major component of cancer stroma [174]. This allows us to visualize the interaction between the two cell types. This proof-of-concept study demonstrates the feasibility of using microfluidic devices to culture cells and study tumor microenvironment *in vitro*.

3.2.2 Ex vivo expansion of CTCs

Studies indicate that CTCs are useful prognostic and predictive markers of recurrence and survival in patients with solid cancers, including lung and esophageal cancer [27, 70, 84, 133, 175-178]. CTCs may serve as reliable biomarkers for detecting cancer recurrence earlier than other commonly used approaches, such as radiographic imaging. By the time metastasis is clinically or radiographically apparent, the tumor burden is too high for available therapies to cure the cancer. Studies in advanced lung and esophageal cancer and other malignancies show that elevated numbers of CTCs are associated with reduced progression free and overall survival [179]. However, these studies also emphasize that not all CTCs lead to metastasis. It is crucial to identify the CTCs that are capable of metastasis from the ones that are mere "passengers" in order to specifically target the former. Importantly, identifying specific genetic signatures in CTCs, the earliest cells with metastasis-initiating capability, will provide new therapeutic targets. However, to achieve this, one needs to characterize CTCs from early cancers at a molecular and genomic level.

In this study, an immunoaffinity-based CTC-capture device was utilized and applied it to early stage lung and esophageal cancer. To overcome rarity of CTCs that limits characterization for clinical utility, these CTCs were isolated and further cultured on chip. To date, culturing of CTCs has only been demonstrated by a few groups, albeit in CTCs recovered from animal models or in a few patients with advanced cancers, where the likelihood of finding higher numbers of CTCs was greater [37, 97, 180]. Different from these previous approaches, and as opposed to culturing CTCs off devices, here the captured CTCs were cultured directly on microfluidic chips. It is only after CTCs are expanded on-chip for a long period of time that they are released for subculture or downstream analysis. To facilitate CTC expansion, tumor associated fibroblasts (CAFs) along with extracellular matrix (ECM) proteins are introduced to construct a tumor microenvironment conducive for CTC growth (Figure 11). We demonstrate that rare CTCs from early stage cancers can be expanded for functional studies such as invasion and tumor spheroid forming assays, as well as sequencing of cancer related genes enabling comparison between CTCs and primary tumor cells.

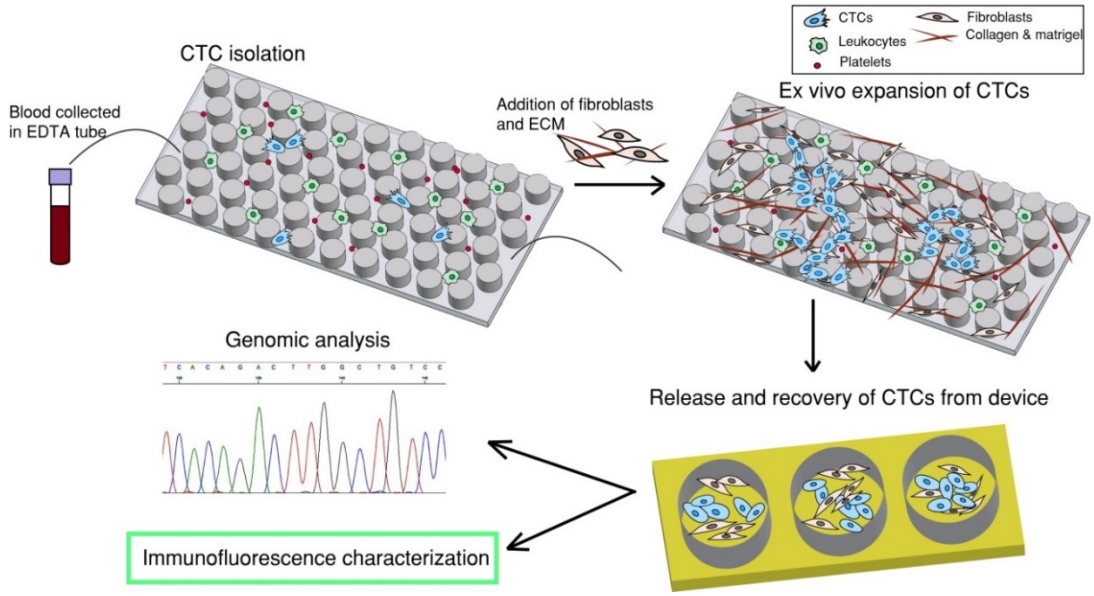

Figure 11. Overall strategy of the 3D microfluidic co-culture model for CTC culturing. The first step is to capture CTCs by flowing patient blood sample through a CTC-capture chip. The second step is to introduce fibroblasts and extracellular matrix (ECM) to the same chip to establish a co-culture environment for *ex-vivo* expansion of CTCs. The third step is to release and recover CTCs from device and the fourth step is downstream characterizations.

3.3 Methods

3.3.1 Design and fabrication of the multi-inlet microfluidic cell culture device

The microfluidic device consisted of three inlets, which were merged to form a middle channel for patterning different types of cells side by side. At the end of the middle channel, there was one outlet. The dimension of the device was determined such that the whole device can be fitted onto a 22mmx22mm cover glass. Each device bonded with a cover glass can be put into one well of a 6-well plate. The inlets were punched with a biopsy punch of 3.5mm in diameter. The big ports served as reservoirs of cell suspension and cell culture medium. The outlet was initially punched with a 0.75mm diameter punch to apply vacuum for establishing the laminar flow. After the cells were patterned and settled down in the device, the outlet was again punched with the 3.5mm punch and served as a reservoir for medium exchange. One completed device needed to

be autoclaved before adding cell suspension. This ensured the culture was free of contamination.

3.3.2 Fluorescein bead testing

To test the patterning efficiency of this device, solution containing fluorescein beads was applied in the middle inlet while the other two inlets on the sides contained plain PEG-800 solution. Specifically, 50μL of 100mg/mL PEG-800 solution in PBS was added to the left and right ports. 50μL of 200mg/mL PEG-800 solution mixed with 0.45 μm fluorescein bead solution (1:1 volume ratio) was added in the middle port. The reason to use PEG-800 solution was that it shared the same viscosity as the cell suspension in Matrigel.

3.3.3 Experimental methods for cell patterning and culturing in the multi-inlet microfluidic device

The human mammary fibroblasts (HMFs) were added to the left and right inlets while the MCF7 cells were loaded in the middle inlet. Both types of cells were suspended in Matrigel (50% by volume) (BD Bioscience) on ice and they were patterned in the middle channel after applying vacuum by a syringe pump. After that, the device was placed in one 6-well plate and was incubated at 37 degree C for 30 minutes to let the Matrigel set. Then medium was added to the inlet and outlet ports to replenish nutrients and exchange waste. Medium was changed every other day. The culture was maintained till cells grew to confluency. IF staining was performed to visualize cancer cells and fibroblasts on chip.

3.3.4 Co-culture techniques for CTC expansion

GFP-tagged A549 (Cell Biolab) and H1650 cells were spiked into whole blood and flowed through the CTC-capture device. One hundred H1650-GFP cells were captured and cultured in the device. Different cell culture environments were tested and compared: 3D co-culturing: 10^5 cancer associated fibroblasts were mixed with 0.97 mg/mL collagen I (BD Bioscience) and 50% Matrigel (BD Bioscience) [181]. The final concentration of collagen I was 0.77 mg/ml. 3D mono-culturing: only the collagen I and

Matrigel mixture was added. 2D co-culturing: only fibroblasts were added. 2D mono-culturing: neither fibroblasts nor gel was added. These experiments were conducted in triplicate for each culturing condition. Collagen, Matrigel and fibroblasts were flowed into the device at a flow rate of 1 mL/hr for a total volume of 200 µl. A scanning electron microscopy image was taken to illustrate the 3D co-culture environment on chip. A proliferation EdU assay (Invitrogen) was carried out to evaluate the proliferation potential of the cultured cancer cells on day 7 in device.

3.3.5 GFP lentivirus transfection of CAFs

CAFs need to be pre-labelled with GFP vectors so that they can be distinguished from the cancer cells after expansion. To label the CAFs, 2X GFP lentivirus was added to each well of one 6-well plate containing around 1000 CAFs and incubated overnight. The next day, viral medium was exchanged with fresh complete medium. The transfected CAFs were cultured till confluency. Finally, the labelled CAFs can be sorted by flow cytometry to select the most expressing populations and to be cultured further for the chip experiments.

3.3.6 CTC expansion with early stage lung and esophageal patient samples

Peripheral blood samples were drawn from early lung and esophageal cancer patients at University of Michigan Hospital under an IRB-approved protocol. Blood specimens from healthy donors were collected according to a separate IRB. The blood sample from each patient was divided equally into 1-1.5mL aliquots and run through 3-4 devices. One device was IF stained for counting CTC numbers on day 0. The remaining devices were used for CTC culturing. To culture CTCs, a mixture of cancer associated fibroblasts-GFP, collagen I and Matrigel was added into the devices. Each device was then incubated in a 37 degree, 7.5% CO_2 incubator for 30 minutes to facilitate gel formation. After that, medium was added to the device for culturing up to 7 days. Medium was RPMI complete medium (10% FBS and 1% Penicillin/Streptomycin).

3.3.7 CTC release and recovery

After 7 days of on-chip culture, cells were released from the device by first incubating with collagenase for 4 hrs and then 0.25% trypsin/EDTA at 37 degree in a 7.5%

CO_2 incubator for 30 minutes. Then cells were flushed outside the device with media at 10 mL/hr flow rate for 3 mL totally. Around 90% of the cells were released from the device. The recovered cells were re-seeded in a well plate and cultured for an additional 7-14 days.

3.3.8 Immunofluorescence cell staining

Cells in well plates were fixed with 4% PFA and permeabilized with 0.1% Triton in PBS. The cells were then blocked with 5% normal goat serum and 1% BSA in PBT solution. Cells were later immunostained with CK7/8 or TTF-1 (Santa Cruz Biotechnology) or Ki67 (Invitrogen) as well as the corresponding secondary antibodies. The CK7/8 positive cells were enumerated. After FACS sorting, CTCs were stained with EGFR (Cell Signaling) and pan-CK (Biolegend).

3.3.9 Spheroid formation assay

CTCs together with fibroblasts cultured in well-plates were trypsinized, counted and re-suspended in a mix of collagen and Matrigel at a concentration of 10^6 cells/mL. Two hundred μL of gel plus cell suspension was added to one well of a 48-well plate following with incubation at 37 degree and 5% CO_2 for at least 30 min. Then 300 μL of culture medium was added to each well, which was then allowed to culture. After culturing, the plate was stained with crystal violet in methanol for imaging.

3.3.10 Invasion assay

Invasion assay was performed with a 24-well transwell plate (Corning). Three CTC samples, pure fibroblasts, one H1650 lung cancer cell line were seeded at 1×10^5 cells in 100 μl medium in the upper units of 8-μm-pore transwells coated with thin Matrigel. Fibroblast conditioned medium was added to the bottom well. After 24 hr incubation at 37^0C, cells in the upper chamber were removed and invaded cells on the lower surface of the porous membrane were fixed with methanol and stained with crystal violet.

3.3.11 RNA extraction and RT-PCR

CTCs cultured in well plates, primary tumor tissue samples as well as controls underwent RNA extraction using the RNeasy Mini Kit (Qiagen). Subsequently, cDNA

was made from the extracted RNA using the High Capacity cDNA Reverse Transcription Kit (Invitrogen). RNA samples isolated from primary tumors, CTCs, positive and negative controls were first converted to cDNA and then preamplified for marker genes of interest using Cells to Ct Kit (Ambion, Life Technologies) with some modification. Finally, preamplified cDNA samples were analyzed for mRNA expression of *CK8, CK18, TTF1, EGFR, β-Catenin, CD45* (marker of WBCs), *GAPDH* and *β-Actin* (housekeeping gene) using TaqMan probes and Gene expression kit (Applied Biosystems) on ABI 7900HT instrument (Applied Biosystems). Data was normalized to expression level of *GAPDH* or *β-Actin* and reported as fold change in expression level among different tested samples.

3.3.12 TP53 sequencing

cDNA from both primary tumors and corresponding CTC samples was PCR amplified with *TP53* primers using Expand High Fidelity PCR System (Roche). The primer sets used in this study that flanked mutated *TP53* fragments were as followings: TP53f1 5'>3' GCTCCGGGGACACTTTGCGTTCG and TP53r1 5'>3' GCAGCGCCTCACAACCTCCGTCAT, flanking bp 105 to 730 of *TP53* gene (of NCBI ID NM_000546), and TP53hsF 5'>3' CCCCCTCCTGGCCCCTGTCATCTTC and TP53hsR 5'>3' TGTTGTTGGGCAGTGCTCGCTTAGTG, which flank the mutation hot-spot region of *TP53* at bp 465 to 1136. The PCR products were characterized with gel electrophoresis and then purified using PCR Purification Kit (Qiagen). The concentration of the purified PCR products was measured and diluted for sequencing. The sequencing was performed at the University of Michigan sequencing core facility.

3.3.13 DNA extraction from FFPE tumor tissue and sequencing

Four regions of distinguishable cancer cells were marked in one FFPE slide stained with H&E reagent provided by Department of Pathology at University of Michigan Hospital. Fixed tissues were scraped from 4 identical slides and collected into 4 different microtubes. Tissue DNA was extracted by the QIAamp DNA FFPE Tissue Kit (Qiagen). DNA of CTCs was extracted by the QIAamp DNA Mini Kit (Qiagen). Extracted DNA was PCR amplified using Expand High Fidelity PCR System (Roche). Table 4 summarizes the primer sets used in this study. The PCR program used is shown

in Figure 12. The PCR products were characterized with gel electrophoresis and then purified using PCR Purification Kit (Qiagen). The concentration of the purified PCR products was measured and diluted for sequencing. The sequencing was performed at the University of Michigan sequencing core facility.

Primer pairs (5'→3')	Direction	Region amplified	Product length
ttcaactctgtctccttcct	F	exon 5	248bp
cagccctgtcgtctctccag	R	exon 5	
gcctctgattcctcactgat	F	exon 6	181bp
ttaacccctcctcccagaga	R	exon 6	
aggcgcactggcctcatctt	F	exon 7	177bp
tgtgcagggtggcaagtggc	R	exon 7	
ttccttactgcctcttgctt	F	exon 8	231bp
aggcataactgcacccttgg	R	exon 8	

Table 4. DNA primer sets of exon 5, 6, 7 and 8 of *TP53* gene. These sets are obtained from International Agency for Research on Cancer (IARC) *TP53* database.

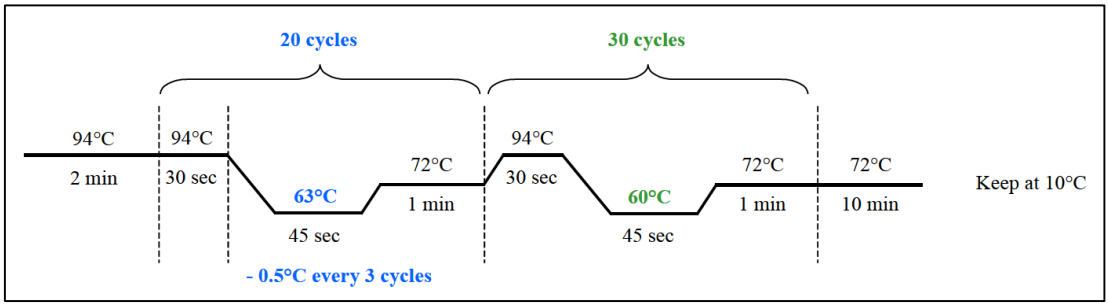

Figure 12. PCR program used for amplifying exon 5, 6, 7 or 8 of *TP53* gene. This program is obtained from IARC *TP53* database.

3.3.14 Next-generation sequencing

RNA was extracted from CTCs and primary tumor and made into cDNA. Genes of interest were PCR amplified and sequenced using mixed primers from Qiagen comprehensive cancer panel for 124 cancer-related genes. Sequencing was performed with Illumina by core facility at the University of Michigan. Sequencing raw data was generated initially by Qiagen online informatics platform, and analyzed by Bioinformatics core facility. Called variants were filtered based on Fisher strand, allele frequency, mean read depth and mapping quality. All filtered variants were classified

based on their position relative to transcript. Following classification, any variant detected in a gene not targeted by the gene panel and present in 1K Genomes data set at a frequency greater than 1% was removed. Variants appeared in healthy controls and pure fibroblasts were removed. All filtered variants were finally validated by viewing in Genome Browser for accuracy.

3.4 Results

3.4.1 Patterning cancer cells and fibroblasts by the multi-inlet microfluidic device

Figure 13 demonstrates that when applying vacuum at the outlet, the fluorescein bead solution is centered in the middle stream flanked by two plain streams on the sides. This shows that the multi-inlet microfluidic device can pattern cells in a side-by-side fashion. The device was tested with two cell lines, MCF7, a breast cancer cell line, and HMFs, human mammary fibroblasts. HMFs acted as the stromal cells in the tumor microenvironment. As shown in Figure 14, MCF7 cells are stained positive for CK (red) while HMFs are stained for cytoskeleton proteins specific to fibroblasts (green). MCF7 cells tend to form spheroids because they are cultured in Matrigel, a 3D environment. These results demonstrate that cancer cells and stromal cells can be cultured in a microfluidic device in a controlled fashion. The patterned cells can be characterized with immunostaining to visualize their interaction.

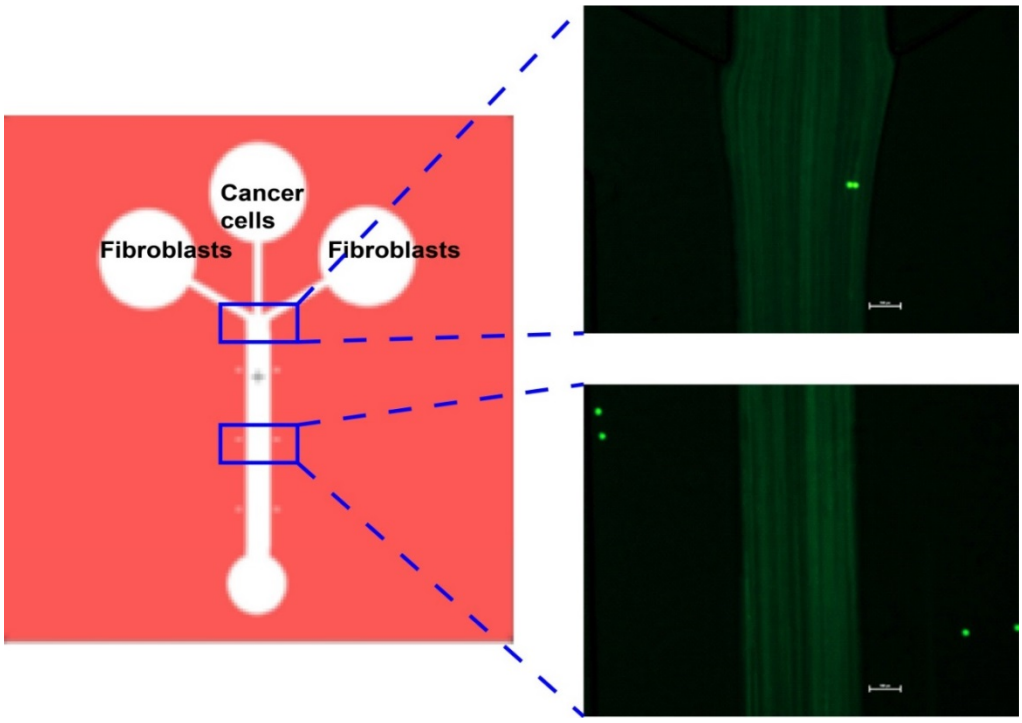

Figure 13. The design of the multi-inlet microfluidic device. The device consists of 3 inlets and 1 outlet. On the right, two fluorescent images demonstrate that if applying fluorescein beads in the middle inlet while adding plain solution in the other inlets, the beads will be confined in the middle of the laminar stream.

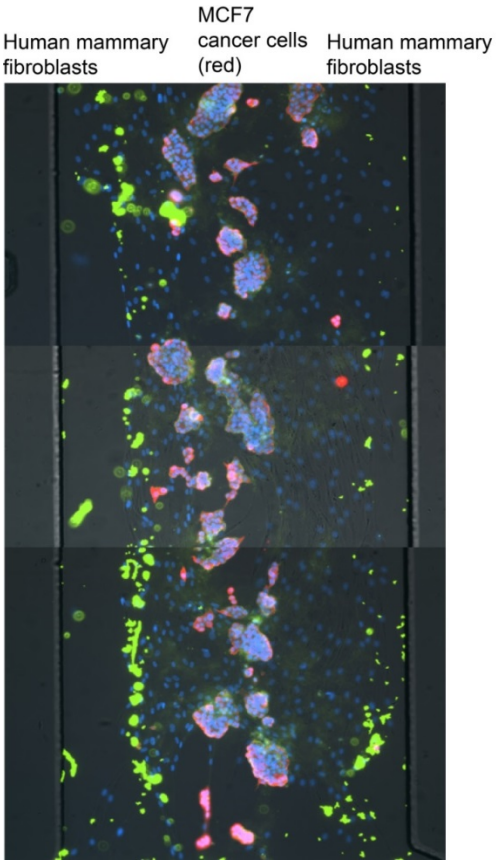

Figure 14. MCF7 cells and human mammary fibroblasts (HMF) are patterned and cultured in the multi-inlet microfluidic device. MCF7 cells are stained for CK (red). Fibroblasts are stained for intracellular cytoskeleton (green).

3.4.2 Testing and optimizing in-situ CTC expansion with cancer cell lines

The CTC culturing was performed in the CTC-capture device after CTCs were isolated. To determine the appropriate strategy for *in-situ* expansion of CTCs after isolation, small numbers of GFP-tagged A549 or H1650 cancer cells (100 cells) were spiked into 1mL of blood and flowed through the device. The numbers of cancer cells in the device on day 0 and day 7 were enumerated for comparison (Figure 15A). We observed that cells grown in the 3D co-culture environment exhibited the highest level of expansion, with an 8-fold (783± 248) increase by day 7 in culture. The 2D co-culture condition also facilitated a 3-fold (281± 52) cell expansion (p=0.049), using t-test compared to 3D co-culture condition. This condition was less efficient than the 3D co-

culture. We did not observe significant expansion using a 3D or 2D mono culture environment (3D mono: 159± 133, p=0.035; 2D mono: 91± 48, p=0.018). Hence, a 3D co-culture environment was selected to be the optimal condition for *in-situ* on-chip CTC expansion in our system. The growth curves of A549-GFP cells in 3D co-culture condition over the 7 day period are shown in Figure 15B. During the initial 1-4 days, the cells grew slowly, perhaps adapting to the environment; however, by day 4, the cells exhibited significant growth. Figure 15C shows a scanning electron microscope (SEM) image of fibroblasts cultured in a mix of collagen and Matrigel beginning to spread in the microfluidic channel. A proliferation EdU assay (Invitrogen) was carried out to evaluate the proliferation potential of the cultured cancer cells on day 7 in device. The experiment was conducted according to protocol by the manufacture. Figure 15D demonstrates more than 90% of H1650-GFP cells are proliferating after being cultured for 7 days. The nucleus of the proliferating cells were stained as red.

After 7 days of on-chip culture, cells were released from the device. Immunofluorescence staining was performed to validate the phenotype of the expanded cells. Figure 15E shows staining of expanded H1975 lung cancer cells with CK (red) and thyroid transcription factor 1 (TTF-1) (cyan) surrounded by GFP-labeled CAFs. The expression of TTF-1, a lung specific marker, was preserved in H1975 cells, known to express this marker [182], in the on-chip cultured environment.

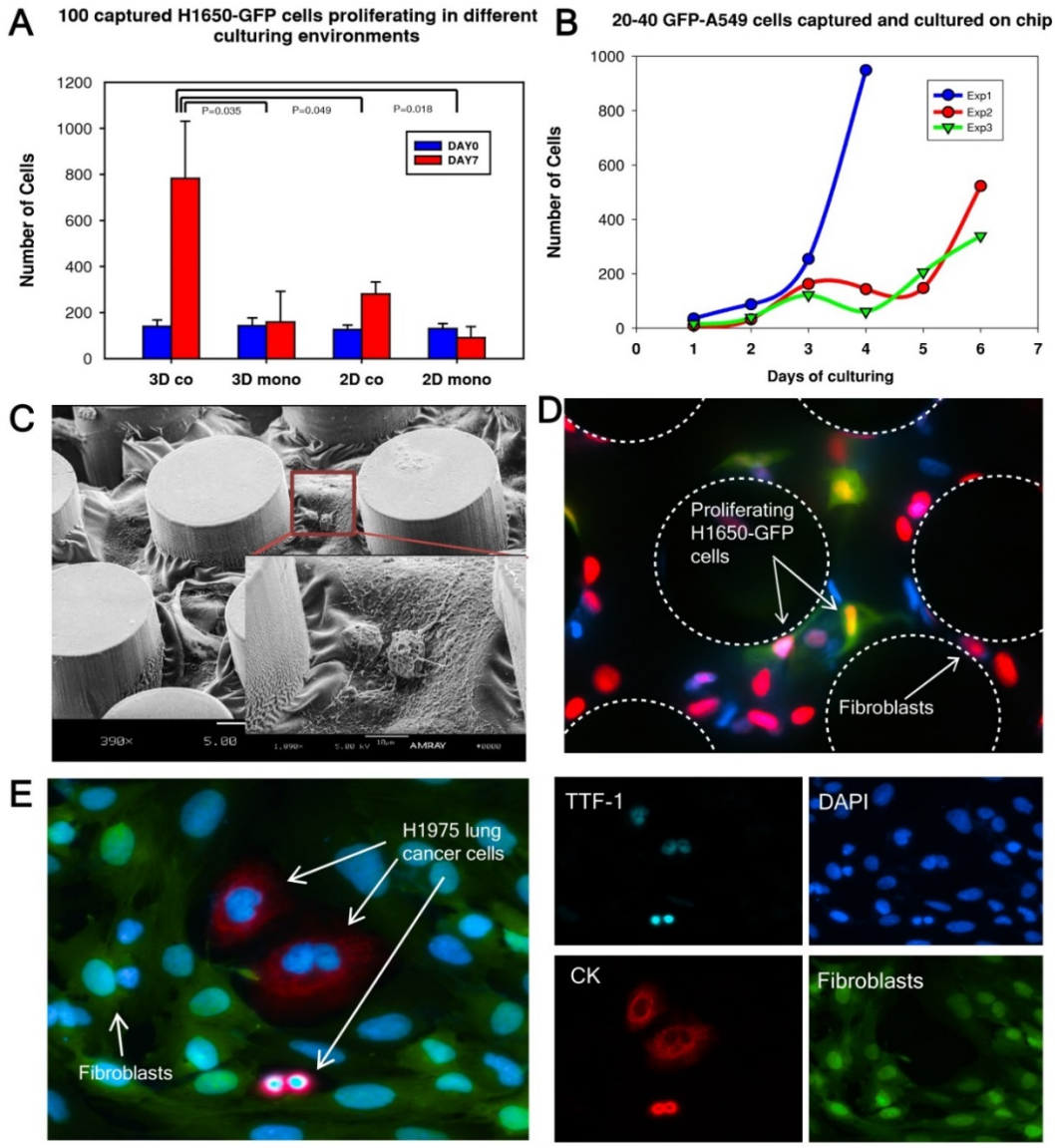

Figure 15. Cancer cell expansion on chip. A. 100 H1650-GFP cells are captured and cultured in different environments (n=3 for each condition). **B.** 20-40 A549-GFP cells are captured and cultured in triplicate (indicated as Exp1, 2 and 3). The curves characterize the growth of the cancer cells. **C.** A scanning electron microscope (SEM) image is taken and showing fibroblasts in gel cultured on chip. **D.** EdU proliferation assay is performed on cancer cells co-cultured with fibroblasts on chip. Green: cancer cells; Red: nucleus of proliferating cells; **E**. Released H1975 lung cancer cells are cultured and IF stained in a well-plate after on-chip culture. TTF-1(cyan), DAPI (blue), Cytokeratin 7/8 (red), Fibroblasts-GFP (green).

3.4.3 Expansion and characterization of CTCs from early stage lung and esophageal cancer patients

The CTC culturing strategy developed and optimized through cell line experiments was applied to test with clinical samples. Specifically, five mL of peripheral blood was drawn from lung and esophageal cancer patients. The blood was drawn before surgery under an IRB-approved protocol at the University of Michigan Hospital. Upon CTC isolation, one of the devices was IF stained with antibodies for enumerating CTCs on day 0. The remaining devices with cells were cultured with collagen I, Matrigel and GFP tagged CAFs for 7 days. Later, expanded patient CTCs were released and cultured up to 14 days in a well-plate. Nineteen lung cancer patient samples and fourteen esophageal cancer patients were tested for capture and expansion efficiency (sample C1-C19 in Table 5, sample E1-E14 in Table 6). Figure 16A lists 19 lung cancer patient samples and 7 healthy controls with the number of CTCs captured on day 0 and on day 14 after expansion. Figure 17A lists 14 esophageal cancer patients and 7 healthy controls with number of CTCs captured on day 0 and on day 14 after expansion. Fourteen of 19 patient samples (73%) had successful expansion of isolated CTCs, 10 of 14 esophageal patient samples (71%) were successful whereas none of the CK positive cells from healthy controls demonstrated capability of expansion in culture.

Patient	Cancer Type	Gender	Age	Tumor histology	Stage	TNM subtypes	CTC count DAY0/1ml	CTC count on DAY14
C1	lung	M	71	SCC	IA	T1bN0M0	6	87
C2	lung	M	72	SCC	IIA	T2aN1M0	2	16
C3	lung	F	50	AC	IIB	T2bN1M0	3	64
C4	lung	M	72	AC	IIIA	T3N1M0	4	118
C5	lung	F	74	AC	IIA	T2bN0M0	1	386
C6	lung	M	62	AC	IB	T2aN0M0	1	12
C7	lung	M	74	AC	IIB	T3N0M0	1	34
C8	lung	F	79	AC	IA	T1bN0M0	3	135
C9	lung	M	69	AC	IIA	T2aN1M0	9	125
C10	lung	F	71	AC	IA	T1bN0M0	3	65
C11	lung	M	86	AC	IA	T1aN0M0	4	42
C12	lung	F	70	SCC	IIA	T2bN0M0	11	70

C13	lung	M	77	SCC	IIIA	T2aN2M0	1	92
C14	lung	M	63	SCC	IB	T2aN0M0	1	83
C15	lung	M	77	AC	IA	T1bN0M0	4	0
C16	lung	F	74	AC	IIA	T2bN0M0	3	0
C17	lung	F	53	SCC	IIA	T2aN1M0	4	0
C18	lung	M	93	SCC	IA	T1bN0M0	6	0
C19	lung	F	71	AC	IA	T1bN0M0	9	0

Table 5. Demographic information of lung cancer patients for samples used for quantifying expansion of CTCs.

Patient	Cancer Type	Gender	Age	Tumor histology	Stage	TNM subtypes	CTC count DAY0/1ml	CTC count on DAY14
E1	esophagus	M	64	AC	IIA	pT3N0	5	29
E2	esophagus	M	59	AC	I	pT1aN0	6	39
E3	esophagus	M	69	SCC	I	T1bN0M0	6	28
E4	esophagus	M	63	AC	IIA	ypT3N0	13	268
E5	esophagus	M	85	SCC	IIA	T3N0	10	88
E6	esophagus	M	51	AC	IIIA	ypT3N1	21	89
E7	esophagus	M	65	AC	IIIB	T3N2	4	44
E8	esophagus	M	62	AC	IA	T1bN0	1	152
E9	esophagus	M	55	AC	IIIA	T2N2	5	86
E10	esophagus	M	67	AC	IIIA	T2N2	4	19
E11	esophagus	M	61	AC	IA	pT1aN0	16	3
E12	esophagus	M	56	AC	IV		1	0
E13	esophagus	M	70	AC	IIA	pT3N0	3	4
E14	esophagus	M	76	AC	IIA	*ypT3N0	10	10

Table 6. Demographic information of esophageal cancer patients for samples used for quantifying expansion of CTCs.

An average of a 54-fold increase of lung CTCs (range 7-385 fold) and a 23-fold increase of esophageal CTCs (range 3-151 fold) was observed in patient samples. Figure 16B and Figure 17B depicts fluorescence images of expanded patient CTCs in well-plates stained for CK 7/8 (red) along with GFP labeled fibroblasts. In one lung cancer patient (C23), the expanded CTCs were stained for TTF-1 (red) and found to be positive (Figure 16C). RT-PCR analysis further confirmed that both the primary tumor and CTCs

demonstrated *TTF-1* expression (Figure 19C). Additional staining for the proliferation marker Ki67 was demonstrated in the expanded CTCs as well (Figure 16C). One CTC sample was positive for epidermal growth factor receptor (EGFR) and pan-cytokeratin (Figure 16D).

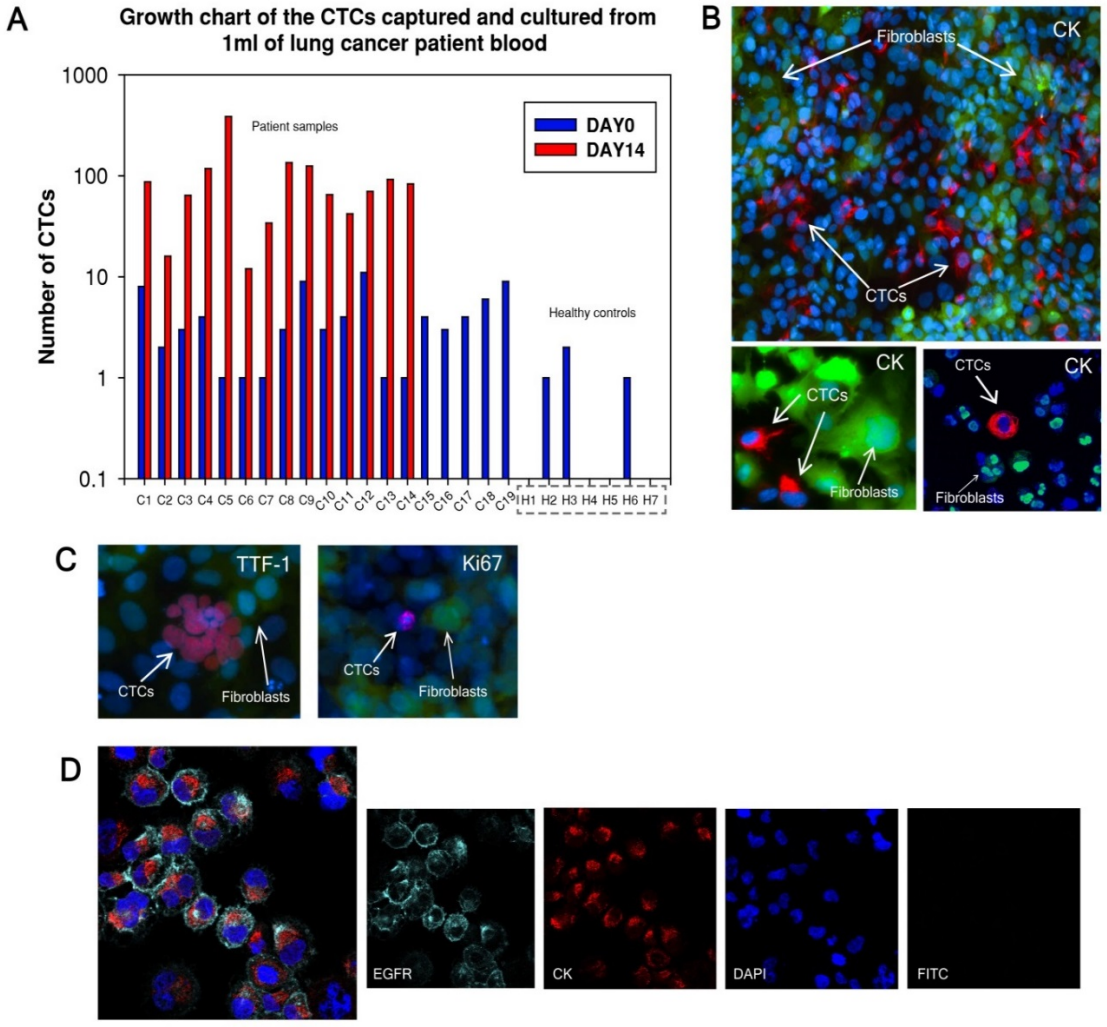

Figure 16. CTC expansion data from lung cancer patients. A. A growth chart shows the number of CTCs captured on day 0 (blue columns) and the number of CTCs on day 14 (red columns) after expansion. CTCs are expanded successfully from 14 out of 19 lung cancer patients. **B**. After expansion, CTCs are characterized in well-plates with CK7/8 (red) surrounded by GFP-fibroblasts. **C**. (left) CTCs from one patient sample (C23) are stained for TTF-1 (red). (right) CTCs from another patient sample are stained positive for Ki67 (purple). **D**. CTCs sorted out from fibroblasts are stained positive for EGFR (cyan) and pan-CK (red) and are negative for FITC suggesting elimination of GFP-fibroblasts.

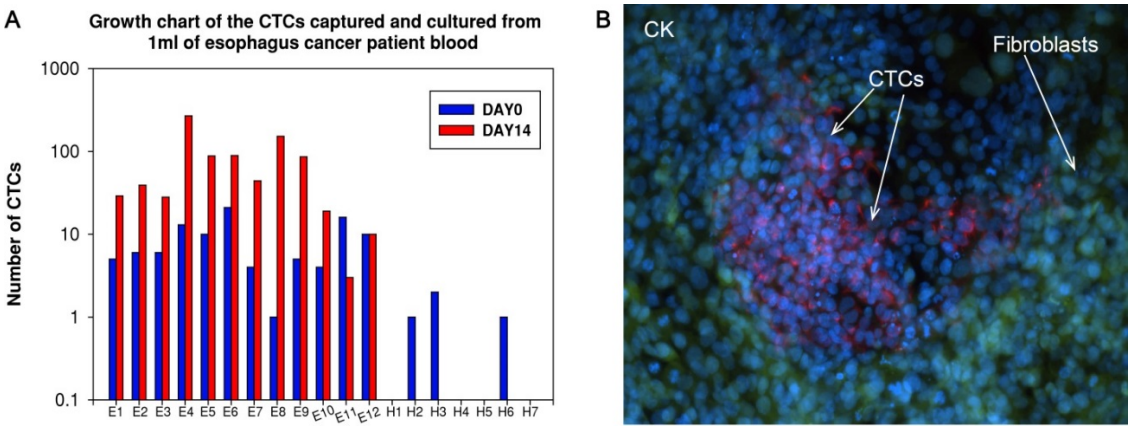

Figure 17. CTC expansion data from esophageal cancer patients. A. A growth chart compares the number of CTCs captured on day 0 (blue columns) and the number of CTCs on day 14 (red columns) after expansion. CTCs are expanded successfully from 10 out of 14 esophageal cancer patients. **B**. After expansion, CTCs are characterized in well-plates with CK7/8 (red) surrounded by GFP-fibroblasts.

To test the tumorigenic properties of expanded CTCs *in vitro*, spheroid formation and invasion assay was performed. Expanded CTCs formed spheroids in three dimension culture whereas fibroblasts did not form spheroids (Figure 18A). One of the key features of tumor cells that are able to leave the primary tumor environment and enter the bloodstream is a capacity to invade [183]. We therefore assessed the invasion abilities of expanded CTCs using a Matrigel-based invasion assay. All three patient CTC samples, similar to H1650 lung cancer cells, demonstrated higher invasion capacity than GFP-fibroblasts (Figure 18B). Fold increase of invaded CTCs compared to fibroblasts ranged from 1.5 to 13-fold. H1650 lung cancer cells exhibited a 2.5-fold increase compared to fibroblasts. The results of this section indicate that patient CTCs can be functionally characterized after a combined on-chip and off-chip culture strategy.

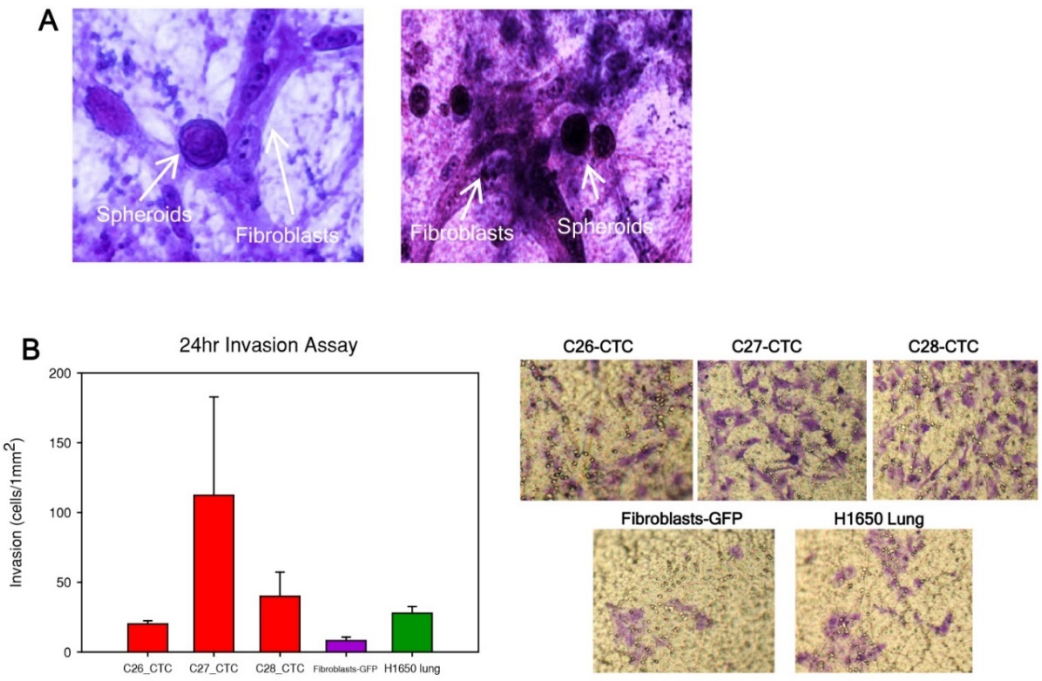

Figure 18. Functional studies of expanded lung CTCs. A. CTC spheroids are formed in a 3D gel assay. **B**. An invasion assay is performed with three CTC samples, fibroblasts-GFP and H1650 cells for 24 hours. Representative images of the transwell membrane are shown on the right.

3.4.4 RNA profiling of expanded lung CTCs and matched primary tumors

RNA was extracted from cultured lung CTCs and matched primary tumors. RT-PCR was conducted to access the expression profile of the cells. This permitted direct comparison between CTCs and primary tumors. Figure 19 summarizes the normalized gene expression level of four cancer-related genes (*CK8*, *CK18*, *TTF-1* and *EGFR*). *CK8* was overexpressed in both the tumor and CTCs of sample C23 compared to the healthy control (Figure 19A, Table 7). *CK18* was highly expressed in sample C22 and C23 both in tumor and CTCs (Figure 19B). *TTF-1* was expressed in both tumor and CTCs of sample C23 (Figure 19C). Importantly, *TTF-1* expression was not observed in cells from the healthy control. We found higher *EGFR* expression in both tumors and CTCs from sample C22 and C23 compared with the healthy control (Figure 19D). Expression of *EGFR* in NSCLC is associated with frequent lymph node metastasis and chemo-resistance [184]. In addition to these genes, we also characterized *β-Catenin* and *CD45*

expression in tumors and CTCs (Figure 19E and F) and found higher expression of *β-Catenin* in patient samples. *β-Catenin* is involved in *WNT* signaling pathway and is important for cell survival [185]. *CD45* was negative in all CTCs samples. In addition to *GAPDH*, the expression level of all of these genes was normalized to *β-Actin* and similar patterns were observed (Figure 20).

Patient	Cancer Type	Gender	Age	Tumor histology	Stage	TNM subtypes	Characterizations performed
C20	lung	F	71	ADC	IA	T1bN0M0	mRNA expression
C21	lung	F	71	ADC	IA	T1bN0M0	mRNA expression
C22	lung	M	79	SCC	IB	T2aPL1N0M0	mRNA expression
C23	lung	F	85	ADC	IIB	T3N0M0	mRNA expression
C24	lung	M	77	SCC	IIIA	T2aN2M0	mRNA expression
C25	lung	M	68	SCC	IA	T1aN0M0	*TP53* sequencing
C26	lung	M	80	SCC	IIIA	T1aN2M0	*TP53* sequencing, Invasion assay
C27	lung	F	37	ADC	IB	T2aN0M0	Invasion assay
C28	lung	M	69	ADC	IIIB	T4N2M0	Invasion assay
C29	lung	F	72	LCC	IIA	T1aN1M0	*TP53* sequencing
C30	lung	M	80	ADC	IA	T1bNxM0	*TP53* sequencing
C31	lung	M	43	ADC	IB	T2aN0 M0	*TP53* sequencing
C32	lung	M	69	SCC	IA	T1aN0M0	Next-generation sequencing
C33	lung	M	73	ADC	IA	T1bNxM0	Next-generation sequencing
C34	lung	M	69	ADC	IIA	T2aN1M0	Next-generation sequencing
C35	lung	F	79	ADC	IA	T1bN0M0	Next-generation sequencing
C36	lung	F	72	LCC	IIA	T1aN1M0	Next-generation sequencing
C37	lung	F	74	ADC	IIA	T2bN0M0	Next-generation sequencing
C38	lung	M	42	ADC	IB	T2aPL1N0M0	Next-generation sequencing
C39	lung	M	75	ADC	IA	T1aN0M0	Next-generation sequencing

Table 7. Demographic information of lung cancer patients for samples used for molecular and functional characterizations.

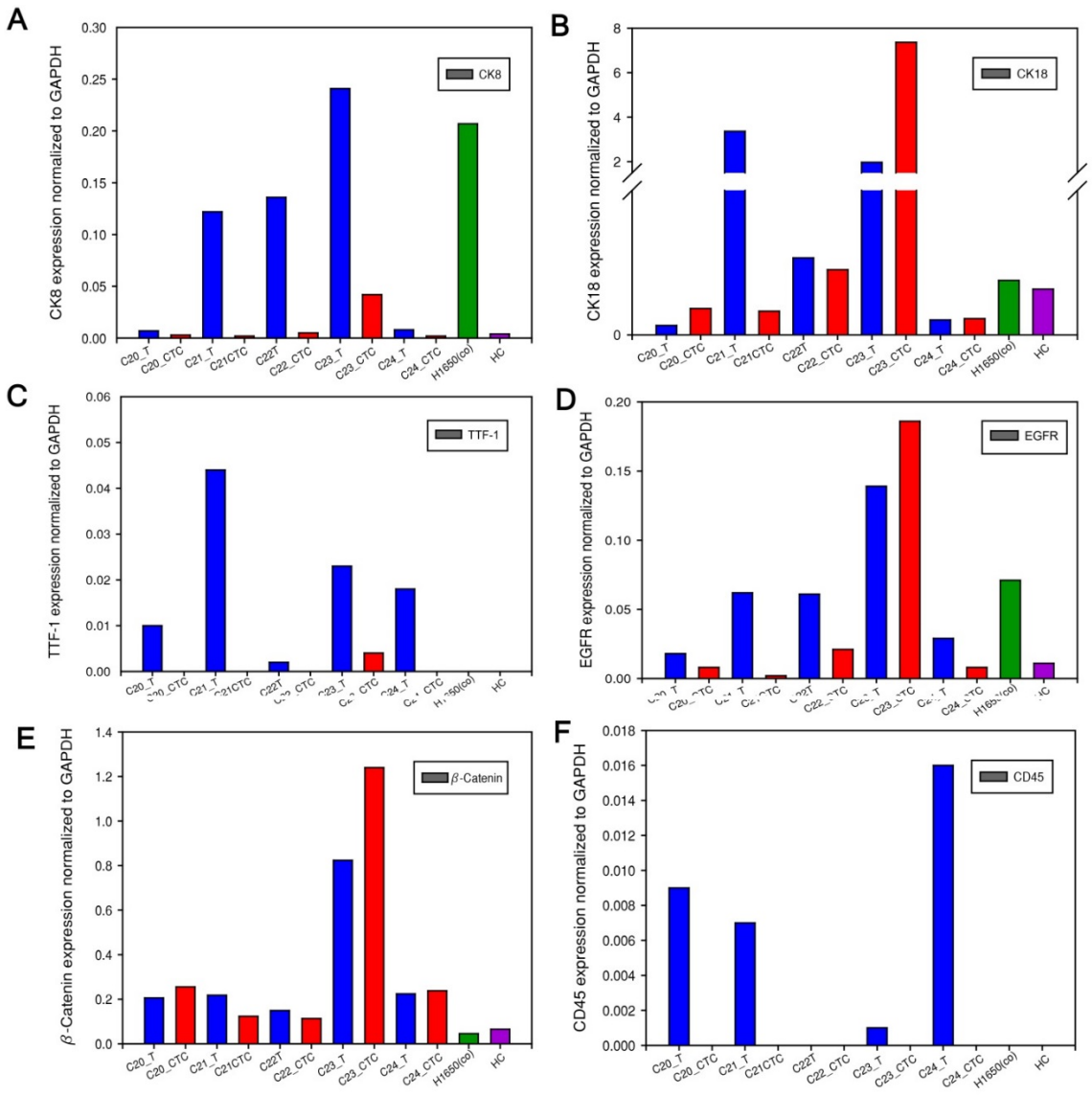

Figure 19. mRNA expression level in primary tumor and CTCs. A to F. Cytokerain8 (*CK8*), cytokeratin18 (*CK18*), *TTF-1*, *EGFR*, *β-Catenin* and *CD45* gene expression levels are normalized to *GAPDH*. Tumor and CTCs mRNA from each patient sample are examined and compared. For example, "C20_T" represents patient C20 tumor (blue column) and "C20_CTC" represents patient C20 expanded CTCs (red column). The positive control is expanded H1650-GFP cells after initially spiking in blood with 100 cells, labeled as "H1650 (co)" (green column). The negative control is one healthy control as "HC" (purple column).

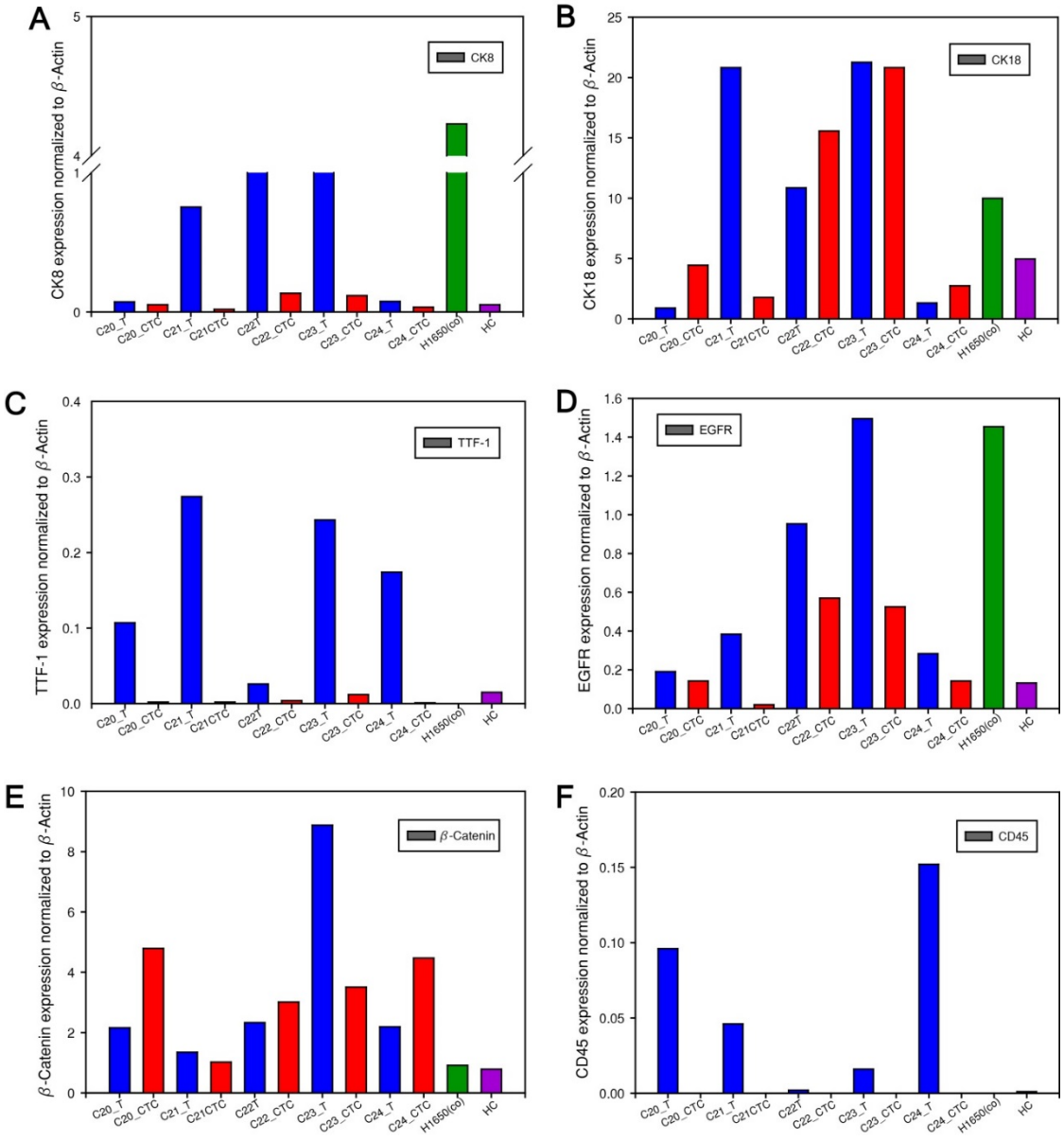

Figure 20. mRNA expression normalized to *β-Actin* in primary tumor and CTCs. A to F. *CK8*, *CK18*, *TTF-1*, *EGFR*, *β-Catenin* and *CD45* expression levels are in the same samples as in Figure 17. Here mRNA expression is normalized to *β-Actin* while Figure 17 has mRNA expression normalized to *GAPDH*.

3.4.5 TP53 sequencing in expanded lung CTCs and matched primary tumors

TP53 is the most commonly mutated gene and is present in nearly 90% of squamous lung carcinomas and in nearly 50% of lung adenocarcinomas [137, 138]. Since *TP53* mutation is an early event in lung tumorigenesis and believed to be preserved to

maintain the malignant phenotype during tumor progression and metastatic spread [186], we hypothesized that CTCs recovered and expanded from early stage lung cancer patients should preserve *TP53* mutations present in the primary patient tumor. RNA was extracted from matching primary tumors and *ex-vivo* cultured CTCs. And the tumor suppressor *TP53* gene was sequenced. Among 15 lung cancer patient samples examined for the *TP53* gene, 9 (60%) had mutations in *TP53* gene. Five of the patient samples had matched mutations in primary tumors and CTCs (Figure 21, 22, Table 7). Figure 21 shows two matched *TP53* mutations between primary lung tumors and cultured CTCs. C25 had a G to A mutation in a non-coding region whereas C26 had G to A mutation in a coding region. However, in 3 patients, *TP53* gene mutations were noted only in the primary tumors and not the matching CTCs, whereas in one patient, the mutation was seen only in the CTCs but not in the primary tumor. The remaining patient samples analyzed exhibited wild type *TP53*. *TP53* mutations were absent from cancer associated GFP-fibroblasts as well as healthy controls, whose blood was run through the devices, co-cultured, released and processed for RNA extraction. These results demonstrate that tumor heterogeneity may exist in cells present in the primary tumor and in the circulation.

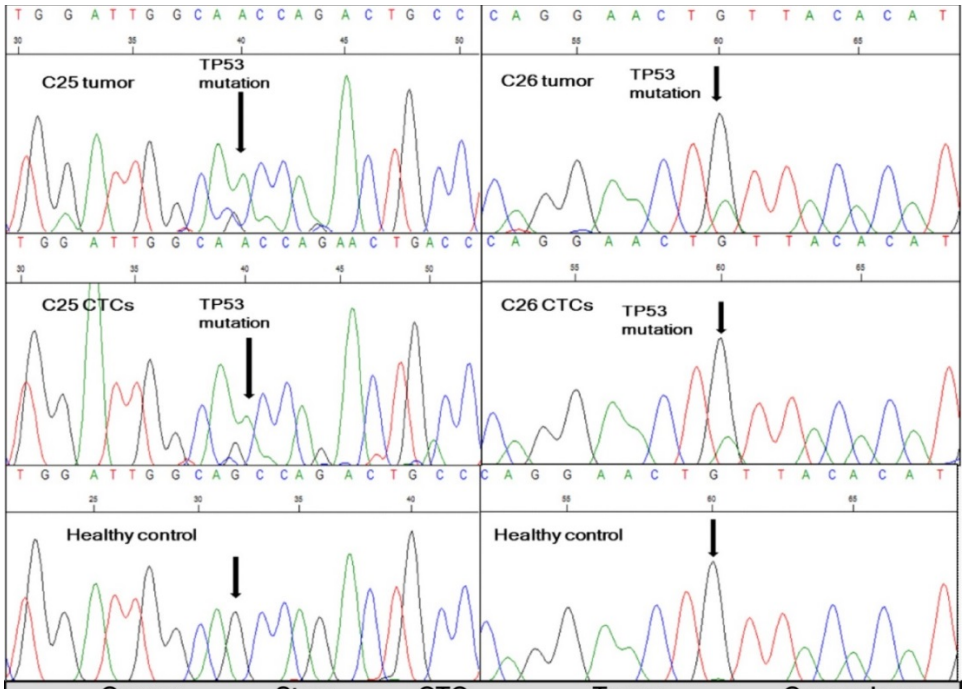

	Cancer	Stage	CTC	Tumor	Concordance
1	Lung SCCA	IA	TP53	TP53	Y
2	Lung AC	I*	TP53	TP53	Y
3	Lung AC	IA	X	X	X
4	Lung AC	IB	TP53	TP53	Y
5	Lung AC	IB	X	X	X
6	Lung LCC	IIA	TP53	TP53	Y
7	Lung AC	IIB	TP53	X	N
8	Lung AC	IIB	X	TP53	N
9	Lung AC	IIB	X	X	X
10	Lung AC	IA	X	TP53	N
11	Lung AC	IA	X	X	X
12	Lung SCC	IA	X	TP53	N
13	Lung NSCLC	IV	X	X	X
14	Lung AC	IIA	X	X	X
15	Lung SCC	IIIA	TP53	TP53	Y

Y: matched, X: wild type, N: not matched

Figure 21. *TP53* sequencing of lung cancer patient samples. One *TP53* point mutation (G to A) is found matched between primary lung tumor and cultured CTCs in patient C25. Another matched point mutation (G to A) is observed between primary tumor and CTCs in patient C26. Healthy controls show no mutations. The table lists *TP53* mutations found in CTCs and corresponding primary tumors in all 15 lung cancer patients tested.

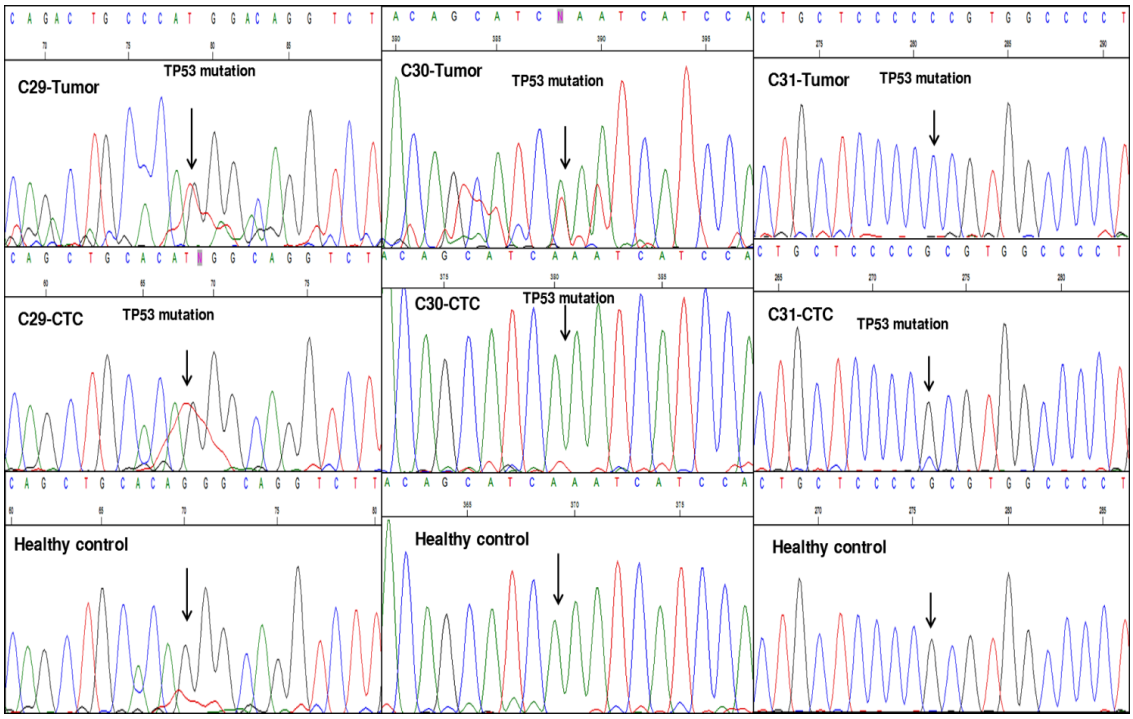

Figure 22. Additional matched *TP53* mutations between CTCs and tumors. Patient C29 has a T insertion. Patient C30 has an A to G mutation. Patient C31 has a G to C mutation.

3.4.6 Investigating tumor heterogeneity

To interrogate tumor heterogeneity and to examine if it can be reflected by CTCs, we sequenced four different regions of one primary tumor. FFPE tissue slides were obtained and four areas of distinct morphological features were identified. We collected tumor tissues separately from the areas and extracted DNA. The primer sets target exon 5, 6, 7 and 8 of *TP53* gene, which cover hotspot regions for mutations. We compared the mutations present in different areas of primary tumor with CTCs to find which area closely resembled CTCs. Figure 23 summarizes the sequencing results. Specifically, region 2, 3 and 4 harbored *TP53* mutations on exon 5 and 7. While region 2 and 3 shared the same mutations (C176F and N239N), region 4 harbored additional mutations on exon 5 (P151P and I162I). CTCs harbored the P151P and I162I mutations on exon 5 and the N239N on exon 7. Therefore, CTCs likely originated from region 2, 3 and 4. Figure 23B and C provide chromatograms of the mutations.

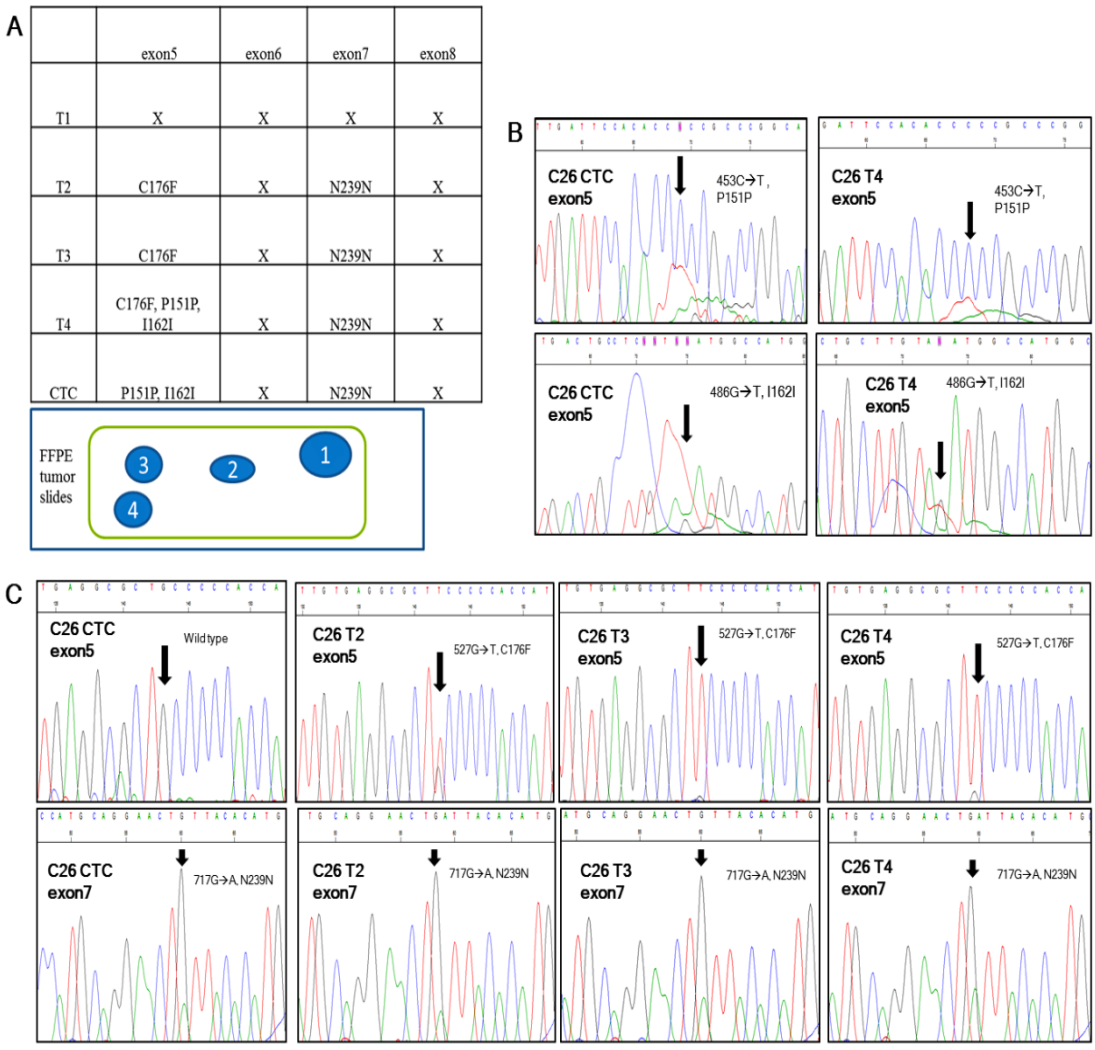

Figure 23. *TP53* mutation status revealing tumor heterogeneity. A. This table summarizes *TP53* mutations in CTCs and four different areas in corresponding primary tumor. "T1,2,3,4" refer to tumor region1,2,3 or 4 from the FFPE slide shown below the table. "X": wild-type; "C176F": codon 176 amino acid change from C to F due to missense mutation; "P151P": codon151 silent mutation; "I162I": codon 162 silent mutation; "N239N": codon 239 silent mutation. **B.** Chromatograms of P151P and I162I seen in CTCs and T4. **C**. Chromatograms of C176F observed only in T2,3 and 4 but not in CTCs, and N239N in CTCs, T2, T3 and T4.

3.4.7 Next-generation sequencing of expanded lung CTCs and matched primary tumors

To further explore the genomic markers CTCs might carry from tumors, next-generation sequencing after targeted exon enrichment was performed with 8 paired primary tumor and CTC samples (sample C32-C39 in Table 7). Figure 24A shows

nonsynonymous (red) and synonymous (green) mutations with mutations in tumor in diamond shape and mutations in CTCs in square shape. Matched mutations between CTCs and primary tumor are highlighted with rectangles. Matched mutations were observed in 3 out of 8 paired CTC-tumor samples in *CASP8, APC*, *TP53* and *ERBB4* genes. The locations of the mutations on the four genes and amino acid alterations are shown in Figure 24B. These results demonstrate that some of the key genes involved in cancer progression are manifested in CTCs and may relate to cancer metastasis.

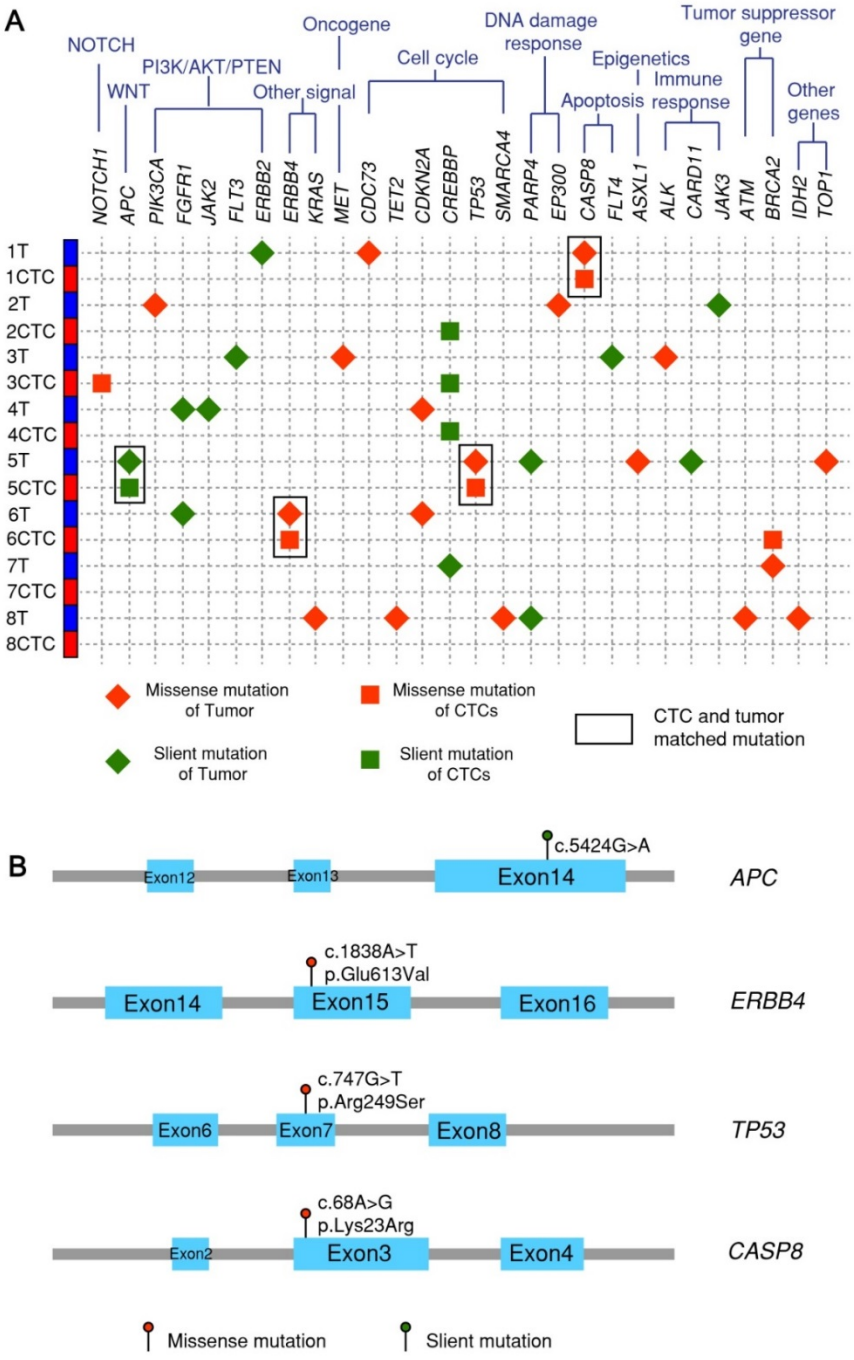

Figure 24. Next-generation sequencing after targeted exon enrichment. A. 8 paired tumor and CTC samples (C32-C39) plus one healthy control and one pure fibroblasts-GFP cell line are sequenced for 124 genes listed in the Qiagen Generead comprehensive cancer panel. Variants in each sample are identified by examining them in genome browser and confirmed by their absence in controls. **B.** Four matched mutations are listed with their locations on exons, base change and amino acid change.

3.5 Discussion

3.5.1 The multi-inlet microfluidic device for cell patterning

We demonstrate the ability to pattern different cell types by a multi-inlet microfluidic device. MCF7 cells and HMFs were spatially patterned in a straight channel. This platform can quantitatively measure the interactions between cancer cells and stromal cells in future studies. Microfluidics can mimic the physiological cues in the cellular environment through spatial and temporal control over gradients of soluble factors and cell-cell contacts in extracellular matrix [172]. It can also pattern cells to create the desired environmental stimuli for cell growth and proliferation [181, 187]. However, to culture cells in a microsystem, one needs to control the tiny environment surrounding the cells. Medium composition, shear stress, chemical gradients and temperature are important parameters to consider when designing the systems [188, 189]. Once the appropriate conditions are obtained, microfluidics provides a tailored, controlled environment for cellular studies.

3.5.2 The microfluidic co-culture model for CTC expansion

For over two decades, studies have shown that tumor cells shed from primary solid tumors, "CTCs" can be detected in the circulation [49, 190]. CTCs may serve as precursors to systemic metastases. Their biological and clinical significance is limited by inability to collect sufficient number of cells. Most studies to date examining biological relevance of CTCs have been carried out in animal models or patients with metastatic disease. Other efforts have been made to release CTCs using a DNA network or hydrogel but suffering cell loss and limited throughput [191, 192]. We present an *in-situ* microfluidic co-culturing model to expand captured CTCs on chip. This is achieved through creating a more physiological tumor microenvironment using a combination of collagen, Matrigel along with cancer associated fibroblasts on a miniaturized device consisted of channels of only 100 μm height. This enables better temporal and spatial control, reduction in material input, and enrichment of signaling molecules such as growth factors and cytokines [172]. This environment likely plays a key role in promoting CTC survival and expansion.

Ex vivo expansion of CTCs allowed us to characterize their phenotypes in multiple aspects. CTCs, but not fibroblasts alone, were able to form spheroids in 3D gel assays (Figure 18A). Additionally, only CTCs stained positive for CK and Ki67, demonstrating that CTCs can be functionally and phenotypically distinguished from fibroblasts (Figure 16). The expanded H1975 lung cancer cells as well as patient CTCs from sample C23 expressed TTF-1 while the cultured fibroblasts lacked expression suggesting tumor specific markers were preserved in our model (Figure 15E and 16C). This observation was confirmed at the gene expression level using RT-PCR to test several cancer-related genes in primary tumors and CTCs (Figure 19). mRNA expression was heterogeneous among different patients. In some patient samples, primary tumors and CTCs demonstrate higher *CK8, CK18* and *EGFR* mRNA expression compared to the healthy control. Invasion assay demonstrated that CTCs possessed invasion capabilities and functional studies were feasible with expanded CTCs.

More importantly, our studies enabled direct comparison of CTCs likely originating from only the primary tumor (as only patients with early stage cancer with no known metastasis were chosen for this study) in early stage patients. Matched *TP53* mutations were detected in patient tumors and CTCs but absent in fibroblasts and healthy controls. This is a strong indication that mutations in *TP53* were preserved in CTCs, which might actively contribute to their ability to enable distant metastasis. We noted that 5/15 lung cancer samples had matched *TP53* mutation between CTCs and primary tumors, whereas 4 samples had unmatched mutations. We believe this may reflect the inherent tumor heterogeneity observed in lung cancer as in most solid tumors [193]. For patient C26, we sequenced 4 areas of the primary tumor and noted the concordance between *TP53* mutations in 3 parts of the tumor and corresponding CTCs, which suggested that tumor heterogeneity likely played a role in CTC shedding (Figure 23). One patient C31, with matched *TP53* mutations recurred within 3 months in the brain and died. Another patient C5 with a 385-fold increase in CTCs after expansion recurred in 3 months in the adrenal gland and died. The follow-up period in the other patients has not been long enough for recurrence data. Although a larger cohort is needed to investigate further the correlation between proliferation, mutational status of CTCs and survival, the presented data demonstrates feasibility of the approach.

Next-generation sequencing of 124 selected cancer-related genes further revealed that concordant mutations (*APC, ERBB4, CASP8*) existed in tumors and cultured CTCs in addition to *TP53*. These genes are related to key signaling pathways for cell growth or apoptosis, which collectively, may lead to tumor progression and metastasis. There are mutations unique to tumors but not in CTCs likely due to intra-tumor heterogeneity or variable abundance of specific mutations. On the other hand, there are mutations not seen in tumors but unique to CTCs such as *NOTCH1* and *BRCA2*. Clinical significance of these mutations related to metastasis will need to be determined using larger cohorts for further investigation.

In summary, we have shown *ex vivo* expansion of CTCs isolated from blood samples of early stage lung and esophageal cancer patients, including patients with Stage I disease. We have found concordant mutations involved in lung cancer progression in CTCs and primary tumors using an unbiased approach (NGS). Albeit, in some cases, we found mutations in genes in the primary tumors that were not noted in the CTCs and vice-versa, which raised the possibility of tumor and CTC heterogeneity. Functionally, expanded CTCs were capable of invasion compared to fibroblasts. Additionally, patients whose CTCs exhibited the greatest capacity to expand *ex vivo* had earlier recurrence and died. Undoubtedly, this is an observation only in 2 patients and further studies are warranted. Finally, this microfluidic co-culture technique may open a new spectrum of opportunities for enriching early stage CTCs and aid in understanding the role of CTCs in metastasis.

Chapter 4
CTC-derived xenograft from *ex vivo* expanded CTCs derived from a NSCLC patient

4.1 Abstract

A CTC-derived xenograft (CDX) presents a valuable model to interrogate cancer metastasis and perform drug susceptibility test, which will aid in personalized medicine and targeted therapy. Previous studies (to date only 4) demonstrated generating CDXs from patients with advanced breast, small-cell lung and colon cancers. Here we showed CTCs expanded from one early stage non-small cell lung cancer (NSCLC) patient successfully generated one xenograft model after 6 months. H&E staining confirmed the CDX had the same histology as the primary cancer. Immunohistochemical staining further characterized the protein expression on the xenograft, which could be correlated with the RNA expression profile by RNA sequencing. Furthermore, we identified several genes enriched in the CTCs, xenograft and primary tumor. These genes are related to the epithelial-mesenchymal transition (EMT) and crosstalk between tumor and stromal cells in the tumor microenvironment.

4.2 Introduction

While the exploration of innovative technologies for enhanced CTC isolation is always at the forefront of research, *ex vivo* culturing and *in vivo* xenograft models have gradually gained momentum in the field. During recent years, attempts have been made to culture CTCs *in vitro* or to generate CTC-derived xenografts (CDXs) from breast, prostate, colon and small-cell lung cancer patients of advanced stages [91, 97-99, 180, 194]. Zhang *et al*. sorted a subset of breast CTCs to form cell lines and tumors in mice [97]. This model identified a novel gene signature associated with development of brain metastasis. Yu *et al*. successfully cultured breast CTCs followed by *in vivo* implantation and drug testing [180]. Cayrefourcq *et al*. established and characterized a cell line derived from colon CTCs, which also generated xenografts [99]. In the study by Hodgkinson *et al*., CTCs from SCLC patients were injected directly to mice [91]. Samples with CTC count >400/7.5ml successfully gave rise to tumors in mice in 2-4 months. CDXs allow examining the tumorigenicity of CTCs as well as drug testing *in vivo* [195]. Our lab has reported *ex vivo* expansion of CTCs from early stage lung cancer patients using a microfluidic co-culture model [77]. In the present study, we utilized the culture strategy described in the previous paper and cultured CTCs from one early stage patient with lung squamous cell carcinoma. The expanded CTCs were injected into immune-compromised mice and generated a xenograft after 6 months. We then performed characterizations of the xenograft and compared it to the primary tumor.

4.3 Methods

4.3.1 CTC isolation and ex vivo expansion

The detailed method can be found in our previous publication [77]. Briefly, 5 mL of the peripheral blood was drawn from the patient before surgery at the University of Michigan Hospital. The CTC-capture device was coated with EpCAM and CD44. The blood was divided and run through two CTC-capture devices to isolate and culture the CTCs. Cancer associated fibroblasts mixed with collagen I and Matrigel was added to the devices. Then the cells were cultured on chip for 2 weeks before releasing them off the

devices. The released cells were further cultured in well-plates for two weeks and tested for spheroid formation capability and immunofluorescence staining to confirm the presence of CTCs.

4.3.2 Generating the CTC-derived xenograft

Cultured CTCs with cancer associated fibroblasts, around 50,000, were injected into one immune-compromised NOD scid gamma (NSG) mouse subcutaneously. The mouse was checked regularly for tumor formation. After harvesting the 1st generation xenograft, a small piece of the xenograft was subcutaneously implanted in two mice. The mice were checked periodically for tumor formation.

4.3.3 H&E and immunohistochemical (IHC) staining

The harvested xenograft tissue was fixed by 10% formalin and submitted to the In-vivo Animal Core Facility at the University of Michigan Medical School to perform H&E and IHC staining. The antibodies used are CD44 (BD Biosciences, clone G44-26), ALDH (BD Biosciences, clone 44/ALDH) and Pan-cytokeratin (Abcam). All the antibodies were tested with a negative and a positive control before staining the actual tumor samples.

4.3.4 CTC isolation from mouse blood

Prior to harvesting the xenograft, mouse blood was drawn in an EDTA tube. The blood was flowed through the CTC-capture device coated with EpCAM and CD44 for CTC isolation. After CTC capturing, the cells were stained for anti-human CK and anti-mouse CD45. The device was scanned with an automated immunofluorescence microscope and the number of CTCs was counted.

4.3.5 RNA sequencing

RNA was extracted from cultured CTCs, the xenograft and the primary tumor by miRNeasy Mini Kit (Qiagen). The RNA concentration and quality was tested with Nanodrop at the Core facility. The extracted RNA was then diluted to the recommended concentrations and submitted for the next generation sequencing, which was performed

on the Illumina platform for 50 paired ends in the Core facility at the University of Michigan.

4.3.6 RNA-seq data analysis

Sequencing reads were mapped to a combination of human transcripts annotated in Gencode v19 and mouse transcripts annotated in Gencode vM2 [196]. Gene expression values were quantified using rSeq [197] in the unit of RPKM [198]. Heatmap and hierarchical clustering were generated using R function "heatmap.2" with Euclidean distance and complete link based on log-transformed gene expression values for genes with average expression value greater than 10 RPKM across the samples. We also performed the differential gene expression and compared the gene expression level of the cultured CTCs, xenograft and primary tumors with pure fibroblasts. The cutoff threshold of the differential gene expression analysis is 0.5. We specifically looked at 340 cancer-associated genes and found some genes were enriched in the cultured CTCs, xenograft and primary tumor.

4.4 Results

4.4.1 Expanded lung CTCs generating a xenograft

Five mL of peripheral blood from each of the four patients with early stage lung cancers was drawn before surgery at the University of Michigan Hospital. The blood samples were obtained under an IRB approved protocol, and run through the CTC-capture devices to isolate and culture CTCs. The culturing method is described in our previous publication in which we have shown CTCs can be expanded in 10/14 early stage lung cancer patients [77]. The cultured CTCs were injected subcutaneously into immune-compromised NGS mice. Only the CTCs from a patient with stage IIIA lung squamous cell carcinoma developed a xenograft after 6 months. Figure 25 is a schematic demonstration of the overall strategy of the study. After the first-generation xenograft was harvested, it was passaged to two new mice. The second-generation xenografts were developed after 4 months with a faster growth rate than the first-generation.

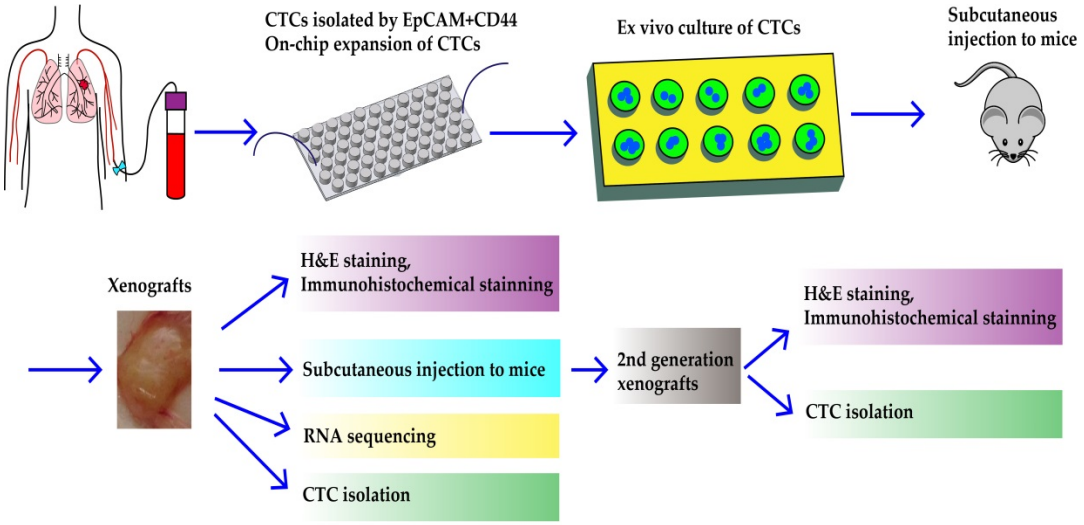

Figure 25. Overall strategy of generating a CDX from one NSCLC patient. After CTCs are isolated and culture *ex vivo*, they are injected into mice and generate a CDX. The 1st generation CDX is characterized and is compared to the primary tumor. It is further passaged to generate 2nd generation CDXs.

4.4.2 Characterization of and comparison between the expanded CTCs, xenografts and primary tumor

H&E staining revealed that the primary tumor was an invasive, poorly differentiated lung squamous cell carcinoma (Figure 26A). The first-generation and second-generation xenografts showed the same histology as the primary tumor (Figure 26A). IHC staining revealed that the first-generation and second-generation xenografts were positive for pan-cytokeratin, CD44 and ALDH (Figure 26B and C).

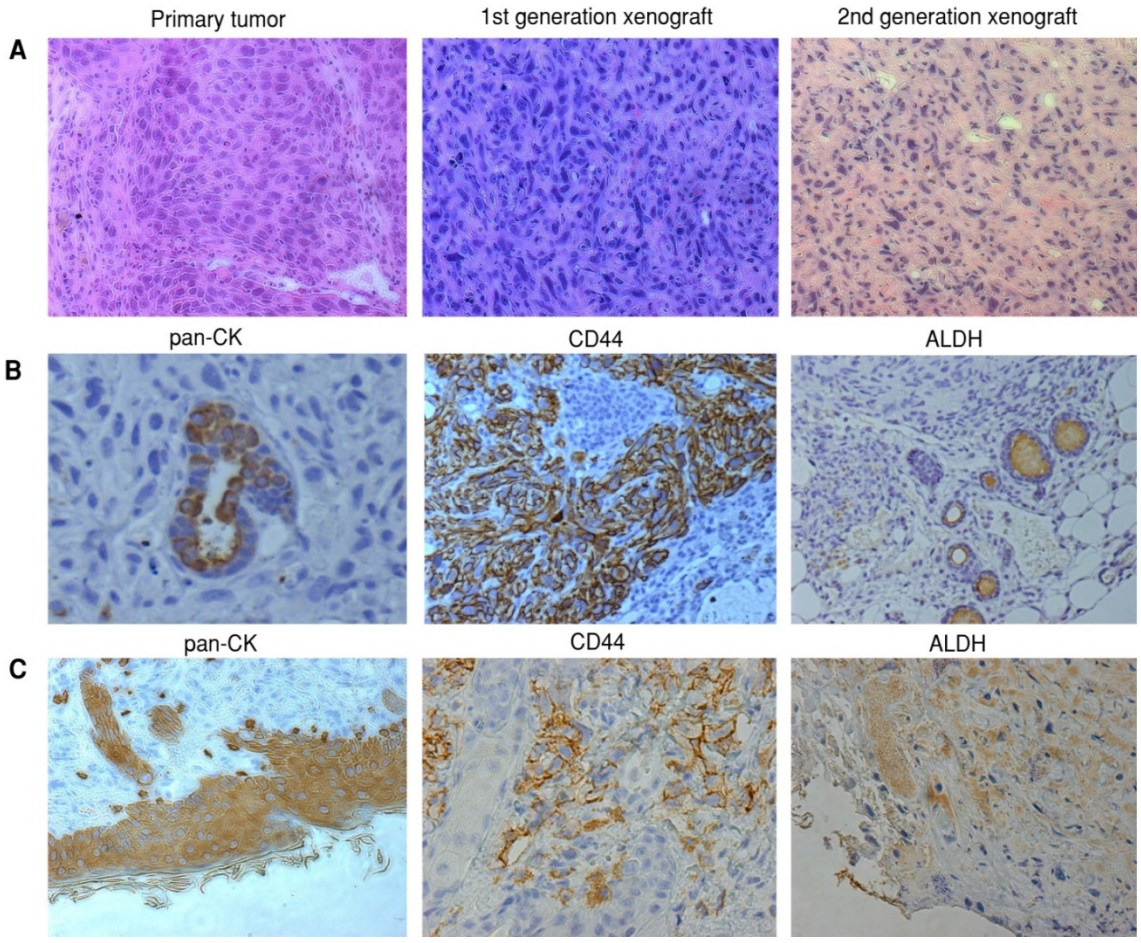

Figure 26. H&E and IHC staining on the primary tumor and xenografts. A. H&E staining on the primary tumor, 1st and 2nd generation xenograft. The primary tumor is poorly differentiated SCC. **B**. IHC staining of pan-CK, CD44 and ALDH on the 1st generation xenograft. **C**. IHC staining of pan-CK, CD44 and ALDH on the 2nd generation xenograft.

We also drew mouse blood and performed CTC isolation. Eight CTCs were identified in the first-generation mouse blood (Figure 27A). An average of 54 CTCs were isolated from blood of the second-generation mice (Figure 27B). These results demonstrate the xenograft model is reliably generated by the expanded CTCs, which suggests their tumorigenicity.

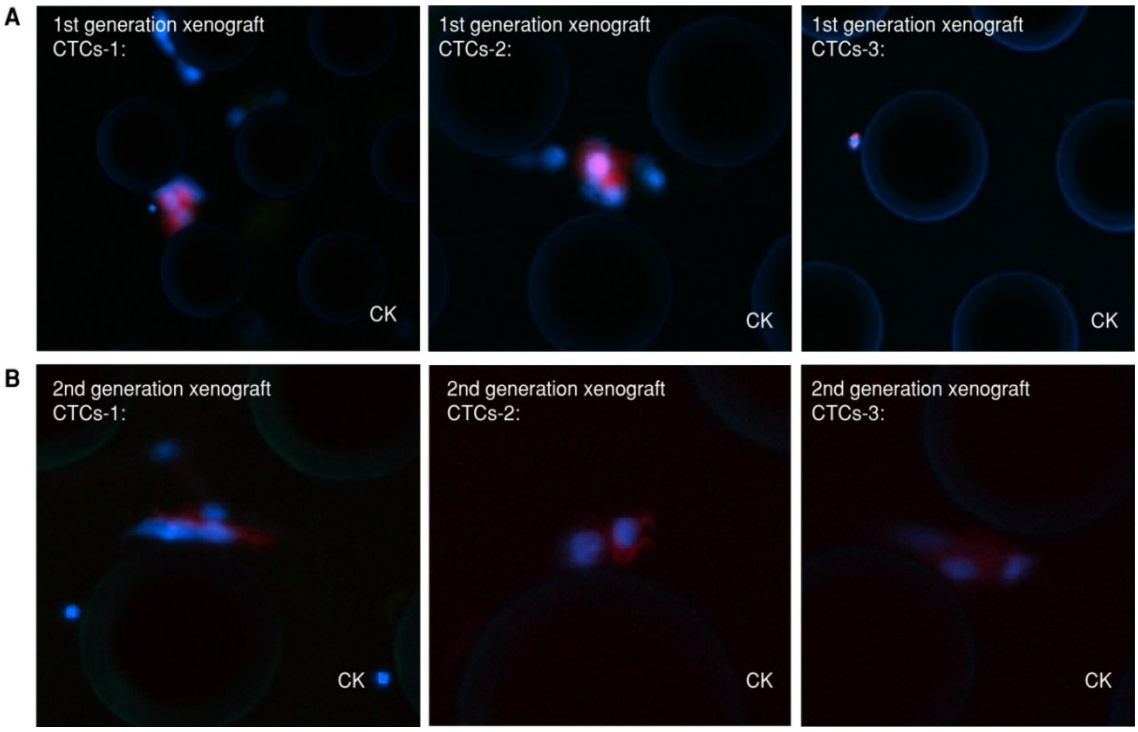

Figure 27. CTCs isolated from mouse blood. CTCs are stained for CK(red), CD45(green) and DAPI. **A**. CTCs from the 1st generation xenograft. **B**. CTCs from the 2nd generation xenografts.

4.4.3 Genomic analysis of the expanded CTCs, CTC derived xenograft and primary tumor

To interrogate the biological pathways enabling the CTCs to grow *in vitro* and *in vivo*, we performed RNA sequencing on the expanded CTCs, the first-generation xenograft, the primary tumor, cancer associated fibroblasts and the normal mouse tissue. Normalized reads were analyzed by hierarchical clustering. Figure 28 shows the global gene expression profile of the samples. CTCs and fibroblasts are clustered closely because of the presence of fibroblasts in the expanded CTCs. The xenograft and primary tumor is clustered together despite there are some mouse genes expressed in the xenograft.

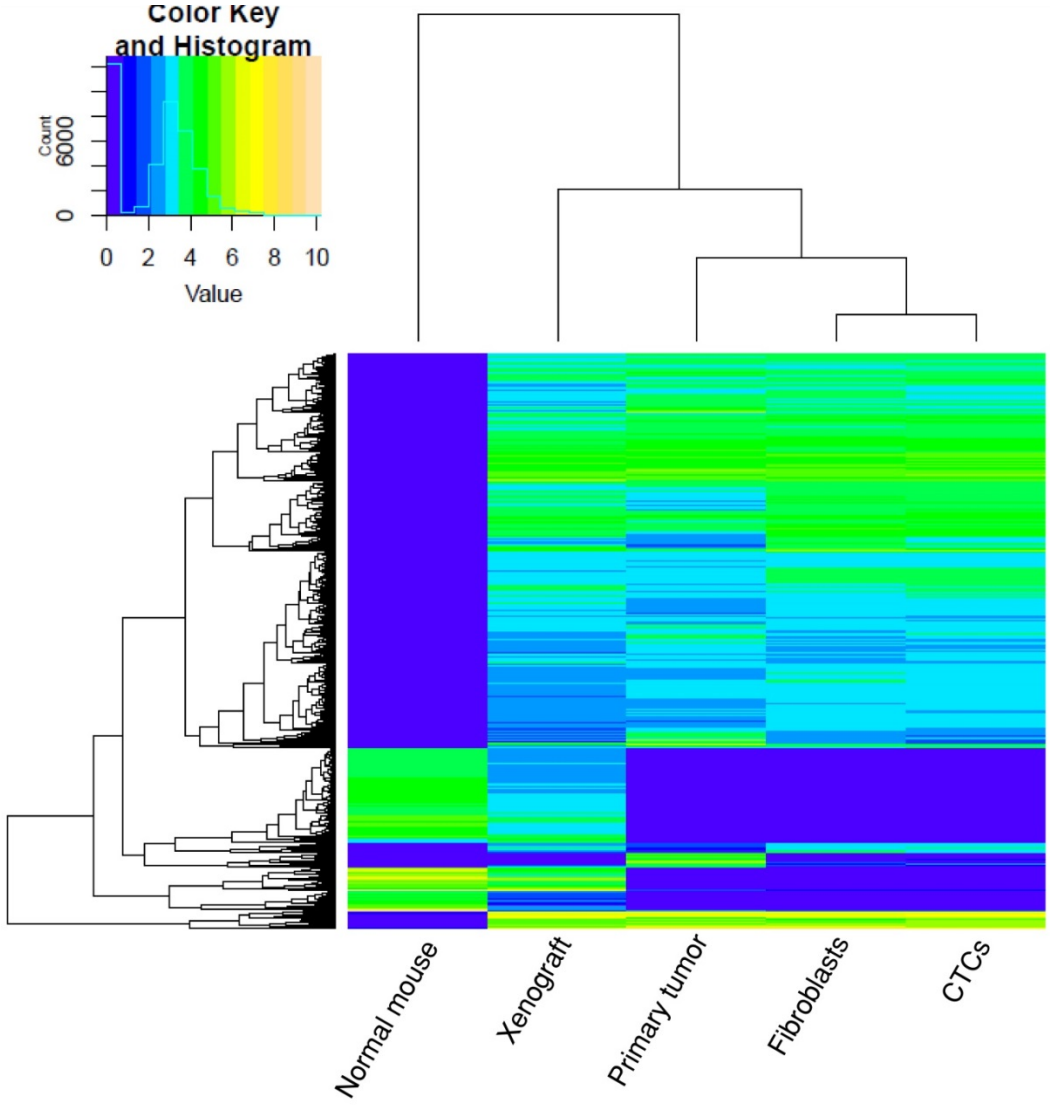

Figure 28. RNA expression analysis. Hierarchical clustering of the normal mouse tissue, the 1st generation xenograft, primary tumor, fibroblasts and CTCs.

We then performed differential gene expression analysis on the CTCs, xenograft and primary tumor by comparing them with the fibroblasts. By examining 340 genes that are associated with cancer, we generated a list of genes that were enriched in the CTCs, xenograft and primary tumor (Figure 29). Notably, *KRT7*, *KRT8*, *KRT14*, *CD44* and *ALDH1A2* were present in the xenograft, which corresponded to the IHC staining (Figure 26B).

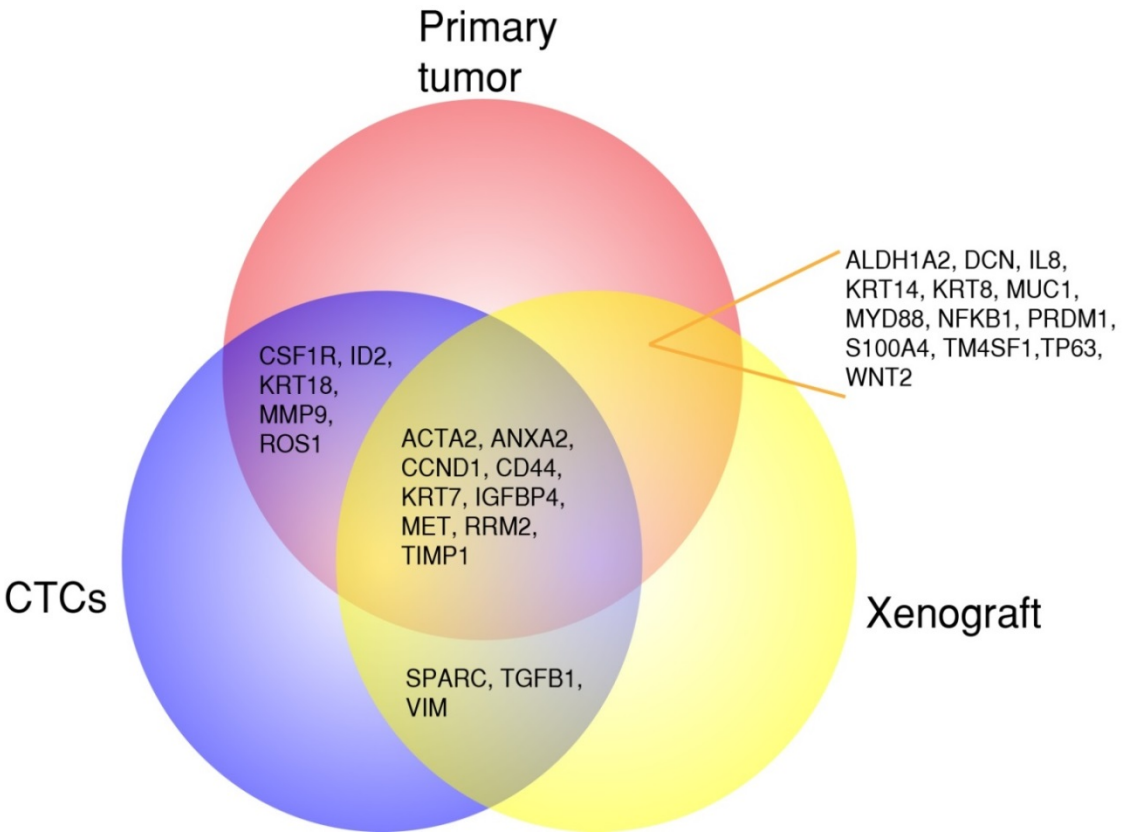

Figure 29. Genes shared between different samples. Venn diagram of the genes enriched in the CTCs, 1st generation xenograft and the primary tumor.

Among the genes shared between the CTCs and primary tumor, *MMP9* acts on remodelling extracellular matrix and aids in metastasis [199]. *CSF1R* is involved in the crosstalk between immune cells and cancer cells to induce cancer cell migration [173]. *ID2* encodes a transcription factor which involves in inhibiting differentiation and enhancing tumor growth [200]. *ROS1* encodes a receptor tyrosine kinase in NSCLC and its overexpression is correlated with poor prognosis [201].

In addition, by examining the genes shared between the CTCs and xenograft, we found *TGFB1*, *VIM* and *SPARC* were expressed. *TGFB1* and *SPARC* are involved in inter-communication between cancer and stromal cells [202, 203]. *VIM* encodes vimentin, an intermediate filament protein associated with epithelial-mesenchymal transition (EMT) and increased tumor growth [204]. *SPARC* is also correlated with EMT and tumor metastasis [205].

There are a number of genes shared between the primary tumor and the xenograft. Among them, *KRT14*, *KRT8*, *MUC1* are epithelial cell markers whereas *S100A4* is involved in EMT [206, 207]. *ALDH1A2* is a cancer stem cell marker [208]. *DCN* is expressed by extracellular matrix of tumor stroma [209]. *IL8* is a chemokine in tumor microenvironment to promote angiogenesis and metastasis [210]. *MYD88* and *NFKB1* are involved in inflammation in the tumor microenvironment [211, 212]. *TP63*, expressed by lung squamous cell carcinoma, is also seen in both the primary tumor and the xenograft [213]. *PRDM1* is shown to localize in the nucleus of lung cancer cells [214]. Additionally, *TM4SF1* is correlated with angiogenesis [215]. *WNT2* is reported to correlate with lung carcinogenesis [216].

Finally, among the genes shared between all three samples, a mix of epithelial genes (*KRT7*) and EMT genes (*IGFBP4*, *TIMP1*, *ACTA2*) were present [217-219]. *MET* is reported as an oncogene in lung cancer and its overexpression is related to tumorigenesis [220]. *MET*, *CCDN1* and *CD44* play roles in proteoglycans in cancer according to the KEGG pathway database. *ANXA2* encodes Annexin A2, which is shown to be upregulated in lung SCC with lymph node metastasis [221]. High expression of *RRM2* is found to be correlated with decreased response to gemcitabine of NSCLC patients and worse prognosis [222]. The overexpression of *CCDN1* has been shown to relate to less differentiated lung cancer [223].

4.5 Discussion

In the present study, one CDX was generated by *ex vivo* expanded CTCs from an early stage lung cancer patient using a microfluidic co-culture model. The CDX exhibited the same histology and phenotypic features as the primary lung cancer. The first-generation xenograft can be stably passaged and generated the second-generation xenografts, which allowed multiple analyses. We performed genomic analysis of the expanded CTCs, xenograft and primary tumor. Together, we observe the expression of *TP63*, which confirms the xenograft is derived from a poorly differentiated lung SCC. The CTCs, xenograft and primary tumor express epithelial (*KRT7, 8, 14, 18* and *MUC1*), EMT markers (*VIM, SPARC, S100A4, IGFBP4, TIMP1* and *ACTA2*), and stem cell

related genes (*ALDH1A2* and *WNT2*) [224]. This suggests the cellular plasticity and EMT contributed significantly to cancer cell invasion and metastasis [225], and there are metastasis initiating niches enabling the xenograft to develop.

Generating CTC-derived xenografts (CDXs) has been demonstrated by several groups using various technologies including flow cytometry sorting in breast cancer [97], depletion of white blood cells through RosetteSep Kit in breast[98], small-cell lung[91] and colon cancer[99] and CTC-iChip in breast cancer [180]. Compared to the previous technologies, our method achieves pre-enrichment of CTCs through *ex vivo* culturing before injecting to mice. Our findings are consistent with the previous work by Ting *et al*., in which they reported the presence of epithelial, EMT and stem cell markers in pancreatic CTCs through single-cell RNA-seq [226]. They also identified genes related to extracellular matrix (ECM) in pancreatic CTCs. Similarly, we find ECM genes such as *MMP9, SPARC, DCN, TIMP1* and *TGFB1,* enriched in the CTCs, xenograft and primary tumor. Additionally, genes such as *CSF1R, IL8, MYD88, NFKB1* and *TM4SF1,* which are involved in the crosstalk between tumor and stromal cells, are upregulated in the samples. These genes suggest the important role tumor microenvironment plays in cancer development [173]. Targeting tumor stroma will contribute to preventing the spread of cancer cells to distant organs.

Genes shared between the CTCs, xenograft or primary tumor may provide insight into the mechanism by which CTCs survive in circulation and ultimately grow *in vitro* and *in vivo*. Pathway analysis indicates Ras signaling is associated with the shared genes ($p=0.004$). Activated Ras proteins enhance tumor development through deregulation of proliferation, programmed cell death, angiogenesis and invasion [227]. The pathway shared between the xenograft and primary tumor is related to anti-apoptosis and cell survival ($p=0.004$). In particular, the activation of NF-κB protects cells against apoptosis [228]. We observe *SPARC*, *TGFβ1* and *VIM* are shared between xenograft and CTCs but are absent in primary tumor. These CTC-specific genes may represent a small population of cells in the primary tumor, and the gene expression patterns may provide unique properties for CTCs to survive in the bloodstream and develop metastases.

The ability to generate xenograft is determined by the number of CTCs isolated and the potential of CTCs to grow *ex vivo*, which may correlate with tumor recurrence and prognosis. In this study, the cancer patient developed a pancreatic cancer two years after the resection of his primary lung tumor. This may correspond to the long time for the CTCs to grow in mice. Although this study is only limited to one xenograft, it is the first report on the generation of a NSCLC CDX from an early stage cancer patient. Our results from RNA-seq demonstrate that EMT and tumor microenvironment plays vital roles in cancer progression. The CDX shows that CTCs from early stage NSCLC cancer patient are tumorigenic. Potentially, CDXs can serve as platforms for testing targeted therapies and predicting patient outcome. Future studies need to include additional CDXs to interrogate metastatic properties of CTCs.

Chapter 5
Demonstration of personalized therapeutics using CTCs: A case of expanded CTCs from *ALK* positive lung cancer patient carrying *EML4-ALK* rearrangement

5.1 Abstract

The emergence of liquid biopsy using circulating tumor cells (CTCs) as a resource to identify genomic alterations in cancer patients has brought up new opportunities to target specific driver mutations earlier in tumor progression. The presented study identified *EML4-ALK* gene rearrangement in expanded CTCs from one patient with *ALK* positive lung adenocarcinoma. A drug resistant mutation, L1196M on *ALK* gene was detected in expanded CTCs. Two ALK inhibitors, crizotinib and ceritinib, were tested on the cultured cells. We demonstrate that it is feasible to detect genetic aberrations in CTCs and perform drug screening. The findings suggest the clinical utility of CTCs for diagnosis and prognosis of non-small cell lung cancer (NSCLC) and the prospect of monitoring CTCs for effective therapeutic intervention.

5.2 Introduction

During recent years, collective efforts have been made to perform genomic profiling of NSCLC to reveal driver mutations [61, 138, 229]. Among all the genomic aberrations identified, mutations on the genes associated with receptor tyrosine kinase are important candidates for targeted therapies. For example, *KRAS* mutations occur in nearly 30% of lung adenocarcinoma [61]. *EGFR* was found over-expressed in around 50% of NSCLC patients while mutations on *EGFR* were found in 10-20% of the patients of lung adenocarcinomas [61, 230, 231]. Gene rearrangement in anaplastic lymphoma kinase (*ALK*), *ROS1* and *RET* was also noted in 3-5% of the patients [61]. Albeit the low occurrence, *ALK* arrangement, most likely with echinoderm microtubule-like protein 4 (*EML4*), can be targeted in 60% of *ALK*-positive patients by a tyrosine kinase inhibitor (TKI), crizotinib, approved by FDA in 2011 [232-234]. However, most patients develop resistance to crizotinib within 1 to 2 years. The mutation G1269A induces stearic obstruction to crizotinib [235]. L1196M mutation, on the other hand, is a gatekeeper mutation that does not allow crizotinib to bind MET [235]. Recently, the second generation ALK inhibitor, ceritinib, was approved by FDA to combat with the acquired drug resistance to crizotinib [235].

With the rapid discoveries in sequencing as well as therapeutics, it is imperative to monitor the molecular evolution of tumors during treatment to provide effective therapies for patients. At the current time, the practice is to biopsy and rebiopsy at the time of radiological recurrence, which is invasive and not without risk. *ALK* rearrangement is identified through fluorescence *in situ* hybridization (FISH) using a break-apart probe [236]. A separation of a red and a green signal indicates gene rearrangement. FISH test of tumor is the only approved method for detecting *ALK* rearrangement [237]. In recent years, *EML4-ALK* rearrangement has been revealed in circulating tumor cells (CTCs) from peripheral blood of NSCLC cancer patients [89, 143]. Sampling of CTCs, as “liquid biopsy”, is less invasive than solid biopsy; and permits real-time monitoring of cancer progression and prediction of treatment response [27, 70, 140, 141, 238]. CTCs are cancer surrogates that have heterogeneous gene-expression

profiles and mirror genetic alterations in tumors [226]. Cultured CTCs or CTC-derived xenografts can serve as *in vitro* or *in vivo* models for drug testing [91, 180].

Here we present a study on one advanced stage lung cancer patient harboring *EML4-ALK* rearrangement in the tumor. CTCs were isolated from the peripheral blood of this patient during the initial and follow-up visit. The cells were cultured through a microfluidic co-culture model reported in our previous study [77]. FISH analysis, *ALK* sequencing and drug testing was performed on the expanded CTCs.

5.3 Methods

5.3.1 CTC isolation and expansion

Five mL of peripheral blood was drawn from the lung cancer patient into lavender EDTA tubes during the initial and follow-up visit. Blood was drawn at University of Michigan Hospital under an IRB-approved protocol. CTCs were captured by EpCAM and CD44 in three CTC-capture devices and cultured with cancer associated fibroblasts (CAFs) in the devices for two weeks and then outside devices for one month. The detailed procedure can be found in our previous study [77].

5.3.2 FISH analysis on CTCs

CTCs were spun onto polylysine-coated slides, and fixed with 1:3 acetic acid and methanol followed by air-drying. FISH test with two-color and break-apart probes was performed on the slides. An isolation of signals indicated *ALK* rearrangement and overlapping signals indicated non-rearranged gene.

5.3.3 ALK sequencing

DNA was extracted from expanded CTCs using the QIAamp DNA Mini Kit (Qiagen). Subsequently, DNA was PCR amplified with *ALK* exon 23 primers using Expand High Fidelity PCR System (Roche). The primer sets used were as followings:

ALK23F: GTAACTTTGTATCCTGTTCCTCCCAG and ALK23R: CACCCTGGGTTCCATCGAGGACTTG, flanking exon 23 of *ALK* gene [239]. The PCR products were characterized with gel electrophoresis and then purified using PCR Purification Kit (Qiagen). The concentration of the purified PCR products was measured and the PCR products were diluted for Sanger sequencing. The sequencing was performed at the University of Michigan sequencing core facility.

5.3.4 Cell lines and reagents

We obtained the cancer-associated fibroblasts (CAFs) from Dr. Diane Simeone's lab and A549, H3122 cell lines from Dr. David Beer's lab both in the Department of Surgery at the University of Michigan Hospital. CAFs, A549 and H3122 cell lines were cultured in RPMI supplemented with 10% FBS and 1% Penicillin-Streptomycin. Crizotinib was purchased from Sigma-Aldrich, and ceritinib was purchased from Selleckchem. They were both reconstituted in DMSO for drug testing experiments *in vitro*.

5.3.5 Drug testing

CTCs, CAFs, A549, or H3122 were plated at a seeding density of 1000 cells/well on 96-well plates. Each drug concentration was tested in triplicate wells. A total of six different concentrations were tested for each drug. Cells were incubated with drugs for 72hrs. After treatment, each well was incubated with Cell Proliferation Reagent WST-1 assay (Roche) for 30min, 1hr, 1.5hr and 2hr. Absorbance was measured with Biotek-Synergy Neo-plate Reader. The optimal duration of incubation was determined. The half maximal inhibitory concentration (IC50) was calculated with nonlinear regression model by Prism Graphpad.

5.4 Results

5.4.1 Detecting ALK rearrangement in expanded CTCs

One patient was presented with metastatic lung adenocarcinoma (AC). The biopsy specimen revealed *ALK* gene rearrangement by FISH. The patient was initially placed on crizotinib. A computerized tomography (CT) scan 6 months after crizotinib revealed near complete resolution of disease. However, a positron emission tomography (PET) scan at 7 months showed progression in right hilum (Figure 30). Patient underwent a bronchoscopy and biopsy of the hilar mass, which revealed a secondary mutation L1196M. He was placed on ceritinib and his repeat scans revealed a decrease in the hilar mass.

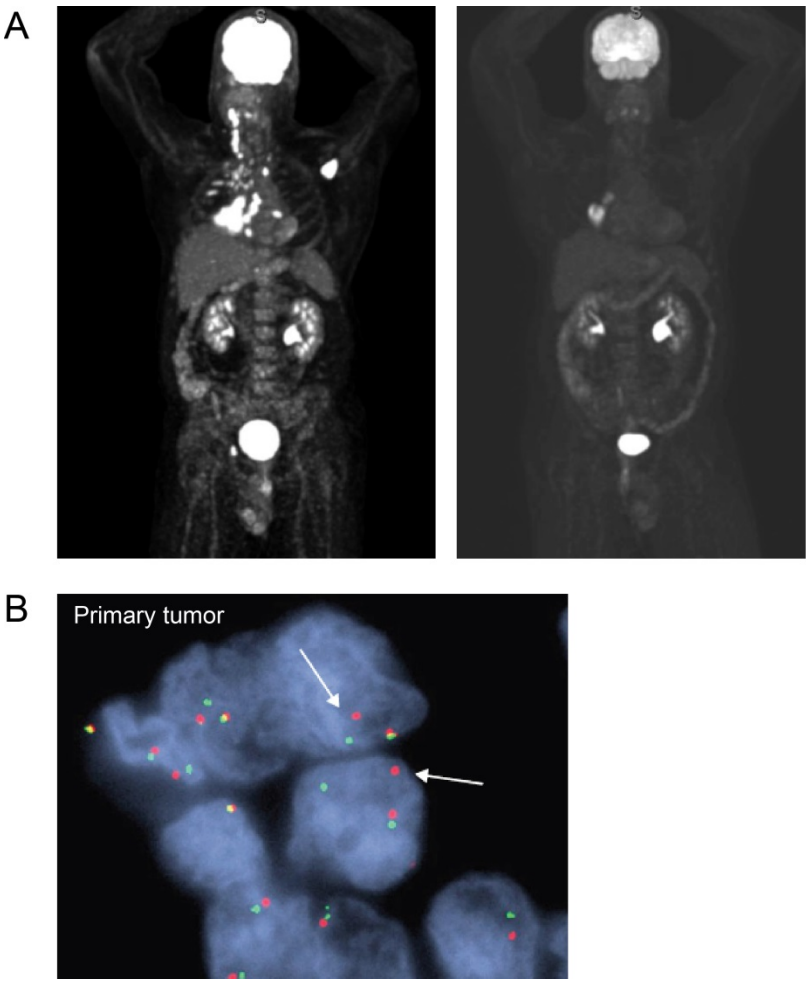

Figure 30. Tumor status of the metastatic lung cancer patient. A. CT scan at baseline and 6 months after crizotinib treatment. **B.** *EML4-ALK* gene rearrangement is detected in the primary tumor biopsy specimen by FISH.

In parallel, we isolated and cultured CTCs from his blood at the time of initial diagnosis and the follow-up visit. CTCs were cultured by a microfluidic co-culture model [77]. By the end of three-week *ex vivo* culture, most of the CAFs were sorted away by flow cytometry. The sorted CTCs were further cultured for one month. We performed FISH analysis on cultured CTCs and these CTCs revealed *ALK* rearrangements (Figure 31). *ALK* rearrangement was noted in both the initial visit and the follow-up visit. Most of the CTCs had 3 copies of *ALK* and few cells with aneuploidy as well. However, there were several CTCs with rearrangement in one allele only, which was expected.

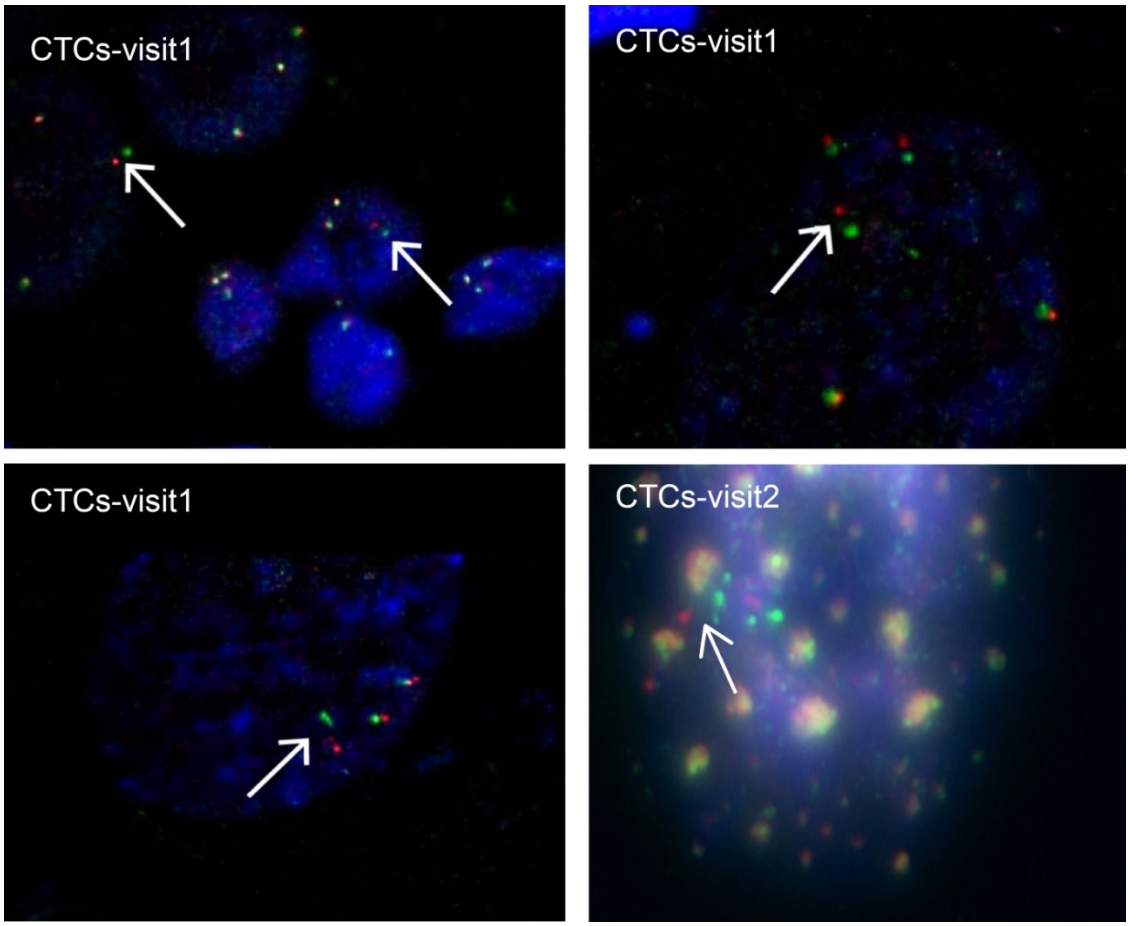

Figure 31. *ALK* rearrangement observed in cultured CTCs. Cultured CTCs, during the initial and follow-up visit, are positive for *EML4-ALK* rearrangement by FISH.

5.4.2 Identifying L1196M mutation in expanded CTCs

To examine the presence of L1196M mutation in cultured CTCs, we performed Sanger sequencing on exon 23 of *ALK* gene. CTCs didn't carry the mutation in the initial visit but they harbored the mutation in the follow-up visit (Figure 32).

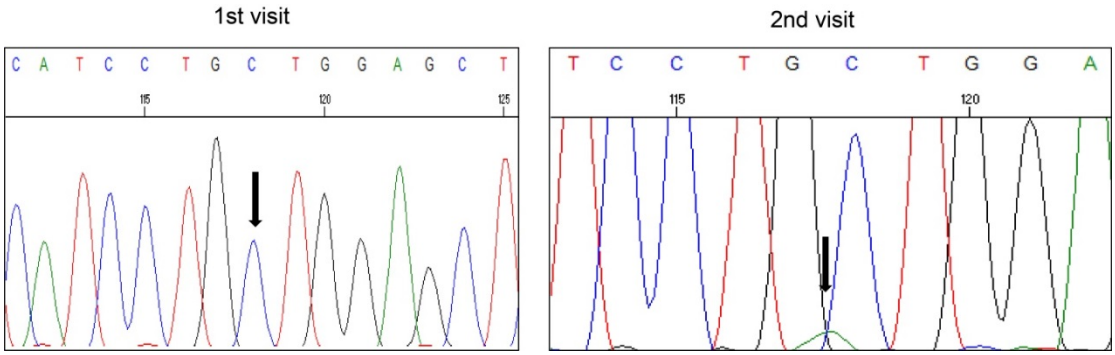

Figure 32. DNA sequencing revealed L1196M mutation in cultured CTCs. During the 1st visit, the mutation is not present in CTCs. During the 2nd visit, a small number of CTCs harbor the mutation.

5.4.3 Drug testing on expanded CTCs

After verifying that the expanded CTCs harbored *EML4-ALK* rearrangement, we conducted *in vitro* experiments to test CTCs with crizotinib and ceritinib, which were applied to the patient. Since the CTCs were mixed with CAFs, we also conducted control experiments on pure CAFs, A549 and H3122 cell lines. A549 cell line serves as a resistant cell line while H3122, harboring the *ALK* rearrangement, is a sensitive cell line. The IC50s of various cells are shown in Figure 33. The IC50 of crizotinib against CTCs is 2268nM and IC50 of ceritinib is 1664nM. These values are higher than H3122 cell line mainly because of the presence of CAFs.

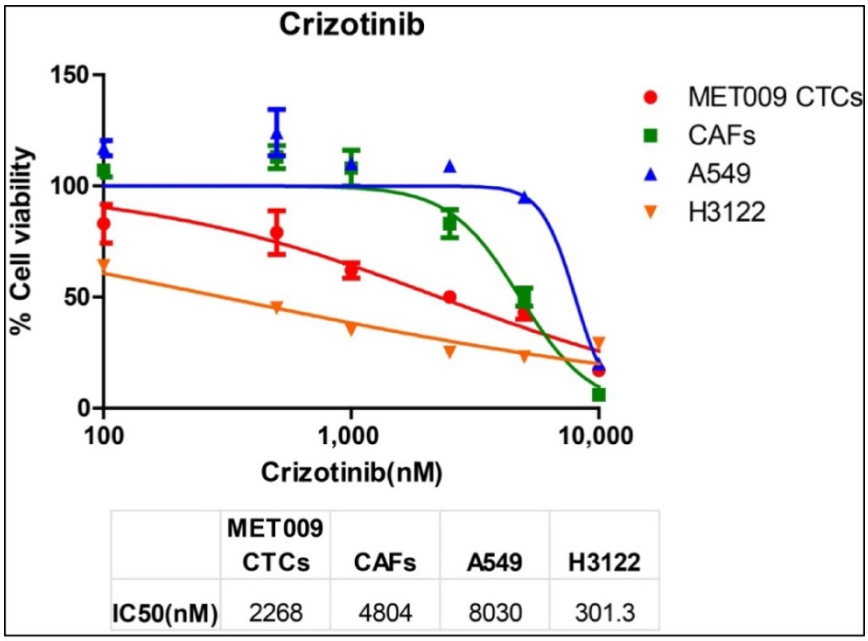

	MET009 CTCs	CAFs	A549	H3122
IC50(nM)	2268	4804	8030	301.3

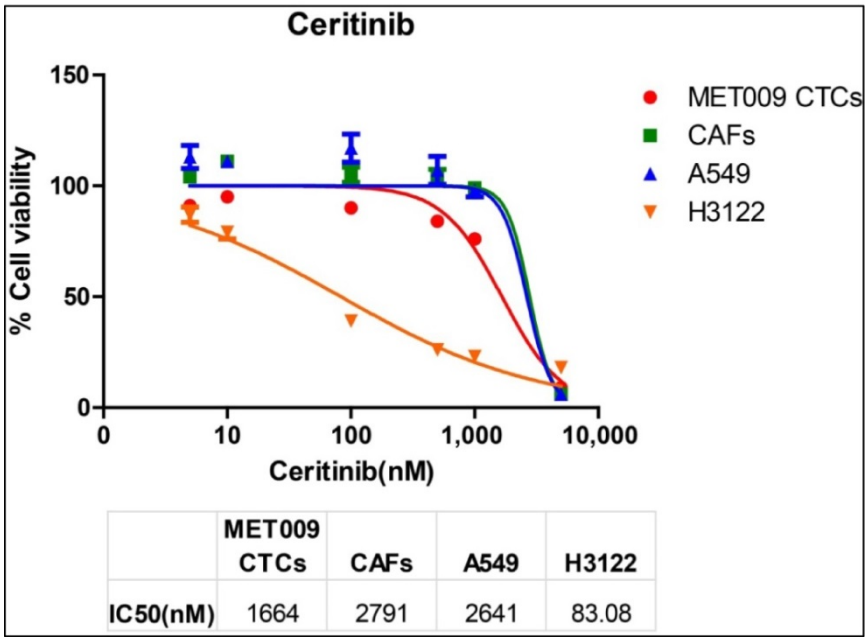

	MET009 CTCs	CAFs	A549	H3122
IC50(nM)	1664	2791	2641	83.08

Figure 33. IC50s of cells treated with crizotinib and ceritinib. Cultured CTCs are compared with pure CAFs, a resistant cell line A549 and a sensitive cell line H3122.

5.5 Discussion

In the present study, we used a microfluidic co-culture method to isolate and culture CTCs for downstream genomic analysis and drug testing. We previously reported this co-culture model effectively isolated and expanded CTCs from early stage lung cancer patients [77]. Pailler *et al*. and Faugeroux *et al*. demonstrated detecting *ALK* rearrangement patterns by the ISET method to guide therapeutic decisions. Detecting CTCs as "liquid biopsy" can complement conventional small-biopsy method, which may be limited by intra-tumoral heterogeneity. This is demonstrated by Abe *et al*. in a study to compare small biopsy with excision samples [139]. Although all 6 excision specimens were positive for *ALK* rearrangement, only 3 small biopsy samples were positive. Cultured CTCs serve as *in vitro* resources for mutation detection and drug testing to compensate for tumor biopsy specimens.

The platform used to recover CTCs is a microfluidic device coated with antibodies against epithelial cell adhesion molecule (EpCAM) and CD44. EpCAM is expressed by epithelial tumor cells in many cancer types [24]. CD44 is reported to be found in 50% of the NSCLC samples [240]. Therefore, it was included in the capturing antibody cocktail to increase the yield of CTCs for subsequent culturing. We observe *ALK* rearrangement in the cultured CTCs of the *ALK* positive patient. Similarly as the other studies, this finding shows the clinical utility of CTCs as they carry concordant driver mutations as the tumor [89, 143]. Moreover, this mutation is preserved through culturing of the CTCs. Additionally, the drug resistant L1196M mutation on *ALK* is detected in the follow-up visit but not in the initial visit. This reflects the emerging dominance of the resistant mutation in the tumor tissue. More importantly, two FDA approved drugs crizotinib and ceritinib were tested on the cultured CTCs. The IC50 of crizotinib is higher than ceritinib (2268nM v 1664nM) as reported by others [235]. Due to the presence of CAFs, the IC50s of CTCs are higher than the H3122 cell line. However, the present study demonstrates the feasibility of performing drug testing on cultured CTCs. In the future, we will perform monoculture of CTCs to circumvent the limitation.

In conclusion, our study demonstrates that the concordant *ALK* rearrangement is present in CTCs. Because of the expansion of the CTCs, drug testing was performed. Our finding is limited to one patient and the cultured CTCs are mixed with fibroblasts affecting the accuracy of the IC50s. Nonetheless, our results highlight that CTCs, as tumor surrogates, can be monitored during treatment; their genomic aberrations reflect the tumor genome in real time and can be potentially used for testing drug efficacy.

Chapter 6

Conclusion

6.1 Summary of research

6.1.1 Isolation and ex vivo expansion of CTCs

In this thesis, a CTC-capture device was developed (Chapter 2) and was further transformed to be a CTC-culture device (Chapter 3). CTCs were isolated from more than 65% early stage lung and esophageal cancer patients. Among them, more than 70% were successfully cultured, which permitted a multitude of downstream molecular assays and functional studies. Since most of the patients enrolled in the study had localized diseases, we compared the genomic aberrations in CTCs with the matched primary tumors. The presence of concordant mutations confirmed the origin of CTCs and served as another validation of the study. Taken together, we demonstrate that CTCs can be isolated from early stage cancer patients therefore may aid in early cancer detection and diagnosis. Isolated and expanded CTCs can undergo immunostaining, RNA profiling and mutation analysis, which indicate the prognostic values of CTCs.

6.1.2 CTC-derived xenograft

We observed the formation of one CTC-derived xenograft from a patient with early stage NSCLC (Chapter 4). This model demonstrated the tumorigenic potential of cultured CTCs and served as a proof-of-concept study to show the feasibility. The first-generation xenograft took about 6 months to develop and the second-generation took around 4 months. RNA-sequencing revealed some of the important genes related to EMT and tumor microenvironment enriched in the xenograft, expanded CTCs and primary tumor. These gene-related pathways may play important roles in metastasis. Future studies will focus on generating and characterizing additional xenografts and interrogate the genes identified in this preliminary study.

6.1.3 CTCs as biomarkers for personalized medicine

In one *ALK* positive patient who had advanced lung adenocarcinoma, we identified the concordant *EML4-ALK* rearrangement in the cultured CTCs during the initial and the follow-up visit (Chapter 5). The emerged point mutation, L1196M, was detected in the follow-up visit when the patient experienced disease progression and developed resistance to crizotinib. We then tested the cultured CTCs with both the first-line and second-line drug, crizotinib and ceritinib respectively. Although the IC50s of cultured CTCs were higher than the sensitive cancer cell line due to the presence of cancer associated fibroblasts, our results demonstrated CTCs mirrored the molecular evolution of tumors in real time during treatment. Future studies need to circumvent the limitation of co-culture by performing monoculture of CTCs, which will result in more accurate IC50 of applied therapeutics.

6.2 Limitations and future directions

6.2.1 Optimizing the CTC isolation technologies and culturing conditions

Microfluidics holds great promise for miniaturization and automation through handling small amount of materials and incorporating control systems. The next generation of microfluidic devices for CTC isolation will aim at achieving high detection efficiency, high cell viability, and high throughput. The CTC research field will also move from enumerating to exploring the biological and clinical significance of the cells. This will facilitate reliable detection of CTCs and incorporating CTC evaluation in routine clinical tests.

The choices of downstream assays depend largely on the isolation technologies. For example, the CellSearch technology requires CTCs to be fixed prior isolation therefore the downstream analysis is limited to immunostaining. Other non-microfluidic technologies, such as ISET and HD-CTC assay, require RBC lysis and have low purity of isolated CTCs, which are also only suitable for immunostaining. On the other hand, the presented CTC-capture device handles unprocessed whole blood and exhibits high purity of isolated CTCs. Therefore, CTCs can be lysed on-chip directly and DNA/RNA can be collected for genomic analysis.

The limitation of the CTC-capture device is that CTCs are bound to the device making functional studies and culturing challenging. In this thesis, we developed the strategy to expand CTCs directly on-chip initially followed by releasing the cells off chip. One of the drawbacks of this approach is that CTCs are co-cultured with CAFs, which can grow faster than cancer cells. Therefore, after cells are cultured on conventional well-plates, CAFs may take over the culture after several weeks. In the future, other microfluidic-based CTC isolation technologies can be used, such that the isolated CTCs are not bound to device. This will permit us to test other culturing methods such as the non-adherent, hypoxia culturing suggested by Yu *et al*. in breast cancer and Cayrefourcq *et al*. in colon cancer [99, 180].

Another limitation of the CTC-capture device is the low flow rate (1mL/hr) and small volume of blood it can process during one hour. It limits the yield of CTCs. The

future CTC-isolation device should be able to process larger volume of blood with a high flow rate. The CTC-iChip presents an example of combining the principle of immunomagnetic isolation with size based isolation, which processes blood samples with high-throughput [96]. And it can operate with either a positive selection or negative depletion mode. The positive selection mode permits CTC isolation with high specificity and purity therefore it is preferred when one wants to perform single-cell analysis or genomic analysis. On the other hand, the negative depletion mode isolates CTCs by depleting blood cells therefore it is not biased toward surface antigen expression. It can be ideal for CTC culturing when one is not sure which subpopulation of CTCs will eventually grow *in vitro*.

Once a versatile microfluidic platform is developed for a specific type of cancer, the CTC culturing conditions should be optimized. Several key factors are worth considering including the medium composition (growth factors and conditioned medium), the incubator environment (hypoxia v normoxia) and culturing environment (2D v 3D). After a reliable culturing condition is determined, culturing CTCs can be included in pre-clinical testing for drug susceptibility and responses to radiation therapy.

6.2.2 CTCs in lung cancer

Over the past decade, the advancement of technological innovation to isolate CTCs has allowed investigation of their clinical utility [168, 241]. We now understand that CTCs contain heterogeneous populations of both epithelial and mesenchymal phenotypes [242]. They harbor genetic alterations that correspond to primary tumor and metastatic sites. The discordant or unique mutations carried by CTCs that are absent in primary tumors reflect heterogeneity in primary tumor or small amount of subclonal populations, which are missed by conventional sequencing methods [243]. Together with cfDNA, CTCs have been shown as promising surrogates of tumor burden and activating mutations for targeted therapies. Specifically, CTCs offer opportunities to perform biological studies such as phenotypic and histological characterization, invasion &

migration assays, *in vitro* expansion, drug testing and deriving xenografts in animal models.

Despite current advances in the field, CTC markers for lung cancer still fall short, when it comes to factoring inter-tumor and intra-tumor heterogeneity [244]. We have seen this as discordance in markers between primary/metastatic cancers and CTC genotypes or phenotypes. Additionally, there is still the problem of contaminating white blood cells, despite the emergence of several technologies that enable positive selection or negative depletion of leukocytes. These factors along with a low yield in earlier stages of lung cancer handicap functional studies related to CTCs (for e.g. ability to detect metastasis initiation properties of lung CTCs as demonstrated in other cancers using EPISPOT [99, 245] or invasion assay[77, 246]). *In vivo* studies of CTCs through generating CTC-derived xenografts generally require larger numbers of cells [91, 98], which are hard to obtain from early stage lung cancer patients; this is to some extent overcome by increasing blood throughput and sensitivity of isolation methods. Biology of metastasis as related to a cascade of events has vast implications in drug development. The study of CTCs opens up a window for understanding this process. One study found that the *WNT2* gene was enriched in breast CTCs and another study showed that genes involved in ECM were highly expressed in pancreatic CTCs [226, 247]. These findings suggested that these genes and pathways could be targeted therapeutically to halt metastasis and likely improve survival. However, this type of study has not been done in lung cancer. Understanding metastasis initiating capabilities of CTCs in lung cancer will have a huge impact on providing specific adjuvant therapies targeted at these CTCs to reduce metastasis and improve survival. The next few years will allow us to further study these biological processes in depth and allow meaningful translation into the clinic.

References

1. Whitesides, G.M. (2006). The origins and the future of microfluidics. Nature *442*, 368-373.
2. Hong, J.W., and Quake, S.R. (2003). Integrated nanoliter systems. Nature biotechnology *21*, 1179-1183.
3. Reyes, D.R., Iossifidis, D., Auroux, P.A., and Manz, A. (2002). Micro total analysis systems. 1. Introduction, theory, and technology. Analytical chemistry *74*, 2623-2636.
4. Auroux, P.A., Iossifidis, D., Reyes, D.R., and Manz, A. (2002). Micro total analysis systems. 2. Analytical standard operations and applications. Analytical chemistry *74*, 2637-2652.
5. Manz, A.e.a. (1992). Planar chips technology for miniaturization and integration of separation techniques into monitoring systems: capillary electrophoresis on a chip. J. Chromatogr, 253–258.
6. Jemal, A., Bray, F., Center, M.M., Ferlay, J., Ward, E., and Forman, D. (2011). Global cancer statistics. CA: a cancer journal for clinicians *61*, 69-90.
7. Siegel, R., Ward, E., Brawley, O., and Jemal, A. (2011). Cancer statistics, 2011: the impact of eliminating socioeconomic and racial disparities on premature cancer deaths. CA: a cancer journal for clinicians *61*, 212-236.
8. Alexis, F.R., J. W. Richie, J. P. Radovic-Moreno, A. F. Langer, R. Farokhzad, O. C. (2008). New frontiers in nanotechnology for cancer treatment. Urologic oncology *26*, 74-85.
9. Seigneuric, R., Markey, L., Nuyten, D.S., Dubernet, C., Evelo, C.T., Finot, E., and Garrido, C. (2010). From nanotechnology to nanomedicine: applications to cancer research. Current molecular medicine *10*, 640-652.
10. Fabian, T.K., Fejerdy, P., and Csermely, P. (2008). Salivary genomics, transcriptomics and proteomics: The emerging concept of the oral ecosystem and their use in the early diagnosis of cancer and other diseases. Curr Genomics *9*, 11-21.
11. Diehl, F., Schmidt, K., Choti, M.A., Romans, K., Goodman, S., Li, M., Thornton, K., Agrawal, N., Sokoll, L., Szabo, S.A., et al. (2008). Circulating mutant DNA to assess tumor dynamics. Nat Med *14*, 985-990.
12. Mitchell, P.S., Parkin, R.K., Kroh, E.M., Fritz, B.R., Wyman, S.K., Pogosova-Agadjanyan, E.L., Peterson, A., Noteboom, J., O'Briant, K.C., Allen, A., et al. (2008). Circulating microRNAs as stable blood-based markers for cancer detection. Proceedings of the National Academy of Sciences *105*, 10513-10518.
13. Roessler, M. (2005). Identification of Nicotinamide N-Methyltransferase as a Novel Serum Tumor Marker for Colorectal Cancer. Clinical Cancer Research *11*, 6550-6557.
14. Valenti, R. (2006). Human Tumor-Released Microvesicles Promote the Differentiation of Myeloid Cells with Transforming Growth Factor- -Mediated Suppressive Activity on T Lymphocytes. Cancer Research *66*, 9290-9298.
15. den Toonder, J. (2011). Circulating tumor cells: the Grand Challenge. Lab on a chip *11*, 375-377.
16. Krivacic, R.T., Ladanyi, A., Curry, D.N., Hsieh, H.B., Kuhn, P., Bergsrud, D.E., Kepros, J.F., Barbera, T., Ho, M.Y., Chen, L.B., et al. (2004). A rare-cell detector for cancer. Proceedings of the National Academy of Sciences of the United States of America *101*, 10501-10504.
17. Heath, J.R., and Davis, M.E. (2008). Nanotechnology and cancer. Annual review of medicine *59*, 251-265.
18. Sorger, P.K. (2008). Microfluidics closes in on point-of-care assays. Nature biotechnology *26*, 1345-1346.

19. Bednarz-Knoll, N., Alix-Panabieres, C., and Pantel, K. (2012). Plasticity of disseminating cancer cells in patients with epithelial malignancies. Cancer Metastasis Rev.
20. Maheswaran, S., and Haber, D.A. (2010). Circulating tumor cells: a window into cancer biology and metastasis. Current Opinion in Genetics & Development *20*, 96-99.
21. Nguyen, D.X., and Massagué, J. (2007). Genetic determinants of cancer metastasis. Nature Reviews Genetics *8*, 341-352.
22. Baeuerle, P.A., and Gires, O. (2007). EpCAM (CD326) finding its role in cancer. Br J Cancer *96*, 417-423.
23. Went, P., Vasei, M., Bubendorf, L., Terracciano, L., Tornillo, L., Riede, U., Kononen, J., Simon, R., Sauter, G., and Baeuerle, P.A. (2006). Frequent high-level expression of the immunotherapeutic target Ep-CAM in colon, stomach, prostate and lung cancers. Br J Cancer *94*, 128-135.
24. Went, P.T., Lugli, A., Meier, S., Bundi, M., Mirlacher, M., Sauter, G., and Dirnhofer, S. (2004). Frequent EpCam protein expression in human carcinomas. Hum Pathol *35*, 122-128.
25. Kaiser, J. (2010). Medicine. Cancer's circulation problem. Science *327*, 1072-1074.
26. Nagrath, S., Sequist, L.V., Maheswaran, S., Bell, D.W., Irimia, D., Ulkus, L., Smith, M.R., Kwak, E.L., Digumarthy, S., Muzikansky, A., et al. (2007). Isolation of rare circulating tumour cells in cancer patients by microchip technology. Nature *450*, 1235-1239.
27. Maheswaran, S., Sequist, L.V., Nagrath, S., Ulkus, L., Brannigan, B., Collura, C.V., Inserra, E., Diederichs, S., Iafrate, A.J., Bell, D.W., et al. (2008). Detection of mutations in EGFR in circulating lung-cancer cells. N Engl J Med *359*, 366-377.
28. Stott, S.L., Lee, R.J., Nagrath, S., Yu, M., Miyamoto, D.T., Ulkus, L., Inserra, E.J., Ulman, M., Springer, S., Nakamura, Z., et al. (2010). Isolation and characterization of circulating tumor cells from patients with localized and metastatic prostate cancer. Sci Transl Med *2*, 25ra23.
29. Saliba, A.E., Saias, L., Psychari, E., Minc, N., Simon, D., Bidard, F.C., Mathiot, C., Pierga, J.Y., Fraisier, V., Salamero, J., et al. (2010). Microfluidic sorting and multimodal typing of cancer cells in self-assembled magnetic arrays. Proceedings of the National Academy of Sciences of the United States of America *107*, 14524-14529.
30. Dharmasiri, U., Balamurugan, S., Adams, A.A., Okagbare, P.I., Obubuafo, A., and Soper, S.A. (2009). Highly efficient capture and enumeration of low abundance prostate cancer cells using prostate-specific membrane antigen aptamers immobilized to a polymeric microfluidic device. Electrophoresis *30*, 3289-3300.
31. Nora Dickson, M., Tsinberg, P., Tang, Z., Bischoff, F.Z., Wilson, T., and Leonard, E.F. (2011). Efficient capture of circulating tumor cells with a novel immunocytochemical microfluidic device. Biomicrofluidics *5*, 34119-3411915.
32. Shannon L. Stott, C.-H.H., Dina I. Tsukrov, Min Yud, David T. Miyamoto, Belinda A. Waltman,, S. Michael Rothenberg, A.M.S., Malgorzata E. Smas, George K. Korir, Frederick P. Floyd, Jr., Anna J. Gilman,, Jenna B. Lord, D.W., Simeon Springer, Daniel Irimia, Sunitha Nagrath, Lecia V. Sequist,, and Richard J. Lee, K.J.I., Shyamala Maheswaran, Daniel A. Haber, and Mehmet Toner (2010). Isolation of circulating tumor cells using a microvortex-generating herringbone-chip. PNAS *107*, 18392-18397.
33. Gleghorn, J.P., Pratt, E.D., Denning, D., Liu, H., Bander, N.H., Tagawa, S.T., Nanus, D.M., Giannakakou, P.A., and Kirby, B.J. (2010). Capture of circulating tumor cells from whole blood of prostate cancer patients using geometrically enhanced differential immunocapture (GEDI) and a prostate-specific antibody. Lab on a chip *10*, 27.
34. Myung, J.H., Launiere, C.A., Eddington, D.T., and Hong, S. (2010). Enhanced tumor cell isolation by a biomimetic combination of E-selectin and anti-EpCAM: implications for the effective separation of circulating tumor cells (CTCs). Langmuir *26*, 8589-8596.

35. Dharmasiri, U., Njoroge, S.K., Witek, M.A., Adebiyi, M.G., Kamande, J.W., Hupert, M.L., Barany, F., and Soper, S.A. (2011). High-throughput selection, enumeration, electrokinetic manipulation, and molecular profiling of low-abundance circulating tumor cells using a microfluidic system. Analytical chemistry *83*, 2301-2309.
36. Hoshino, K., Huang, Y.Y., Lane, N., Huebschman, M., Uhr, J.W., Frenkel, E.P., and Zhang, X. (2011). Microchip-based immunomagnetic detection of circulating tumor cells. Lab on a chip *11*, 3449-3457.
37. Kang, J.H., Krause, S., Tobin, H., Mammoto, A., Kanapathipillai, M., and Ingber, D.E. (2012). A combined micromagnetic-microfluidic device for rapid capture and culture of rare circulating tumor cells. Lab on a chip *12*, 2175-2181.
38. Santos, J., Punnoose, E.A., Atwal, S.K., Spoerke, J.M., Savage, H., Pandita, A., Yeh, R.-F., Pirzkall, A., Fine, B.M., Amler, L.C., et al. (2010). Molecular Biomarker Analyses Using Circulating Tumor Cells. PLoS ONE *5*, e12517.
39. Hou, H.W., Bhagat, A.A.S., Lee, W.C., Huang, S., Han, J., and Lim, C.T. (2011). Microfluidic Devices for Blood Fractionation. Micromachines *2*, 319-343.
40. Zheng, S., Lin, H., Liu, J.-Q., Balic, M., Datar, R., Cote, R.J., and Tai, Y.-C. (2007). Membrane microfilter device for selective capture, electrolysis and genomic analysis of human circulating tumor cells. Journal of Chromatography A *1162*, 154-161.
41. Zheng, S., Lin, H.K., Lu, B., Williams, A., Datar, R., Cote, R.J., and Tai, Y.C. (2011). 3D microfilter device for viable circulating tumor cell (CTC) enrichment from blood. Biomed Microdevices *13*, 203-213.
42. Kuo, J.S., Zhao, Y., Schiro, P.G., Ng, L., Lim, D.S., Shelby, J.P., and Chiu, D.T. (2010). Deformability considerations in filtration of biological cells. Lab on a chip *10*, 837-842.
43. Hur, S.C., Henderson-MacLennan, N.K., McCabe, E.R., and Di Carlo, D. (2011). Deformability-based cell classification and enrichment using inertial microfluidics. Lab on a chip *11*, 912-920.
44. Lim, E.J., Ober, T.J., Edd, J.F., McKinley, G.H., and Toner, M. (2012). Visualization of microscale particle focusing in diluted and whole blood using particle trajectory analysis. Lab on a chip *12*, 2199.
45. Cristofanilli, M., Budd, G.T., Ellis, M.J., Stopeck, A., Matera, J., Miller, M.C., Reuben, J.M., Doyle, G.V., Allard, W.J., Terstappen, L.W., et al. (2004). Circulating tumor cells, disease progression, and survival in metastatic breast cancer. N Engl J Med *351*, 781-791.
46. Talasaz, A.H., Powell, A.A., Huber, D.E., Berbee, J.G., Roh, K.H., Yu, W., Xiao, W., Davis, M.M., Pease, R.F., Mindrinos, M.N., et al. (2009). Isolating highly enriched populations of circulating epithelial cells and other rare cells from blood using a magnetic sweeper device. Proceedings of the National Academy of Sciences *106*, 3970-3975.
47. Moon, H.-S., Kwon, K., Kim, S.-I., Han, H., Sohn, J., Lee, S., and Jung, H.-I. (2011). Continuous separation of breast cancer cells from blood samples using multi-orifice flow fractionation (MOFF) and dielectrophoresis (DEP). Lab on a chip *11*, 1118.
48. Chen, C.L., Chen, K.C., Pan, Y.C., Lee, T.P., Hsiung, L.C., Lin, C.M., Chen, C.Y., Lin, C.H., Chiang, B.L., and Wo, A.M. (2011). Separation and detection of rare cells in a microfluidic disk via negative selection. Lab on a chip *11*, 474-483.
49. Sieuwerts, A.M., Kraan, J., Bolt, J., van der Spoel, P., Elstrodt, F., Schutte, M., Martens, J.W., Gratama, J.W., Sleijfer, S., and Foekens, J.A. (2009). Anti-epithelial cell adhesion molecule antibodies and the detection of circulating normal-like breast tumor cells. J Natl Cancer Inst *101*, 61-66.
50. Society, A.C. (2014). Cancer Facts & Figures 2014. Atlanta: American Cancer Society.
51. Siegel, R., Ma, J., Zou, Z., and Jemal, A. (2014). Cancer statistics, 2014. CA: a cancer journal for clinicians *64*, 9-29.
52. Services, U.S.D.o.H.a.H. (2004). The Health Consequences of Smoking: A Report of the Surgeon General. Atlanta, GA: U.S. Department of Health and Human Services, Centers

for Disease Control and Prevention, National Center for Chronic Disease Prevention and Health Promotion, Office on Smoking and Health, .

53. Namba, Y., Kijima, T., Yokota, S., Niinaka, M., Kawamura, S., Iwasaki, T., Takeda, Y., Kimura, H., Okada, T., Yamaguchi, T., et al. (2004). Gefitinib in patients with brain metastases from non-small-cell lung cancer: review of 15 clinical cases. Clin Lung Cancer *6*, 123-128.
54. Siegel, R., Naishadham, D., and Jemal, A. (2013). Cancer statistics, 2013. CA: a cancer journal for clinicians *63*, 11-30.
55. Ries LAG, Y.J., Keel GE, Eisner MP, Lin YD, Horner M-J (editors) (2007). SEER Survival Monograph: Cancer Survival Among Adults: U.S. SEER Program, 1988-2001, Patient and Tumor Characteristics. National Cancer Institute, SEER Program, NIH Pub. No. 07-6215, Bethesda, MD, 2007.
56. Aberle, D.R., Adams, A.M., Berg, C.D., Black, W.C., Clapp, J.D., Fagerstrom, R.M., Gareen, I.F., Gatsonis, C., Marcus, P.M., and Sicks, J.D. (2011). Reduced lung-cancer mortality with low-dose computed tomographic screening. N Engl J Med *365*, 395-409.
57. Ettinger, D.S., Akerley, W., Borghaei, H., Chang, A.C., Cheney, R.T., Chirieac, L.R., D'Amico, T.A., Demmy, T.L., Ganti, A.K., Govindan, R., et al. (2012). Non-small cell lung cancer. J Natl Compr Canc Netw *10*, 1236-1271.
58. Kobayashi, S., Boggon, T.J., Dayaram, T., Janne, P.A., Kocher, O., Meyerson, M., Johnson, B.E., Eck, M.J., Tenen, D.G., and Halmos, B. (2005). EGFR mutation and resistance of non-small-cell lung cancer to gefitinib. N Engl J Med *352*, 786-792.
59. Engelman, J.A., Zejnullahu, K., Mitsudomi, T., Song, Y., Hyland, C., Park, J.O., Lindeman, N., Gale, C.M., Zhao, X., Christensen, J., et al. (2007). MET amplification leads to gefitinib resistance in lung cancer by activating ERBB3 signaling. Science *316*, 1039-1043.
60. Alix-Panabieres, C., and Pantel, K. (2013). Circulating tumor cells: liquid biopsy of cancer. Clin Chem *59*, 110-118.
61. Alix-Panabieres, C., and Pantel, K. (2014). Challenges in circulating tumour cell research. Nat Rev Cancer *14*, 623-631.
62. Bettegowda, C., Sausen, M., Leary, R.J., Kinde, I., Wang, Y., Agrawal, N., Bartlett, B.R., Wang, H., Luber, B., Alani, R.M., et al. (2014). Detection of circulating tumor DNA in early- and late-stage human malignancies. Sci Transl Med *6*, 224ra224.
63. Shen, J., Liao, J., Guarnera, M.A., Fang, H., Cai, L., Stass, S.A., and Jiang, F. (2014). Analysis of MicroRNAs in sputum to improve computed tomography for lung cancer diagnosis. J Thorac Oncol *9*, 33-40.
64. Diaz, L.A., Jr., and Bardelli, A. (2014). Liquid biopsies: genotyping circulating tumor DNA. J Clin Oncol *32*, 579-586.
65. Nilsson, R.J., Balaj, L., Hulleman, E., van Rijn, S., Pegtel, D.M., Walraven, M., Widmark, A., Gerritsen, W.R., Verheul, H.M., Vandertop, W.P., et al. (2011). Blood platelets contain tumor-derived RNA biomarkers. Blood *118*, 3680-3683.
66. Gevensleben, H., Garcia-Murillas, I., Graeser, M.K., Schiavon, G., Osin, P., Parton, M., Smith, I.E., Ashworth, A., and Turner, N.C. (2013). Noninvasive detection of HER2 amplification with plasma DNA digital PCR. Clin Cancer Res *19*, 3276-3284.
67. Thierry, A.R., Mouliere, F., El Messaoudi, S., Mollevi, C., Lopez-Crapez, E., Rolet, F., Gillet, B., Gongora, C., Dechelotte, P., Robert, B., et al. (2014). Clinical validation of the detection of KRAS and BRAF mutations from circulating tumor DNA. Nat Med *20*, 430-435.
68. Taly, V., Pekin, D., Benhaim, L., Kotsopoulos, S.K., Le Corre, D., Li, X., Atochin, I., Link, D.R., Griffiths, A.D., Pallier, K., et al. (2013). Multiplex picodroplet digital PCR to detect KRAS mutations in circulating DNA from the plasma of colorectal cancer patients. Clin Chem *59*, 1722-1731.

69. Tjensvoll, K., Nordgard, O., and Smaaland, R. (2014). Circulating tumor cells in pancreatic cancer patients: methods of detection and clinical implications. Int J Cancer *134*, 1-8.
70. Krebs, M.G., Sloane, R., Priest, L., Lancashire, L., Hou, J.M., Greystoke, A., Ward, T.H., Ferraldeschi, R., Hughes, A., Clack, G., et al. (2011). Evaluation and prognostic significance of circulating tumor cells in patients with non-small-cell lung cancer. J Clin Oncol *29*, 1556-1563.
71. Cristofanilli, M., Hayes, D.F., Budd, G.T., Ellis, M.J., Stopeck, A., Reuben, J.M., Doyle, G.V., Matera, J., Allard, W.J., Miller, M.C., et al. (2005). Circulating tumor cells: a novel prognostic factor for newly diagnosed metastatic breast cancer. J Clin Oncol *23*, 1420-1430.
72. Botteri, E., Sandri, M.T., Bagnardi, V., Munzone, E., Zorzino, L., Rotmensz, N., Casadio, C., Cassatella, M.C., Esposito, A., Curigliano, G., et al. (2010). Modeling the relationship between circulating tumour cells number and prognosis of metastatic breast cancer. Breast Cancer Res Tr *122*, 211-217.
73. Kurihara, T., Itoi, T., Sofuni, A., Itokawa, F., Tsuchiya, T., Tsuji, S., Ishii, K., Ikeuchi, N., Tsuchida, A., Kasuya, K., et al. (2008). Detection of circulating tumor cells in patients with pancreatic cancer: a preliminary result. J Hepatobiliary Pancreat Surg *15*, 189-195.
74. Shah, S.P., Morin, R.D., Khattra, J., Prentice, L., Pugh, T., Burleigh, A., Delaney, A., Gelmon, K., Guliany, R., Senz, J., et al. (2009). Mutational evolution in a lobular breast tumour profiled at single nucleotide resolution. Nature *461*, 809-U867.
75. Pantel, K., and Alix-Panabieres, C. (2013). Real-time liquid biopsy in cancer patients: fact or fiction? Cancer Res *73*, 6384-6388.
76. Cen, P., Ni, X., Yang, J., Graham, D.Y., and Li, M. (2012). Circulating tumor cells in the diagnosis and management of pancreatic cancer. Biochim Biophys Acta *1826*, 350-356.
77. Zhang, Z., Shiratsuchi, H., Lin, J., Chen, G.A., Reddy, R.M., Azizi, E., Fouladdel, S., Chang, A.C., Lin, L., Jiang, H., et al. (2014). Expansion of CTCs from early stage lung cancer patients using a microfluidic co-culture model. Oncotarget *5*, 12383-12397.
78. Soeth, E., Grigoleit, U., Moellmann, B., Roder, C., Schniewind, B., Kremer, B., Kalthoff, H., and Vogel, I. (2005). Detection of tumor cell dissemination in pancreatic ductal carcinoma patients by CK 20 RT-PCR indicates poor survival. Journal of cancer research and clinical oncology *131*, 669-676.
79. Khoja, L., Backen, A., Sloane, R., Menasce, L., Ryder, D., Krebs, M., Board, R., Clack, G., Hughes, A., Blackhall, F., et al. (2012). A pilot study to explore circulating tumour cells in pancreatic cancer as a novel biomarker. Br J Cancer *106*, 508-516.
80. Hoffmann, K., Kerner, C., Wilfert, W., Mueller, M., Thiery, J., Hauss, J., and Witzigmann, H. (2007). Detection of disseminated pancreatic cells by amplification of cytokeratin-19 with quantitative RT-PCR in blood, bone marrow and peritoneal lavage of pancreatic carcinoma patients. World journal of gastroenterology : WJG *13*, 257-263.
81. de Albuquerque, A., Kubisch, I., Breier, G., Stamminger, G., Fersis, N., Eichler, A., Kaul, S., and Stolzel, U. (2012). Multimarker gene analysis of circulating tumor cells in pancreatic cancer patients: a feasibility study. Oncology *82*, 3-10.
82. Punnoose, E.A., Atwal, S., Liu, W., Raja, R., Fine, B.M., Hughes, B.G., Hicks, R.J., Hampton, G.M., Amler, L.C., Pirzkall, A., et al. (2012). Evaluation of circulating tumor cells and circulating tumor DNA in non-small cell lung cancer: association with clinical endpoints in a phase II clinical trial of pertuzumab and erlotinib. Clin Cancer Res *18*, 2391-2401.
83. Muinelo-Romay, L., Vieito, M., Abalo, A., Nocelo, M.A., Baron, F., Anido, U., Brozos, E., Vazquez, F., Aguin, S., Abal, M., et al. (2014). Evaluation of Circulating Tumor Cells and Related Events as Prognostic Factors and Surrogate Biomarkers in Advanced NSCLC Patients Receiving First-Line Systemic Treatment. Cancers (Basel) *6*, 153-165.

84. Tanaka, F., Yoneda, K., Kondo, N., Hashimoto, M., Takuwa, T., Matsumoto, S., Okumura, Y., Rahman, S., Tsubota, N., Tsujimura, T., et al. (2009). Circulating Tumor Cell as a Diagnostic Marker in Primary Lung Cancer. Clinical Cancer Research *15*, 6980-6986.
85. Krebs, M.G., Hou, J.M., Sloane, R., Lancashire, L., Priest, L., Nonaka, D., Ward, T.H., Backen, A., Clack, G., Hughes, A., et al. (2012). Analysis of circulating tumor cells in patients with non-small cell lung cancer using epithelial marker-dependent and -independent approaches. J Thorac Oncol *7*, 306-315.
86. Hofman, V., Bonnetaud, C., Ilie, M.I., Vielh, P., Vignaud, J.M., Flejou, J.F., Lantuejoul, S., Piaton, E., Mourad, N., Butori, C., et al. (2011). Preoperative circulating tumor cell detection using the isolation by size of epithelial tumor cell method for patients with lung cancer is a new prognostic biomarker. Clin Cancer Res *17*, 827-835.
87. Wendel, M., Bazhenova, L., Boshuizen, R., Kolatkar, A., Honnatti, M., Cho, E.H., Marrinucci, D., Sandhu, A., Perricone, A., Thistlethwaite, P., et al. (2012). Fluid biopsy for circulating tumor cell identification in patients with early-and late-stage non-small cell lung cancer: a glimpse into lung cancer biology. Phys Biol *9*, 016005.
88. Ni, X.H., Zhuo, M.L., Su, Z., Duan, J.C., Gao, Y., Wang, Z.J., Zong, C.H., Bai, H., Chapman, A.R., Zhao, J., et al. (2013). Reproducible copy number variation patterns among single circulating tumor cells of lung cancer patients. Proceedings of the National Academy of Sciences of the United States of America *110*, 21083-21088.
89. Pailler, E., Adam, J., Barthelemy, A., Oulhen, M., Auger, N., Valent, A., Borget, I., Planchard, D., Taylor, M., Andre, F., et al. (2013). Detection of circulating tumor cells harboring a unique ALK rearrangement in ALK-positive non-small-cell lung cancer. J Clin Oncol *31*, 2273-2281.
90. Pailler, E., Auger, N., Lindsay, C.R., Vielh, P., Islas-Morris-Hernandez, A., Borget, I., Ngo-Camus, M., Planchard, D., Soria, J.C., Besse, B., et al. (2015). High Level of Chromosomal Instability in Circulating Tumor Cells of ROS1-Rearranged Non-Small-Cell Lung Cancer. Ann Oncol.
91. Hodgkinson, C.L., Morrow, C.J., Li, Y., Metcalf, R.L., Rothwell, D.G., Trapani, F., Polanski, R., Burt, D.J., Simpson, K.L., Morris, K., et al. (2014). Tumorigenicity and genetic profiling of circulating tumor cells in small-cell lung cancer. Nat Med *20*, 897-903.
92. Riethdorf, S., Fritsche, H., Muller, V., Rau, T., Schindlbeck, C., Rack, B., Janni, W., Coith, C., Beck, K., Janicke, F., et al. (2007). Detection of circulating tumor cells in peripheral blood of patients with metastatic breast cancer: a validation study of the CellSearch system. Clin Cancer Res *13*, 920-928.
93. Ruiz, C., Li, J.L., Luttgen, M.S., Kolatkar, A., Kendall, J.T., Flores, E., Topp, Z., Samlowski, W.E., McClay, E., Bethel, K., et al. (2015). Limited genomic heterogeneity of circulating melanoma cells in advanced stage patients. Physical Biology *12*.
94. Talasaz, A.H., Powell, A.A., Huber, D.E., Berbee, J.G., Roh, K.H., Yu, W., Xiao, W.Z., Davis, M.M., Pease, R.F., Mindrinos, M.N., et al. (2009). Isolating highly enriched populations of circulating epithelial cells and other rare cells from blood using a magnetic sweeper device. Proceedings of the National Academy of Sciences of the United States of America *106*, 3970-3975.
95. Vona, G., Sabile, A., Louha, M., Sitruk, V., Romana, S., Schutze, K., Capron, F., Franco, D., Pazzagli, M., Vekemans, M., et al. (2000). Isolation by size of epithelial tumor cells : a new method for the immunomorphological and molecular characterization of circulatingtumor cells. Am J Pathol *156*, 57-63.
96. Ozkumur, E., Shah, A.M., Ciciliano, J.C., Emmink, B.L., Miyamoto, D.T., Brachtel, E., Yu, M., Chen, P.I., Morgan, B., Trautwein, J., et al. (2013). Inertial focusing for tumor

antigen-dependent and -independent sorting of rare circulating tumor cells. Sci Transl Med *5*, 179ra147.
97. Zhang, L., Ridgway, L.D., Wetzel, M.D., Ngo, J., Yin, W., Kumar, D., Goodman, J.C., Groves, M.D., and Marchetti, D. (2013). The identification and characterization of breast cancer CTCs competent for brain metastasis. Sci Transl Med *5*, 180ra148.
98. Baccelli, I., Schneeweiss, A., Riethdorf, S., Stenzinger, A., Schillert, A., Vogel, V., Klein, C., Saini, M., Bauerle, T., Wallwiener, M., et al. (2013). Identification of a population of blood circulating tumor cells from breast cancer patients that initiates metastasis in a xenograft assay. Nature biotechnology *31*, 539-U143.
99. Cayrefourcq, L., Mazard, T., Joosse, S., Solassol, J., Ramos, J., Assenat, E., Schumacher, U., Costes, V., Maudelonde, T., Pantel, K., et al. (2015). Establishment and characterization of a cell line from human circulating colon cancer cells. Cancer Res *75*, 892-901.
100. Yoon, H.J., Kim, T.H., Zhang, Z., Azizi, E., Pham, T.M., Paoletti, C., Lin, J., Ramnath, N., Wicha, M.S., Hayes, D.F., et al. (2013). Sensitive capture of circulating tumour cells by functionalized graphene oxide nanosheets. Nat Nanotechnol *8*, 735-741.
101. Miller, M.C., Doyle, G.V., and Terstappen, L.W. (2010). Significance of Circulating Tumor Cells Detected by the CellSearch System in Patients with Metastatic Breast Colorectal and Prostate Cancer. J Oncol *2010*, 617421.
102. Chen, X., Wang, X., He, H., Liu, Z., Hu, J.F., and Li, W. (2015). Combination of circulating tumor cells with serum carcinoembryonic antigen enhances clinical prediction of non-small cell lung cancer. PLoS One *10*, e0126276.
103. Stott, S.L., Hsu, C.H., Tsukrov, D.I., Yu, M., Miyamoto, D.T., Waltman, B.A., Rothenberg, S.M., Shah, A.M., Smas, M.E., Korir, G.K., et al. (2010). Isolation of circulating tumor cells using a microvortex-generating herringbone-chip. Proceedings of the National Academy of Sciences of the United States of America *107*, 18392-18397.
104. Wang, C., Ye, M., Cheng, L., Li, R., Zhu, W., Shi, Z., Fan, C., He, J., Liu, J., and Liu, Z. (2015). Simultaneous isolation and detection of circulating tumor cells with a microfluidic silicon-nanowire-array integrated with magnetic upconversion nanoprobes. Biomaterials *54*, 55-62.
105. Wit, S., Dalum, G., Lenferink, A.T., Tibbe, A.G., Hiltermann, T.J., Groen, H.J., van Rijn, C.J., and Terstappen, L.W. (2015). The detection of EpCAM(+) and EpCAM(-) circulating tumor cells. Sci Rep *5*, 12270.
106. De Giorgi, V., Pinzani, P., Salvianti, F., Panelos, J., Paglierani, M., Janowska, A., Grazzini, M., Wechsler, J., Orlando, C., Santucci, M., et al. (2010). Application of a Filtration- and Isolation-by-Size Technique for the Detection of Circulating Tumor Cells in Cutaneous Melanoma. J Invest Dermatol *130*, 2440-2447.
107. Desitter, I., Guerrouahen, B.S., Benali-Furet, N., Wechsler, J., Janne, P.A., Kuang, Y., Yanagita, M., Wang, L., Berkowitz, J.A., Distel, R.J., et al. (2011). A new device for rapid isolation by size and characterization of rare circulating tumor cells. Anticancer Res *31*, 427-441.
108. Kim, M.S., Sim, T.S., Kim, Y.J., Kim, S.S., Jeong, H., Park, J.M., Moon, H.S., Kim, S.I., Gurel, O., Lee, S.S., et al. (2012). SSA-MOA: a novel CTC isolation platform using selective size amplification (SSA) and a multi-obstacle architecture (MOA) filter. Lab on a chip *12*, 2874-2880.
109. Di Carlo, D. (2009). Inertial microfluidics. Lab on a chip *9*, 3038-3046.
110. Di Carlo, D., Edd, J.F., Irimia, D., Tompkins, R.G., and Toner, M. (2008). Equilibrium separation and filtration of particles using differential inertial focusing. Analytical chemistry *80*, 2204-2211.
111. Huang, T., Jia, C.P., Jun, Y., Sun, W.J., Wang, W.T., Zhang, H.L., Cong, H., Jing, F.X., Mao, H.J., Jin, Q.H., et al. (2014). Highly sensitive enumeration of circulating tumor

cells in lung cancer patients using a size-based filtration microfluidic chip. Biosensors & Bioelectronics *51*, 213-218.
112. Hosokawa, M., Yoshikawa, T., Negishi, R., Yoshino, T., Koh, Y., Kenmotsu, H., Naito, T., Takahashi, T., Yamamoto, N., Kikuhara, Y., et al. (2013). Microcavity array system for size-based enrichment of circulating tumor cells from the blood of patients with small-cell lung cancer. Analytical chemistry *85*, 5692-5698.
113. Hosokawa, M., Kenmotsu, H., Koh, Y., Yoshino, T., Yoshikawa, T., Naito, T., Takahashi, T., Murakami, H., Nakamura, Y., Tsuya, A., et al. (2013). Size-Based Isolation of Circulating Tumor Cells in Lung Cancer Patients Using a Microcavity Array System. PLoS One *8*.
114. Fan, X., Jia, C., Yang, J., Li, G., Mao, H., Jin, Q., and Zhao, J. (2015). A microfluidic chip integrated with a high-density PDMS-based microfiltration membrane for rapid isolation and detection of circulating tumor cells. Biosensors & Bioelectronics *71*, 380-386.
115. Sun, Y.F., Yang, X.R., Zhou, J., Qiu, S.J., Fan, J., and Xu, Y. (2011). Circulating tumor cells: advances in detection methods, biological issues, and clinical relevance. Journal of cancer research and clinical oncology *137*, 1151-1173.
116. Dong, Y., Skelley, A.M., Merdek, K.D., Sprott, K.M., Jiang, C., Pierceall, W.E., Lin, J., Stocum, M., Carney, W.P., and Smirnov, D.A. (2013). Microfluidics and circulating tumor cells. J Mol Diagn *15*, 149-157.
117. Liu, Z.B., Zhang, W., Huang, F., Feng, H.T., Shu, W.L., Xu, X.P., and Chen, Y. (2013). High throughput capture of circulating tumor cells using an integrated microfluidic system. Biosensors & Bioelectronics *47*, 113-119.
118. Pappas, D., and Wang, K. (2007). Cellular separations: a review of new challenges in analytical chemistry. Anal Chim Acta *601*, 26-35.
119. Satelli, A., Brownlee, Z., Mitra, A., Meng, Q.H., and Li, S. (2015). Circulating tumor cell enumeration with a combination of epithelial cell adhesion molecule- and cell-surface vimentin-based methods for monitoring breast cancer therapeutic response. Clin Chem *61*, 259-266.
120. Chang, C.L., Huang, W.F., Jalal, S.I., Chan, B.D., Mahmood, A., Shahda, S., O'Neil, B.H., Matei, D.E., and Savran, C.A. (2015). Circulating tumor cell detection using a parallel flow micro-aperture chip system. Lab on a chip *15*, 1677-1688.
121. Mascalchi, M., Falchini, M., Maddau, C., Salvianti, F., Nistri, M., Bertelli, E., Sali, L., Zuccherelli, S., Vella, A., Matucci, M., et al. (2015). Prevalence and number of circulating tumour cells and microemboli at diagnosis of advanced NSCLC. Journal of cancer research and clinical oncology.
122. Carlsson, A., Nair, V.S., Luttgen, M.S., Keu, K.V., Horng, G., Vasanawala, M., Kolatkar, A., Jamali, M., Iagaru, A.H., Kuschner, W., et al. (2014). Circulating tumor microemboli diagnostics for patients with non-small-cell lung cancer. J Thorac Oncol *9*, 1111-1119.
123. Zamay, G.S., Kolovskaya, O.S., Zamay, T.N., Glazyrin, Y.E., Krat, A.V., Zubkova, O., Spivak, E., Wehbe, M., Gargaun, A., Muharemagic, D., et al. (2015). Aptamers Selected to Postoperative Lung Adenocarcinoma Detect Circulating Tumor Cells in Human Blood. Mol Ther.
124. Dorsey, J.F., Kao, G.D., MacArthur, K.M., Ju, M., Steinmetz, D., Wileyto, E.P., Simone, C.B., 2nd, and Hahn, S.M. (2015). Tracking viable circulating tumor cells (CTCs) in the peripheral blood of non-small cell lung cancer (NSCLC) patients undergoing definitive radiation therapy: pilot study results. Cancer *121*, 139-149.
125. Juan, O., Vidal, J., Gisbert, R., Munoz, J., Macia, S., and Gomez-Codina, J. (2014). Prognostic significance of circulating tumor cells in advanced non-small cell lung cancer patients treated with docetaxel and gemcitabine. Clin Transl Oncol *16*, 637-643.

126. Sienel, W., Seen-Hibler, R., Mutschler, W., Pantel, K., and Passlick, B. (2003). Tumour cells in the tumour draining vein of patients with non-small cell lung cancer: detection rate and clinical significance. Eur J Cardio-Thorac *23*, 451-456.
127. Hashimoto, M., Tanaka, F., Yoneda, K., Takuwa, T., Matsumoto, S., Okumura, Y., Kondo, N., Tsubota, N., Tsujimura, T., Tabata, C., et al. (2014). Significant increase in circulating tumour cells in pulmonary venous blood during surgical manipulation in patients with primary lung cancer. Interact Cardiovasc Thorac Surg *18*, 775-783.
128. Funaki, S., Sawabata, N., Abulaiti, A., Nakagiri, T., Shintani, Y., Inoue, M., Minami, M., and Okumura, M. (2013). Significance of tumour vessel invasion in determining the morphology of isolated tumour cells in the pulmonary vein in non-small-cell lung cancer. Eur J Cardiothorac Surg *43*, 1126-1130.
129. Chudasama, D., Rice, A., Soppa, G., and Anikin, V. (2015). Circulating tumour cells in patients with lung cancer undergoing endobronchial cryotherapy. Cryobiology.
130. Wu, S., Liu, S., Liu, Z., Huang, J., Pu, X., Li, J., Yang, D., Deng, H., Yang, N., and Xu, J. (2015). Classification of circulating tumor cells by epithelial-mesenchymal transition markers. PLoS One *10*, e0123976.
131. Nel, I., Jehn, U., Gauler, T., and Hoffmann, A.C. (2014). Individual profiling of circulating tumor cell composition in patients with non-small cell lung cancer receiving platinum based treatment. Transl Lung Cancer Res *3*, 100-106.
132. van Meerbeeck, J.P., Fennell, D.A., and De Ruysscher, D.K. (2011). Small-cell lung cancer. Lancet *378*, 1741-1755.
133. Hou, J.M., Krebs, M.G., Lancashire, L., Sloane, R., Backen, A., Swain, R.K., Priest, L.J.C., Greystoke, A., Zhou, C., Morris, K., et al. (2012). Clinical Significance and Molecular Characteristics of Circulating Tumor Cells and Circulating Tumor Microemboli in Patients With Small-Cell Lung Cancer. Journal of Clinical Oncology *30*, 525-532.
134. Huang, C.H., Wick, J.A., Sittampalam, G.S., Nirmalanandhan, V.S., Ganti, A.K., Neupane, P.C., Williamson, S.K., Godwin, A.K., Schmitt, S., Smart, N.J., et al. (2014). A multicenter pilot study examining the role of circulating tumor cells as a blood-based tumor marker in patients with extensive small-cell lung cancer. Front Oncol *4*, 271.
135. Pirozzi, G., Tirino, V., Camerlingo, R., La Rocca, A., Martucci, N., Scognamiglio, G., Franco, R., Cantile, M., Normanno, N., and Rocco, G. (2013). Prognostic value of cancer stem cells, epithelial-mesenchymal transition and circulating tumor cells in lung cancer. Oncol Rep *29*, 1763-1768.
136. Kris, M.G., Johnson, B.E., Berry, L.D., Kwiatkowski, D.J., Iafrate, A.J., Wistuba, I.I., Varella-Garcia, M., Franklin, W.A., Aronson, S.L., Su, P.F., et al. (2014). Using Multiplexed Assays of Oncogenic Drivers in Lung Cancers to Select Targeted Drugs. Jama-J Am Med Assoc *311*, 1998-2006.
137. (2014). Comprehensive molecular profiling of lung adenocarcinoma. Nature *511*, 543-550.
138. (2012). Comprehensive genomic characterization of squamous cell lung cancers. Nature *489*, 519-525.
139. Abe, H., Kawahara, A., Azuma, K., Taira, T., Takase, Y., Fukumitsu, C., Murata, K., Yamaguchi, T., Akiba, J., Ishii, H., et al. (2015). Heterogeneity of anaplastic lymphoma kinase gene rearrangement in non-small-cell lung carcinomas: a comparative study between small biopsy and excision samples. J Thorac Oncol *10*, 800-805.
140. Marchetti, A., Del Grammastro, M., Felicioni, L., Malatesta, S., Filice, G., Centi, I., De Pas, T., Santoro, A., Chella, A., Brandes, A.A., et al. (2014). Assessment of EGFR mutations in circulating tumor cell preparations from NSCLC patients by next generation sequencing: toward a real-time liquid biopsy for treatment. PLoS One *9*, e103883.

141. Breitenbuecher, F., Hoffarth, S., Worm, K., Cortes-Incio, D., Gauler, T.C., Kohler, J., Herold, T., Schmid, K.W., Freitag, L., Kasper, S., et al. (2014). Development of a highly sensitive and specific method for detection of circulating tumor cells harboring somatic mutations in non-small-cell lung cancer patients. PLoS One *9*, e85350.
142. Taniguchi, K., Uchida, J., Nishino, K., Kumagai, T., Okuyama, T., Okami, J., Higashiyama, M., Kodama, K., Imamura, F., and Kato, K. (2011). Quantitative detection of EGFR mutations in circulating tumor DNA derived from lung adenocarcinomas. Clin Cancer Res *17*, 7808-7815.
143. Faugeroux, V., Pailler, E., Auger, N., Taylor, M., and Farace, F. (2014). Clinical Utility of Circulating Tumor Cells in ALK-Positive Non-Small-Cell Lung Cancer. Front Oncol *4*, 281.
144. Thiery, J.P., Acloque, H., Huang, R.Y., and Nieto, M.A. (2009). Epithelial-mesenchymal transitions in development and disease. Cell *139*, 871-890.
145. Weinberg, R.A. (2008). Mechanisms of malignant progression. Carcinogenesis *29*, 1092-1095.
146. Rhim, A.D., Mirek, E.T., Aiello, N.M., Maitra, A., Bailey, J.M., McAllister, F., Reichert, M., Beatty, G.L., Rustgi, A.K., Vonderheide, R.H., et al. (2012). EMT and dissemination precede pancreatic tumor formation. Cell *148*, 349-361.
147. Ilie, M., Hofman, V., Long-Mira, E., Selva, E., Vignaud, J.M., Padovani, B., Mouroux, J., Marquette, C.H., and Hofman, P. (2014). "Sentinel" circulating tumor cells allow early diagnosis of lung cancer in patients with chronic obstructive pulmonary disease. PLoS One *9*, e111597.
148. Chen, Y.Y., and Xu, G.B. (2014). Effect of circulating tumor cells combined with negative enrichment and CD45-FISH identification in diagnosis, therapy monitoring and prognosis of primary lung cancer. Med Oncol *31*, 240.
149. Yu, Y., Chen, Z., Dong, J., Wei, P., Hu, R., Zhou, C., Sun, N., Luo, M., Yang, W., Yao, R., et al. (2013). Folate receptor-positive circulating tumor cells as a novel diagnostic biomarker in non-small cell lung cancer. Transl Oncol *6*, 697-702.
150. Lou, J., Ben, S., Yang, G., Liang, X., Wang, X., Ni, S., and Han, B. (2013). Quantification of rare circulating tumor cells in non-small cell lung cancer by ligand-targeted PCR. PLoS One *8*, e80458.
151. Fiorelli, A., Accardo, M., Carelli, E., Angioletti, D., Santini, M., and Di Domenico, M. (2015). Circulating Tumor Cells in Diagnosing Lung Cancer: Clinical and Morphologic Analysis. Ann Thorac Surg.
152. Howlader N, N.A., Krapcho M, Garshell J, Miller D, Altekruse SF, Kosary CL, Yu M, Ruhl J, Tatalovich Z,Mariotto A, Lewis DR, Chen HS, Feuer EJ, Cronin KA (eds) SEER Cancer Statistics Review, 1975-2012. National Cancer Institute. Bethesda, MD, http://seer.cancer.gov/csr/1975_2012/, based on November 2014 SEER data submission, posted to the SEER web site, April 2015.
153. Siegel, R.L., Miller, K.D., and Jemal, A. (2015). Cancer statistics, 2015. CA: a cancer journal for clinicians *65*, 5-29.
154. Siewert, J.R., Stein, H.J., Feith, M., Bruecher, B.L.D.M., Bartels, H., and Fink, U. (2001). Histologic tumor type is an independent prognostic parameter in esophageal cancer: Lessons from more than 1,000 consecutive resections at a single center in the Western world. Ann Surg *234*, 360-367.
155. Brown, L.M., Hoover, R., Silverman, D., Baris, D., Hayes, R., Swanson, G.M., Schoenberg, J., Greenberg, R., Liff, J., Schwartz, A., et al. (2001). Excess incidence of squamous cell esophageal cancer among US black men: Role of social class and other risk factors. Am J Epidemiol *153*, 114-122.

156. Garidou, A., Tzonou, A., Lipworth, L., Signorello, L.B., Kalapothaki, V., and Trichopoulos, D. (1996). Life-style factors and medical conditions in relation to esophageal cancer by histologic type in a low-risk population. Int J Cancer *68*, 295-299.
157. Lagergren, J., Bergstrom, R., Lindgren, A., and Nyren, O. (1999). Symptomatic gastroesophageal reflux as a risk factor for esophageal adenocarcinoma. New Engl J Med *340*, 825-831.
158. Enzinger, P.C., and Mayer, R.J. (2003). Esophageal cancer. N Engl J Med *349*, 2241-2252.
159. Mealy, K., Feely, J., Reid, I., McSweeney, J., Walsh, T., and Hennessy, T.P.J. (1996). Tumour marker detection in oesophageal carcinoma. Eur J Surg Oncol *22*, 505-507.
160. Sclafani, F., Smyth, E., Cunningham, D., Chau, I., Turner, A., and Watkins, D. (2014). A pilot study assessing the incidence and clinical significance of circulating tumor cells in esophagogastric cancers. Clin Colorectal Cancer *13*, 94-99.
161. Matsushita, D., Uenosono, Y., Arigami, T., Yanagita, S., Nishizono, Y., Hagihara, T., Hirata, M., Haraguchi, N., Arima, H., Kijima, Y., et al. (2015). Clinical Significance of Circulating Tumor Cells in Peripheral Blood of Patients with Esophageal Squamous Cell Carcinoma. Ann Surg Oncol *22*, 3674-3680.
162. Consoli, F., Arcangeli, G., Ferrari, V., Grisanti, S., Almici, C., Bordonali, T., and Simoncini, E. (2011). Circulating tumor cells and cardiac metastasis from esophageal cancer: a case report. Case Rep Oncol *4*, 299-303.
163. Reeh, M., Effenberger, K.E., Koenig, A.M., Riethdorf, S., Eichstadt, D., Vettorazzi, E., Uzunoglu, F.G., Vashist, Y.K., Izbicki, J.R., Pantel, K., et al. (2015). Circulating Tumor Cells as a Biomarker for Preoperative Prognostic Staging in Patients With Esophageal Cancer. Ann Surg *261*, 1124-1130.
164. Li, H., Song, P., Zou, B., Liu, M., Cui, K., Zhou, P., Li, S., and Zhang, B. (2015). Circulating Tumor Cell Analyses in Patients With Esophageal Squamous Cell Carcinoma Using Epithelial Marker-Dependent and -Independent Approaches. Medicine (Baltimore) *94*, e1565.
165. Bobek, V., Matkowski, R., Gurlich, R., Grabowski, K., Szelachowska, J., Lischke, R., Schutzner, J., Harustiak, T., Pazdro, A., Rzechonek, A., et al. (2014). Cultivation of circulating tumor cells in esophageal cancer. Folia Histochem Cytobiol *52*, 171-177.
166. Flores, L.M., Kindelberger, D.W., Ligon, A.H., Capelletti, M., Fiorentino, M., Loda, M., Cibas, E.S., Janne, P.A., and Krop, I.E. (2010). Improving the yield of circulating tumour cells facilitates molecular characterisation and recognition of discordant HER2 amplification in breast cancer. Br J Cancer *102*, 1495-1502.
167. Allard, W.J. (2004). Tumor Cells Circulate in the Peripheral Blood of All Major Carcinomas but not in Healthy Subjects or Patients With Nonmalignant Diseases. Clinical Cancer Research *10*, 6897-6904.
168. Yu, M., Stott, S., Toner, M., Maheswaran, S., and Haber, D.A. (2011). Circulating tumor cells: approaches to isolation and characterization. J Cell Biol *192*, 373-382.
169. Haun, J.B., Devaraj, N.K., Hilderbrand, S.A., Lee, H., and Weissleder, R. (2010). Bioorthogonal chemistry amplifies nanoparticle binding and enhances the sensitivity of cell detection. Nat Nanotechnol *5*, 660-665.
170. Regehr, K.J., Domenech, M., Koepsel, J.T., Carver, K.C., Ellison-Zelski, S.J., Murphy, W.L., Schuler, L.A., Alarid, E.T., and Beebe, D.J. (2009). Biological implications of polydimethylsiloxane-based microfluidic cell culture. Lab on a chip *9*, 2132-2139.
171. Young, E.W., and Beebe, D.J. (2010). Fundamentals of microfluidic cell culture in controlled microenvironments. Chem Soc Rev *39*, 1036-1048.
172. El-Ali, J., Sorger, P.K., and Jensen, K.F. (2006). Cells on chips. Nature *442*, 403-411.
173. Joyce, J.A., and Pollard, J.W. (2009). Microenvironmental regulation of metastasis. Nat Rev Cancer *9*, 239-252.

174. Orimo, A., and Weinberg, R.A. (2006). Stromal fibroblasts in cancer: a novel tumor-promoting cell type. Cell Cycle *5*, 1597-1601.
175. Hofman, V., Ilie, M.I., Long, E., Selva, E., Bonnetaud, C., Molina, T., Vénissac, N., Mouroux, J., Vielh, P., and Hofman, P. (2011). Detection of circulating tumor cells as a prognostic factor in patients undergoing radical surgery for non-small-cell lung carcinoma: comparison of the efficacy of the CellSearch Assay™ and the isolation by size of epithelial tumor cell method. International Journal of Cancer *129*, 1651-1660.
176. Hofman, V., Bonnetaud, C., Ilie, M.I., Vielh, P., Vignaud, J.M., Flejou, J.F., Lantuejoul, S., Piaton, E., Mourad, N., Butori, C., et al. (2010). Preoperative Circulating Tumor Cell Detection Using the Isolation by Size of Epithelial Tumor Cell Method for Patients with Lung Cancer Is a New Prognostic Biomarker. Clinical Cancer Research *17*, 827-835.
177. Punnoose, E.A., Atwal, S., Liu, W., Raja, R., Fine, B.M., Hughes, B.G.M., Hicks, R.J., Hampton, G.M., Amler, L.C., Pirzkall, A., et al. (2012). Evaluation of Circulating Tumor Cells and Circulating Tumor DNA in Non-Small Cell Lung Cancer: Association with Clinical Endpoints in a Phase II Clinical Trial of Pertuzumab and Erlotinib. Clinical Cancer Research *18*, 2391-2401.
178. Alix-Panabieres, C., Riethdorf, S., and Pantel, K. (2008). Circulating Tumor Cells and Bone Marrow Micrometastasis. Clinical Cancer Research *14*, 5013-5021.
179. Tanaka, F., Yoneda, K., Kondo, N., Hashimoto, M., Takuwa, T., Matsumoto, S., Okumura, Y., Rahman, S., Tsubota, N., Tsujimura, T., et al. (2009). Circulating tumor cell as a diagnostic marker in primary lung cancer. Clin Cancer Res *15*, 6980-6986.
180. Yu, M., Bardia, A., Aceto, N., Bersani, F., Madden, M.W., Donaldson, M.C., Desai, R., Zhu, H., Comaills, V., Zheng, Z., et al. (2014). Cancer therapy. Ex vivo culture of circulating breast tumor cells for individualized testing of drug susceptibility. Science *345*, 216-220.
181. Sung, K.E., Yang, N., Pehlke, C., Keely, P.J., Eliceiri, K.W., Friedl, A., and Beebe, D.J. (2011). Transition to invasion in breast cancer: a microfluidic in vitro model enables examination of spatial and temporal effects. Integr Biol (Camb) *3*, 439-450.
182. Yamaguchi, T., Yanagisawa, K., Sugiyama, R., Hosono, Y., Shimada, Y., Arima, C., Kato, S., Tomida, S., Suzuki, M., Osada, H., et al. (2012). NKX2-1/TITF1/TTF-1-Induced ROR1 is required to sustain EGFR survival signaling in lung adenocarcinoma. Cancer Cell *21*, 348-361.
183. Fidler, I.J. (2003). The pathogenesis of cancer metastasis: the 'seed and soil' hypothesis revisited. Nat Rev Cancer *3*, 453-458.
184. Bethune, G., Bethune, D., Ridgway, N., and Xu, Z. (2010). Epidermal growth factor receptor (EGFR) in lung cancer: an overview and update. J Thorac Dis *2*, 48-51.
185. You, L., He, B., Xu, Z., Uematsu, K., Mazieres, J., Mikami, I., Reguart, N., Moody, T.W., Kitajewski, J., McCormick, F., et al. (2004). Inhibition of Wnt-2-mediated signaling induces programmed cell death in non-small-cell lung cancer cells. Oncogene *23*, 6170-6174.
186. Mogi, A., and Kuwano, H. (2011). TP53 mutations in nonsmall cell lung cancer. J Biomed Biotechnol *2011*, 583929.
187. Wong, A.P., Perez-Castillejos, R., Christopher Love, J., and Whitesides, G.M. (2008). Partitioning microfluidic channels with hydrogel to construct tunable 3-D cellular microenvironments. Biomaterials *29*, 1853-1861.
188. Walker, G.M., Zeringue, H.C., and Beebe, D.J. (2004). Microenvironment design considerations for cellular scale studies. Lab on a chip *4*, 91-97.
189. Sung, J.H., and Shuler, M.L. (2012). Microtechnology for mimicking in vivo tissue environment. Ann Biomed Eng *40*, 1289-1300.
190. Pantel, K., Brakenhoff, R.H., and Brandt, B. (2008). Detection, clinical relevance and specific biological properties of disseminating tumour cells. Nat Rev Cancer *8*, 329-340.

191. Zhao, W., Cui, C.H., Bose, S., Guo, D., Shen, C., Wong, W.P., Halvorsen, K., Farokhzad, O.C., Teo, G.S.L., Phillips, J.A., et al. (2012). Bioinspired multivalent DNA network for capture and release of cells. Proceedings of the National Academy of Sciences *109*, 19626-19631.
192. Shah, A.M., Yu, M., Nakamura, Z., Ciciliano, J., Ulman, M., Kotz, K., Stott, S.L., Maheswaran, S., Haber, D.A., and Toner, M. (2012). Biopolymer System for Cell Recovery from Microfluidic Cell Capture Devices. Analytical chemistry *84*, 3682-3688.
193. Gerlinger, M., Rowan, A.J., Horswell, S., Larkin, J., Endesfelder, D., Gronroos, E., Martinez, P., Matthews, N., Stewart, A., Tarpey, P., et al. (2012). Intratumor heterogeneity and branched evolution revealed by multiregion sequencing. N Engl J Med *366*, 883-892.
194. Gao, D., Vela, I., Sboner, A., Iaquinta, P.J., Karthaus, W.R., Gopalan, A., Dowling, C., Wanjala, J.N., Undvall, E.A., Arora, V.K., et al. (2014). Organoid cultures derived from patients with advanced prostate cancer. Cell *159*, 176-187.
195. Maheswaran, S., and Haber, D.A. (2015). Ex Vivo Culture of CTCs: An Emerging Resource to Guide Cancer Therapy. Cancer Res *75*, 2411-2415.
196. Harrow, J., Denoeud, F., Frankish, A., Reymond, A., Chen, C.K., Chrast, J., Lagarde, J., Gilbert, J.G., Storey, R., Swarbreck, D., et al. (2006). GENCODE: producing a reference annotation for ENCODE. Genome Biol *7 Suppl 1*, S4 1-9.
197. Jiang, H., and Wong, W.H. (2009). Statistical inferences for isoform expression in RNA-Seq. Bioinformatics *25*, 1026-1032.
198. Mortazavi, A., Williams, B.A., McCue, K., Schaeffer, L., and Wold, B. (2008). Mapping and quantifying mammalian transcriptomes by RNA-Seq. Nat Methods *5*, 621-628.
199. Balkwill, F. (2004). Cancer and the chemokine network. Nat Rev Cancer *4*, 540-550.
200. Perk, J., Iavarone, A., and Benezra, R. (2005). Id family of helix-loop-helix proteins in cancer. Nat Rev Cancer *5*, 603-614.
201. Lee, H.J., Seol, H.S., Kim, J.Y., Chun, S.M., Suh, Y.A., Park, Y.S., Kim, S.W., Choi, C.M., Park, S.I., Kim, D.K., et al. (2013). ROS1 receptor tyrosine kinase, a druggable target, is frequently overexpressed in non-small cell lung carcinomas via genetic and epigenetic mechanisms. Ann Surg Oncol *20*, 200-208.
202. Bierie, B., and Moses, H.L. (2006). Tumour microenvironment: TGFbeta: the molecular Jekyll and Hyde of cancer. Nat Rev Cancer *6*, 506-520.
203. Tai, I.T., and Tang, M.J. (2008). SPARC in cancer biology: its role in cancer progression and potential for therapy. Drug Resist Updat *11*, 231-246.
204. Satelli, A., and Li, S.L. (2011). Vimentin in cancer and its potential as a molecular target for cancer therapy. Cell Mol Life Sci *68*, 3033-3046.
205. Podhajcer, O.L., Benedetti, L.G., Girotti, M.R., Prada, F., Salvatierra, E., and Llera, A.S. (2008). The role of the matricellular protein SPARC in the dynamic interaction between the tumor and the host. Cancer Metast Rev *27*, 691-705.
206. Schneider, M., Hansen, J.L., and Sheikh, S.P. (2008). S100A4: a common mediator of epithelial-mesenchymal transition, fibrosis and regeneration in diseases? J Mol Med (Berl) *86*, 507-522.
207. Guddo, F., Giatromanolaki, A., Koukourakis, M.I., Reina, C., Vignola, A.M., Chlouverakis, G., Hilkens, J., Gatter, K.C., Harris, A.L., and Bonsignore, G. (1998). MUC1 (episialin) expression in non-small cell lung cancer is independent of EGFR and c-erbB-2 expression and correlates with poor survival in node positive patients. J Clin Pathol *51*, 667-671.
208. Ma, I., and Allan, A.L. (2011). The role of human aldehyde dehydrogenase in normal and cancer stem cells. Stem Cell Rev *7*, 292-306.
209. Goldoni, S., and Iozzo, R.V. (2008). Tumor microenvironment: Modulation by decorin and related molecules harboring leucine-rich tandem motifs. Int J Cancer *123*, 2473-2479.

210. Waugh, D.J., and Wilson, C. (2008). The interleukin-8 pathway in cancer. Clin Cancer Res *14*, 6735-6741.
211. Karin, M., Cao, Y., Greten, F.R., and Li, Z.W. (2002). NF-kappaB in cancer: from innocent bystander to major culprit. Nat Rev Cancer *2*, 301-310.
212. Mantovani, A., Allavena, P., Sica, A., and Balkwill, F. (2008). Cancer-related inflammation. Nature *454*, 436-444.
213. Wu, M., Wang, B., Gil, J., Sabo, E., Miller, L., Gan, L., and Burstein, D.E. (2003). p63 and TTF-1 immunostaining. A useful marker panel for distinguishing small cell carcinoma of lung from poorly differentiated squamous cell carcinoma of lung. Am J Clin Pathol *119*, 696-702.
214. Zhang, T.H., Meng, L., Dong, W., Shen, H.C., Zhang, S.M., Liu, Q., and Du, J.J. (2013). High expression of PRDM14 correlates with cell differentiation and is a novel prognostic marker in resected non-small cell lung cancer. Medical Oncology *30*.
215. Lin, C.I., Merley, A., Sciuto, T.E., Li, D., Dvorak, A.M., Melero-Martin, J.M., Dvorak, H.F., and Jaminet, S.C. (2014). TM4SF1: a new vascular therapeutic target in cancer. Angiogenesis *17*, 897-907.
216. You, L., He, B., Xu, Z.D., Uematsu, K., Mazieres, J., Mikami, I., Reguart, N., Moody, T.W., Kitajewski, J., McCormick, F., et al. (2004). Inhibition of Wnt-2-mediated signaling induces programmed cell death in non-small-cell lung cancer cells. Oncogene *23*, 6170-6174.
217. Praveen Kumar, V.R., Sehgal, P., Thota, B., Patil, S., Santosh, V., and Kondaiah, P. (2014). Insulin like growth factor binding protein 4 promotes GBM progression and regulates key factors involved in EMT and invasion. J Neurooncol *116*, 455-464.
218. Jung, Y.S., Liu, X.W., Chirco, R., Warner, R.B., Fridman, R., and Kim, H.R. (2012). TIMP-1 induces an EMT-like phenotypic conversion in MDCK cells independent of its MMP-inhibitory domain. PLoS One *7*, e38773.
219. Lee, H.W., Park, Y.M., Lee, S.J., Cho, H.J., Kim, D.H., Lee, J.I., Kang, M.S., Seol, H.J., Shim, Y.M., Nam, D.H., et al. (2013). Alpha-Smooth Muscle Actin (ACTA2) Is Required for Metastatic Potential of Human Lung Adenocarcinoma. Clinical Cancer Research *19*, 5879-5889.
220. Pao, W., and Girard, N. (2011). New driver mutations in non-small-cell lung cancer. Lancet Oncol *12*, 175-180.
221. Yao, H.X., Zhang, Z.Q., Xiao, Z.Q., Chen, Y.H., Li, C., Zhang, P.F., Li, M.X., Liu, Y.F., Guan, Y.J., Yu, Y.H., et al. (2009). Identification of metastasis associated proteins in human lung squamous carcinoma using two-dimensional difference gel electrophoresis and laser capture microdissection. Lung Cancer *65*, 41-48.
222. Boukovinas, I., Papadaki, C., Mendez, P., Taron, M., Mavroudis, D., Koutsopoulos, A., Sanchez-Ronco, M., Sanchez, J.J., Trypaki, M., Staphopoulos, E., et al. (2008). Tumor BRCA1, RRM1 and RRM2 mRNA expression levels and clinical response to first-line gemcitabine plus docetaxel in non-small-cell lung cancer patients. PLoS One *3*, e3695.
223. Betticher, D.C., Heighway, J., Hasleton, P.S., Altermatt, H.J., Ryder, W.D., Cerny, T., and Thatcher, N. (1996). Prognostic significance of CCND1 (cyclin D1) overexpression in primary resected non-small-cell lung cancer. Br J Cancer *73*, 294-300.
224. He, B., Barg, R.N., You, L., Xu, Z., Reguart, N., Mikami, I., Batra, S., Rosell, R., and Jablons, D.M. (2005). Wnt signaling in stem cells and non-small-cell lung cancer. Clin Lung Cancer *7*, 54-60.
225. Chaffer, C.L., and Weinberg, R.A. (2011). A perspective on cancer cell metastasis. Science *331*, 1559-1564.
226. Ting, D.T., Wittner, B.S., Ligorio, M., Vincent Jordan, N., Shah, A.M., Miyamoto, D.T., Aceto, N., Bersani, F., Brannigan, B.W., Xega, K., et al. (2014). Single-cell RNA

sequencing identifies extracellular matrix gene expression by pancreatic circulating tumor cells. Cell Rep *8*, 1905-1918.
227. Shields, J.M., Pruitt, K., McFall, A., Shaub, A., and Der, C.J. (2000). Understanding Ras: 'it ain't over 'til it's over'. Trends Cell Biol *10*, 147-154.
228. Martinon, F., Holler, N., Richard, C., and Tschopp, J. (2000). Activation of a pro-apoptotic amplification loop through inhibition of NF-kappa B-dependent survival signals by caspase-mediated inactivation of RIP. Febs Lett *468*, 134-136.
229. Ding, L., Getz, G., Wheeler, D.A., Mardis, E.R., McLellan, M.D., Cibulskis, K., Sougnez, C., Greulich, H., Muzny, D.M., Morgan, M.B., et al. (2008). Somatic mutations affect key pathways in lung adenocarcinoma. Nature *455*, 1069-1075.
230. Sharma, S.V., Bell, D.W., Settleman, J., and Haber, D.A. (2007). Epidermal growth factor receptor mutations in lung cancer. Nat Rev Cancer *7*, 169-181.
231. Paez, J.G., Janne, P.A., Lee, J.C., Tracy, S., Greulich, H., Gabriel, S., Herman, P., Kaye, F.J., Lindeman, N., Boggon, T.J., et al. (2004). EGFR mutations in lung cancer: correlation with clinical response to gefitinib therapy. Science *304*, 1497-1500.
232. Camidge, D.R., Bang, Y.J., Kwak, E.L., Iafrate, A.J., Varella-Garcia, M., Fox, S.B., Riely, G.J., Solomon, B., Ou, S.H., Kim, D.W., et al. (2012). Activity and safety of crizotinib in patients with ALK-positive non-small-cell lung cancer: updated results from a phase 1 study. Lancet Oncol *13*, 1011-1019.
233. Kwak, E.L., Bang, Y.J., Camidge, D.R., Shaw, A.T., Solomon, B., Maki, R.G., Ou, S.H., Dezube, B.J., Janne, P.A., Costa, D.B., et al. (2010). Anaplastic lymphoma kinase inhibition in non-small-cell lung cancer. N Engl J Med *363*, 1693-1703.
234. Katayama, R., Khan, T.M., Benes, C., Lifshits, E., Ebi, H., Rivera, V.M., Shakespeare, W.C., Iafrate, A.J., Engelman, J.A., and Shaw, A.T. (2011). Therapeutic strategies to overcome crizotinib resistance in non-small cell lung cancers harboring the fusion oncogene EML4-ALK. Proceedings of the National Academy of Sciences of the United States of America *108*, 7535-7540.
235. Friboulet, L., Li, N., Katayama, R., Lee, C.C., Gainor, J.F., Crystal, A.S., Michellys, P.Y., Awad, M.M., Yanagitani, N., Kim, S., et al. (2014). The ALK inhibitor ceritinib overcomes crizotinib resistance in non-small cell lung cancer. Cancer Discov *4*, 662-673.
236. Gandhi, L., and Janne, P.A. (2012). Crizotinib for ALK-rearranged non-small cell lung cancer: a new targeted therapy for a new target. Clin Cancer Res *18*, 3737-3742.
237. Lindeman, N.I., Cagle, P.T., Beasley, M.B., Chitale, D.A., Dacic, S., Giaccone, G., Jenkins, R.B., Kwiatkowski, D.J., Saldivar, J.S., Squire, J., et al. (2013). Molecular testing guideline for selection of lung cancer patients for EGFR and ALK tyrosine kinase inhibitors: guideline from the College of American Pathologists, International Association for the Study of Lung Cancer, and Association for Molecular Pathology. J Thorac Oncol *8*, 823-859.
238. Pailler, E., Auger, N., Lindsay, C.R., Vielh, P., Islas-Morris-Hernandez, A., Borget, I., Ngo-Camus, M., Planchard, D., Soria, J.C., Besse, B., et al. (2015). High level of chromosomal instability in circulating tumor cells of ROS1-rearranged non-small-cell lung cancer. Ann Oncol *26*, 1408-1415.
239. McDermott, U., Lafrate, A.J., Gray, N.S., Shioda, T., Classon, M., Maheswaran, S., Zhou, W., Choi, H.G., Smith, S.L., Dowell, L., et al. (2008). Genomic alterations of anaplastic lymphoma kinase may sensitize tumors to anaplastic lymphoma kinase inhibitors. Cancer Research *68*, 3389-3395.
240. Leung, E.L., Fiscus, R.R., Tung, J.W., Tin, V.P., Cheng, L.C., Sihoe, A.D., Fink, L.M., Ma, Y., and Wong, M.P. (2010). Non-small cell lung cancer cells expressing CD44 are enriched for stem cell-like properties. PLoS One *5*, e14062.
241. Kling, J. (2012). Beyond counting tumor cells. Nature biotechnology *30*, 578-580.

242. Yu, M., Bardia, A., Wittner, B.S., Stott, S.L., Smas, M.E., Ting, D.T., Isakoff, S.J., Ciciliano, J.C., Wells, M.N., Shah, A.M., et al. (2013). Circulating breast tumor cells exhibit dynamic changes in epithelial and mesenchymal composition. Science *339*, 580-584.
243. Heitzer, E., Auer, M., Gasch, C., Pichler, M., Ulz, P., Hoffmann, E.M., Lax, S., Waldispuehl-Geigl, J., Mauermann, O., Lackner, C., et al. (2013). Complex tumor genomes inferred from single circulating tumor cells by array-CGH and next-generation sequencing. Cancer Res *73*, 2965-2975.
244. Pantel, K., and Alix-Panabieres, C. (2010). Circulating tumour cells in cancer patients: challenges and perspectives. Trends Mol Med *16*, 398-406.
245. Deneve, E., Riethdorf, S., Ramos, J., Nocca, D., Coffy, A., Daures, J.P., Maudelonde, T., Fabre, J.M., Pantel, K., and Alix-Panabieres, C. (2013). Capture of viable circulating tumor cells in the liver of colorectal cancer patients. Clin Chem *59*, 1384-1392.
246. Fan, T., Zhao, Q., Chen, J.J., Chen, W.T., and Pearl, M.L. (2009). Clinical significance of circulating tumor cells detected by an invasion assay in peripheral blood of patients with ovarian cancer. Gynecol Oncol *112*, 185-191.
247. Yu, M., Ting, D.T., Stott, S.L., Wittner, B.S., Ozsolak, F., Paul, S., Ciciliano, J.C., Smas, M.E., Winokur, D., Gilman, A.J., et al. (2012). RNA sequencing of pancreatic circulating tumour cells implicates WNT signalling in metastasis. Nature *487*, 510-513.